HHS Public Access

Author manuscript

Adv Drug Deliv Rev. Author manuscript; available in PMC 2019 March 15.

Published in final edited form as:

Adv Drug Deliv Rev. 2018 March 15; 128: 3–28. doi:10.1016/j.addr.2017.09.013.

Recent Advances of Controlled Drug Delivery Using Microfluidic Platforms

Sharma T. Sanjay[+,1], **Wan Zhou**[+,1], **Maowei Dou**[+,1,2], **Hamed Tavakoli**[1], **Lei Ma**[1], **Feng Xu**[3], and **XiuJun Li**[1,4,5,6,*]

[1]Department of Chemistry, University of Texas at El Paso, 500 West University Ave, El Paso, Texas, 79968, USA, Richland, Washington, 99354, USA

[2]Environmental Molecular Sciences Laboratory, Pacific Northwest National Laboratory

[3]Bioinspired Engineering and Biomechanics Center (BEBC), Xi'an Jiaotong University, Xi'an 710049, P.R. China

[4]Border Biomedical Research Center, University of Texas at El Paso, 500 West University Ave, El Paso, Texas, 79968, USA, Richland, Washington, 99354, USA

[5]Biomedical Engineering, University of Texas at El Paso, 500 West University Ave, El Paso, Texas, 79968, USA, Richland, Washington, 99354, USA

[6]Environmental Science and Engineering, University of Texas at El Paso, 500 West University Ave, El Paso, Texas, 79968, USA, Richland, Washington, 99354, USA

Abstract

Conventional systematically-administered drugs distribute evenly throughout the body, get degraded and excreted rapidly while crossing many biological barriers, leaving minimum amounts of the drugs at pathological sites. Controlled drug delivery aims to deliver drugs to the target sites at desired rates and time, thus enhancing the drug efficacy, pharmacokinetics, and bioavailability while maintaining minimal side effects. Due to a number of unique advantages of the recent microfluidic lab-on-a-chip technology, microfluidic lab-on-a-chip has provided unprecedented opportunities for controlled drug delivery. Drugs can be efficiently delivered to the target sites at desired rates in a well-controlled manner by microfluidic platforms via integration, implantation, localization, automation, and precise control of various microdevice parameters. These features accordingly make reproducible, on-demand, and tunable drug delivery become feasible. On-demand self-tuning dynamic drug delivery systems have shown great potential for personalized drug delivery. This review presents an overview of recent advances in controlled drug delivery using microfluidic platforms. The review first briefly introduces microfabrication techniques of microfluidic platforms, followed by detailed descriptions of numerous microfluidic drug delivery

[*]Corresponding author: xli4@utep.edu.
[+]Denotes those authors contribute equally to this work

Declaration of interest: All the authors declare no conflict of interest.

systems that have significantly advanced the field of controlled drug delivery. Those microfluidic systems can be separated into four major categories, namely drug carrier-free micro-reservoir-based drug delivery systems, highly integrated carrier-free microfluidic lab-on-a-chip systems, drug carrier-integrated microfluidic systems, and microneedles. Microneedles can be further categorized into five different types, i.e. solid, porous, hollow, coated, and biodegradable microneedles, for controlled transdermal drug delivery. At the end, we discuss current limitations and future prospects of microfluidic platforms for controlled drug delivery.

Graphical abstract

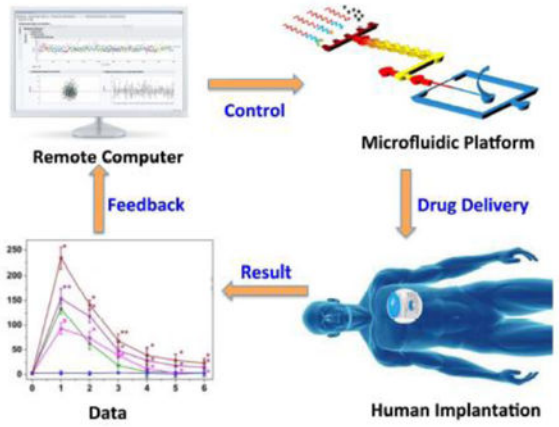

This article reviews recent advances of controlled drug delivery using microfluidic platforms which can be implanted in human bodies to control drug release in real time through an on-demand feedback mechanism.

Keywords

Controlled drug delivery; Microfluidic lab-on-a-chip platforms; Microfluidic devices; Micro-reservoir; Drug Carriers; Microneedles; Nanomaterials for drug delivery

1. Introduction

Drug delivery systems to administer a therapeutic substance to a biological system have been crucial to ensuring that the administered substances/drugs lead to desired therapeutic efficacy with minimal side effects. Drugs can be delivered through various routes including hypodermic injections, oral administration, inhalation, and transdermal administration [1]. Drug delivery systems ensure maximum efficacy of the therapeutic drugs by delivering drugs to the target sites, immediately releasing the drugs, lengthening the release of drugs or making a pulsatile release based upon disease conditions and working mechanisms of the drugs.

Conventional methods of drug delivery possess several drawbacks although they are the most common delivery methods. One of the major drawbacks of conventional drug delivery is the difficulty associated with achieving targeted delivery to specific cells and tissues as

they are evenly distributed throughout the body before reaching pathological sites of action and may get inactivated or degraded while crossing different biological barriers [2]. Further, drugs may become less effective as the final effective concentrations at the site of action are lowered. Almost 80 % of the drugs are administered orally [1]. Oral administrations have limitations in terms of absorption and metabolism. Enzymatic degradation, degradation due to change in pH within the body, side effects, varying transit times, and first-pass metabolism represent some other limitations associated with oral administration [3]. Hypodermic injections lead to pain because of long needles that pierce through the nerve endings. In addition, conventional drug delivery systems usually have a burst release of drugs instead of sustained release, which decreases the efficacy of therapeutic drugs. Drugs may have to be used at higher concentrations, ultimately increasing cytotoxicity and side effects of the drugs. Finally, conventional methods are also limited by drug's poor solubility, non-specificity, and undesired release profiles [4]. Sustained release of drugs where the drugs' concentrations remain within the therapeutic range for a long time is often required for the desired therapeutic efficacy. For some specific therapeutic effects, it is desired to deliver drugs according to the circadian behavior of the disease. These chrono-therapeutic drugs for diseases such as arthritis, epilepsy, asthma, ulcer, and diabetes, where pharmacokinetics is not constant within 24 h due to rhythmic circadian of the body, may require the pulsatile release of the drugs [5, 6].

Controlled drug delivery systems started in the early 1950s with the development of oral and transdermal sustained release systems, followed by the development of zero-order release systems, microtechnology- and nanotechnology-based delivery, and self-regulated drug delivery systems [7]. The growth in the field has led to the development of numerous novel systems for controlled drug delivery, including micro-reservoir implants, transdermal patches, nanoparticles (NPs), antibody-drug conjugates, and microneedles (MNs) [8]. Controlled drug delivery systems help to improve the administration, efficiency, and pharmacokinetics of therapeutic drugs such as peptides, vaccines, enzymes, and other drugs. They improve the bioavailability of therapeutic drugs by increasing the uptake, preventing the premature degradation, maintaining drugs at the therapeutic window, and reducing the side effects by targeting drugs to particular cells or tissues. A drug delivery system that can be controlled to release the drugs in the desired amount would enable patients to achieve reproducible, on-demand, and tunable dosing at the required time. Such a system allows accurate regulation of dosage for desired effects, minimizes the related side effects, and averts repeated drug administration or implantation of devices, ultimately increasing the patient compliance [9].

1.1. Microtechnology for controlled drug delivery

Microfluidic lab-on-a-chip (LOC) is a rapidly growing field where a tiny amount of fluids is manipulated within a device with micro-scale structures inside. Microfluidic devices produced by microfabrication techniques integrate multiple components and functionalities ranging from sampling and synthesis to testing within a small device and can be automated to analyze complex biological fluids or deliver therapeutic compounds [10]. In addition, it has several other remarkable features including low-cost, portable, well-controlled microenvironments, and high throughput. Processes within a miniaturized microfluidic

device can be controlled precisely and efficiently. LOC finds applications in varieties of fields including drug and gene delivery, particles and drug-carriers synthesis, detection of infectious diseases and cancers, cellular analysis, tissue engineering and so on [9, 11-14]. The microtechnology for controlled drug delivery involves the fabrication and assembly of various components for drug delivery devices, implantation of the devices within human or animal bodies, synthesis of therapeutic vessels/carriers, and delivery of the drugs to the targeted cells or tissues. Both the synthesis of therapeutic drugs and delivery to specific sites can also be integrated into a single device [15].

To address various drawbacks of conventional delivery systems, microfluidic devices are being widely used in controlled drug delivery as they have certain unique features such as the precise control of flow and integrated processing [16-18]. LOC-based devices can deliver drugs at a sustained rate, increasing the therapeutic efficiency and overcoming the burst release in conventional methods and its associated side effects [19]. Peptides, proteins or DNA-based drugs may be ineffective due to enzymatic degradation while traveling through the long pathway in conventional drug delivery system [20]. Recent developments in microfluidic technologies can help controlled and targeted drug delivery (e.g. through implanted microdevices) and minimize the delivery pathway. As LOC technology can precisely manipulate nano-liter volumes of liquid, it can synthesize drug carriers with precise sizes, shapes, and compositions, leading to a more predictable drug release profile [21, 22]. To obtain a reproducible release profile, mono-dispersed drug carriers are required, which is very challenging without the use of LOC technologies as conventional methods of emulsification generally produce multi-dispersed carriers. In addition, miniaturized microfluidic devices help to reduce pain and improve portability and safety, and in some cases, do not require trained personnel.

This article reviews recent advances in controlled drug delivery using microfluidic platforms. After a brief description of drug delivery systems and microfabrication techniques, this article reviews different microfluidic controlled drug delivery platforms based upon three broad categories, i.e. drug carrier-free microfluidic systems, drug carrier-integrated microfluidic LOC systems, and MNs-based drug delivery systems. Because MNs have attracted a lot of attention, we separate MNs into a stand-alone section. Drug carrier-free microfluidic systems further include micro-reservoir systems and microfluidic LOC devices, because of different degree of integrations. Certain drug carriers can improve the delivery and effectiveness of drugs. Hence, different kinds of drug carriers including microcapsules, nanoemulsions, and NPs, are discussed within drug carriers-integrated microfluidic systems. Similarly, MNs-based drug delivery systems include different varieties of MNs including solid, porous, hollow, coated, and dissolvable MNs, based upon their structures and modes of delivery of therapeutics drugs. Lastly, we briefly discuss current limitations and future trends in the field of controlled drug delivery using microfluidic platforms.

1.2 Microfabrication techniques

Currently, there are a variety of techniques to fabricate these microsystems, including micromilling, micromachining, photolithography, etching, deposition, mold replication, laser

ablation, and assembly [10, 23-26]. In general, there are basically four processes to fabricate these microsystems, involving patterning, deposition, etching, and bonding [23]. Particularly, in microfabrication techniques, patterning is the fundamental process, which is applied to transfer the designed sketches of each component, like microchannels, onto a chip substrate such as silicon, glass, metals, and polymers [24, 27]. Photolithography and soft lithography have been widely used for patterning by transferring a pattern from a photomask onto a photoresist layer under the exposure to ultraviolet illumination [21, 24, 28, 29]. In addition, deposition of thin films is another crucial procedure, in which thin films with the thickness of micrometers are deposited usually via the physical deposition or chemical deposition or grown on a substrate. Evaporation, sputtering and electroplating are commonly used as deposition techniques for metal substrates [23]. Besides, etching methods such as isotropic and anisotropic etching are applied to remove materials selectively to create different types of features for defined patterns, with a complementary set of materials and etchants [16]. Most structures can be displayed after the sequential etching processes. Moreover, in many situations, there is a need to form a closed system. Therefore, two or even more substrates are required to be bonded together reversibly or irreversibly via various bonding processes, such as thermal bonding, anodic bonding, and photopolymer adhesives [30-34]. Since microfabrication is not the focus of this review article, more detailed information regarding microfabrication techniques can be found from these review articles and books [10, 35, 36].

2. Drug carrier-free microfluidic systems for controlled drug delivery

Microfluidic platforms have been increasingly applied for controlled drug delivery, either through the direct drug carrier-free delivery, or the integration of drug carriers on a chip [21]. Drug carrier-free microfluidic systems can be separated into two categories, namely simple micro-reservoir-based devices and highly integrated microfluidic LOC devices, with tremendous interest in implantable devices [16, 23, 25, 37].

2.1. Micro-reservoir systems

Micro-reservoir systems consisting of one or more drug reservoirs are utilized for temporary storage of drugs and have been applied to provide well-controlled platforms for carrier-free drugs loading and delivery at the microscale [38, 39]. Micro-reservoir systems which are fabricated via the microfabrication technology provide more precise control over drug delivery rates and allow physicians to actively start, modify, and stop drug release at desired locations in an interactive format [40]. Micro-reservoir systems also have the capacity to accommodate various delivery schemes, such as zero order, pulsatile, and on-demand dosing, compared with conventional burst release delivery systems [41-44]. Moreover, the use of micro-reservoirs in drug delivery, whether external to the body or implanted, has shown increased drug stability and prolonged delivery time [41]. Recently, the development of micro-reservoir-based systems for controlled drug delivery shows potential for difficult-to-treat medical applications (e.g., ocular diseases) [40, 45, 46].

Current drug delivery strategies in drug carrier-free micro-reservoir systems can be categorized into two main modes based on different actuation mechanisms: the passive mode

and the active mode. Stable and prolong drug release profiles can be achieved in the passive mode, while the release time and rates can be precisely and promptly controlled in the active mode [47-49].

In the passive mode, drugs are released slowly via the osmotic potential, diffusive transport, concentration gradients, or in response to other external environmental stimuli [40, 50]. The passive mode is applied for drug delivery when the release rate is decided in advance, and usually used in self-regulated drug delivery systems [51].

For instance, Adrus and Ulbricht fabricated a micro-reservoir system within a confined support membrane as “sieving networks” to delivery dextrans by using a temperature-responsive poly(N-isopropylacrylamide) (PNIPAAm) hydrogel, with the diameter between 200 to 5000 nm. The hydrogel was synthesized via photoinitiated *in situ* copolymerization through grafting of linear PNIPAAm chains as pre-modification steps (Fig. 1 (A)). Specifically, the linear polymer chains were grafted to the surface of the support membrane via pre-adsorption of a photoinitiator during UV exposure. Desired transport properties of dextrans were achieved via identifying suitable filling conditions, resulting in a tunable size-selectivity delivery mechanism. Stable drug delivery can also be obtained with higher selectivity under diffusive than under convective flow conditions. When temperature increased up to 32 °C, the flux increased and rejection decreased significantly, resulting in a reversible microfiltration behavior. This temperature-responsive strategy showed broader implications on the passively controlled microfluidic systems for drug delivery [52]. Barash *et al.* developed another passively controlled drug delivery system for therapeutic proteins, which was based on an *in situ* cross-linking hybrid hydrogel combining polysaccharide hydrogels and gelatin [53]. The hybrid hydrogel was formed by injecting two compositions into a rubber mold sandwiched between two glass slides, with the whole diameter of 1.2 cm and the thickness of 3.5 mm. The addition of gelatin made the hydrogels less porous, thus contributing to a prolonged release process of proteins for more than 3 weeks. Moreover, bioactivity studies of proteins during the releasing process were conducted and the results showed high activity (>70%) maintained throughout the releasing process. This system consisted of the microporous structure as depots or micro-reservoirs for the local or systemic release of proteins, in which the protein release was tuned by varying the initial polysaccharide composition. The system was easy to fabricate and handle, where therapeutic proteins could be delivered via minimally invasive methods.

Similarly, Spieth *et al.* proposed another micro-reservoir-based implantable micropump for passive drug delivery [54]. Each micro-reservoir was preloaded with 0.25 μL of drug solutions before implantation, and the drug was displaced from the reservoirs due to local and irreversible thermal expansion by short heating pulses applied to a polydimethylsiloxane (PDMS) layer containing Expancel microspheres. While implanted, the system released drugs to neural tissues by diffusion, in which 0.06 μL of a drug solution could be released within the first three days after implantation. Such a system was proved to be advantageous for behavioral experiments of small animals in neuroscience, yet further improvement could be made, such as increasing the long-term stability and replacing the micropump with wireless control. In general, passive controlled micro-reservoir devices are usually less complex and much easier to fabricate, in which no external power is needed. However, drug

release in passive micro-reservoir systems demonstrates limited control during delivery processes and is susceptible to environmental stimuli, such as temperature, pH, biological agents, ionic strength, and drug degradation rates [55].

In the active mode, drugs can be released at desired time and release rates from a pre-pressurized reservoir, either via mechanical, electrochemical and laser means, thermal, or magnetic actuation [38]. Generally, microelectromechanical technology has been commonly used in the fabrication of the active micro-reservoir systems, which provides great potential to develop drug delivery devices with precise electronic control of drug release, especially for implantable devices [56-58]. Particularly, actuators [59] and active valves [60] that are controlled using electrochemical and electrothermal methods are commonly employed for the precise dose release of stored drugs inside each reservoir [58, 61]. For instance, Song *et al.* reported an implantable microelectromechanical system (MEMS)-based device, which was actively controlled for the *in vitro* programmed delivery of doxorubicin [59]. This device, containing a micro-reservoir, a cannula layer, and a flexible membrane, was fabricated and sealed by PDMS and silicon with high biocompatibility. The drug release was electrochemically actuated through a diaphragm membrane. Individualized disease treatment schedules were programmed and studied by delivering doxorubicin to two pancreatic cancer cell line cultures. Colony growths turned out to be inhibited for both cell lines via the MEMS drug delivery strategy. In comparison with other MEMS devices used for *in vitro*/*in vivo* cancer treatment, the presented device enabled a relatively higher dosage of drugs (one dose of 100 μL) with good flexibility. A long-term treatment (up to seven days) was achieved by using this device, confirming the reliability of the system without the aid of replantation.

Alternatively, another MEMS-based controlled drug delivery device was proposed by Zhuang *et al.* which was actuated by a piston and applied for drug release in the alimentary canal [60]. The device was fabricated with a length of 30.0 mm and an external diameter of 10.6 mm, involving four components: a time module, a driving unit, a microfluidic chamber for drug reservoir, and a power supply, as shown in Fig. 1 (B-1). All components were integrated to form a swallowable capsule, which had an interface to set the timing parameter and an indicator signal to monitor the working state. Once the system was powered on, the desired dose of the fluid drug (up to 0.5 mL) was thus released from the reservoir through a one-way valve activated by a piston (Fig. 1 (B-2)). The proposed micro-reservoir system was further tested both *in vitro* and *in vivo*. As a proof-of-concept, this device was claimed to be superior in the accuracy of drug release time and turned out to be unaffected by digestive tract liquid, though the presented device could be further miniaturized.

Recently, some important improvement of actively controlled micro-reservoir drug delivery systems has emerged to apply wireless actuation strategy. However, the usage of the external power, especially the wired connection of electrical circuitry, causes complexities and inconvenience for drug release [40, 62, 63]. Farra *et al.* developed an implantable MicroCHIPS® device which can be triggered wirelessly. This device was fabricated using a biodegradable polymer containing lyophilized proteins and small molecular compounds and could be used to activate individually addressable reservoirs which held 300 nL of the drug, human parathyroid hormone fragment (1-34) [PTH(1-34)], through a thermal mechanism.

The drug dosing can be terminated without the aid of device extraction. This MicroCHIPS® device has been further used for successful human clinical trials of subcutaneous delivery of an anabolic agent for the treatment of osteoporosis [64]. Similarly, Rahimi and Takahata developed another implantable micro-reservoir drug delivery device which was wirelessly controlled by radiofrequency magnetic fields [65]. This device was fabricated with thermos-responsive hydrogel microvalves which could be activated by a specific resonant frequency. Therefore, the model drug (fluorescein) was released from reservoirs at the desired rate by tuning the frequency of the magnetic field and showed no detectable leak for 12 hours.

In addition, Huang *et al.* proposed another wirelessly controlled drug delivery system using electrolysis [66]. The reservoirs were fabricated and sealed using PDMS through soft lithography, and each reservoir was 210 μm in length and 110 μm in width. Wireless components including a receiver, microcontrol unit, regulator, clock divider, and power-on reset were integrated for remote drug activation with the total size of 2.48 mm^2. The printed circuit board (PCB) was also integrated on the chip. Electrolysis was applied to generate microbubbles with the power of 7.57 mW to provide the force to open the reservoirs, thus releasing drugs. *In vivo* studies were conducted by delivering a model drug, a fluorescent dye (Rhodamine B). Fast response was achieved after the drug was released, and only 1.5 s was needed to open the reservoir after the opening command was given to the device. This approach provided a novel method to introduce the wireless control by using electrolysis and further broadened its biomedical applications. Another wireless implantable chip was presented by Fong *et al.*, in which a nitinol-based pump was integrated for radio-controlled local drug delivery [63]. This device was fabricated with a polyimide casing (10 × 10 × 2 mm^3), and consisted of a drug reservoir with the volume of 76 μL, a positive displacement pump, and check valves created by micromachining Parylene C. Pumping in the device was achieved by a wireless shape-memory alloy (SMA) actuator, which was based on a biocompatible nitinol, serving as a frequency-sensitive heater. The chip was designed to have a rectangular spiral-coil shape with an integrated capacitor to form an inductor-capacitor (LC) tank, and the working principle is illustrated in Fig. 1(C). The stress layers of the compressive SiO_2 film were patterned on the nitinol spiral coil to fix the capacitor side on the substrate. The resonant radio-frequency (RF) nitinol actuator was applied for wireless control by tuning the radiation of the RF electromagnetic field, through which enough force was produced to pump the drug-filled Parylene chamber, thus releasing the drug with a single release volume of 219 nL. This device was further used for anabolic osteoporosis treatment, and demonstrated good drug- loading and delivery performance for up to 5 months without refilling, with an output power of 1.1 W. The frequency-sensitive wireless control principle provided promising potential to integrate multiple actuators directly for the delivery of multiple drugs from a single chip, whereas the device design could be optimized to improve the performance of the wireless actuator in force as well as the speed.

Along with the integration of wireless actuation, there has been some other improvement on actively controlled devices recently, in order to meet the requirements of different kinds of drugs, such as developing multi-reservoir microdevices, and the use of refillable drug reservoirs [37, 67-70]. By developing multi-reservoir devices, the consequences of a reservoir loading failure can be minimized, and the dosing from each reservoir can be controlled simply and individually at its desired release rate without metering by actuators or

valves [68, 69]. The development of refillable micro-reservoirs can reduce the dependency on a large reservoir size, thus increasing the drug loading volume as well as reducing the sizes of whole devices. However, there are some issues while using refillable micro-reservoirs drug delivery systems, involving running risks to the patients when the devices were implanted to a fragile and sensitive part of the body like eye tissues, and difficulties to avoid the overfilling of the reservoir due to the lack of filling indicators [71-76]. Overall, actively controlled micro-reservoir drug delivery systems demonstrated to be advantageous over the passively controlled counterparts at the release time, rates, and real-time adjustment, especially after implantation. However, the complexities of the design and fabrication and inconveniences for the connection between actuation powers and drug release sections on actively controlled devices restricted their broad applications [77, 78].

2.2. Highly integrated drug carrier-free microfluidic lab-on-a-chip devices

Other than micro-reservoir devices, highly integrated drug carrier-free microfluidic lab-on-a-chip (LOC) devices, which integrates more components than micro-reservoirs have also been applied in controlled drug delivery systems. In comparison with micro-reservoir devices, these devices usually consist of substrates, micro-reservoirs, microchannels or microcapillaries, and micro-valves or actuators [16, 22, 23, 25]. The fabrication procedures for these devices are more complicated and require intensive integrations as compared to the fabrication of micro-reservoir systems.

Similar to micro-reservoir systems, highly integrated microfluidic LOC devices can also be categorized into the passive mode and the active mode [23]. In the passive mode, osmotic potentials, diffusive transports, and concentration gradients have been widely applied in microfluidic LOC devices, where the release profiles involving the dosage and rates can be simply modulated by changing the geometries of micro-channels [16, 25]. For example, Lee *et al.* proposed an implantable microfluidic LOC drug delivery device for releasing bupivacaine hydrochloride (BHCl) at a constant rate [79]. The device was constructed by using 85/15 poly (L-lactide-co-glycolide) and contained a drug reservoir (80 μm in depth) and two microchannels (20 μm in width × 20 μm in depth), which were finally bonded via a thermal bonding process. Furthermore, a co-delivery profile of acidic additives was applied to minimize the issue of BHCl precipitation. Cumulative release profiles of the devices with BHCl and other acidic additives were investigated *in vitro* by varying different geometric parameters. The amount of drug release was measured by the specific absorption of UV light at 262 nm. The release rate via diffusion was demonstrated to follow the Fick's law, thus forming a zero-order drug delivery profile for a week without the initial burst. Lee *et al.* developed another implantable drug-delivery microchip for controlled delivery of diclofenac sodium (DS). The microchip was made of poly(methyl methacrylate) (PMMA), consisting of a pair of microchannels and micro-wells [80]. A water-soluble polymer, polyethylene glycol (PEG), was used to fill the microchannels and worked as a drug diffusion barrier. The release rates varied according to the channel dimensions. The cross-sectional areas and lengths of micro-channels were optimized to modulate the drug release profile. As a result, this microchip with micro-channels exhibited almost zero-order drug release for 31 days (R^2 > 0.996) after the immediate release onset on day 0.5. DS could be released in a sustained manner with a minimized initial burst. After implantation in living rats, the microchip

showed good biocompatibility and the released drug in the blood maintained at 148 ng/mL-225 ng/mL for the first 23 days.

Alternatively, another passive implantable ocular drug delivery device was fabricated using PDMS by Marsh *et al.,* which consisted of microchannels embedded between cover layers with a drug reservoir [81]. Six different microchannel configurations were designed (within a range of 1.5 ~ 8.0 mm in length, 5 ~ 100 μm in depth, and 50 ~ 500 μm in width), and analyzed for their diffusion characteristics. The obtained result showed that the delivery of the Fluocinolone Acetonide drug was driven only by the concentration gradient. Two devices were finally selected to meet the diffusion rate specifications (less than 0.07 nL/min) for the ocular drug delivery, which produced a constant delivery rate, and was favorable for the eye disease treatment. Additionally, Ferrati *et al.* developed another passively controlled drug delivery on another implantable LOC device with nanochannels as small as 2.5 nm. These nanochannels controlled the release of drugs by physical-electrostatic confinement, resulting in constant drug diffusion, as shown in Fig. 2(A) [82]. By varying the size of nanochannels, sustained and constant plasma levels of various drugs such as leuprolide, letrozole, octreotide, and human growth hormone were delivered at clinically relevant doses. This device was demonstrated to maintain sustaining target doses for up to 70 days after its implantation. Further validation was achieved by introducing a PhoA pathway inhibitor on the drug delivery system to prevent chronic rejection of cardiac allografts in rats. This platform has the potential for long-term treatment, especially in chronic conditions.

In the active mode, various controllers or actuators have been integrated on microfluidic LOC devices for drug delivery, in which drug release was actuated and controlled either manually by applying an external power, or wirelessly by using a magnetic field. Lee *et al.* presented a microfluidic-based device to generate on-demand combinatorial dilutions of all input samples in the range of a 3D simplexcentroid [83]. The combinatorial device was designed based on a microfluidic network which allowed adjusting the mixing ratios and desirable concentrations of samples. This combinatorial dilution module could generate a full set of seven combinations of the three drugs (Mitomycin C, Doxorubicin, and 5-FU) while the diluted samples flowed through the device. The device was also integrated with an initial PDMS concentration control module involving a single common channel to dilute samples independently in response to variable input flows. Computational simulations were performed to investigate the performance of the initial concentration controller. As a proof-of-concept, this integrated device was applied to perform a simple combinatorial cytotoxicity test using three drugs on MCF-7 cancer cells. Another microfluidic LOC platform was proposed by Nagai *et al.* for controlled transscleral co-delivery of two drugs, edaravone (EDV) and unoprostone (UNO), to the retina in rats in the active mode [84]. This LOC device, as shown in Fig. 2(B), was integrated with a controlled-release cover and drug formulations. The drug formulations and the cover were fabricated based on the photopolymerized tri(ethyleneglycol)dimethacrylate (TEGDM) and poly(ethyleneglycol)dimethacrylate (PEGDM). The drug release of both EDV and UNO could be controlled at independent release rates via the transscleral route. The active release of both drugs was achieved by changing the ratio of PEGDM/TEGDM in the formulations and its cover. This system provided better synergistic retinal neuroprotection against light

injury in rats, compared with single-drug-loaded devices, and thus a safer and more bioavailable therapeutic method than intravitreal injections for retinal disease treatment.

Similarly, Pirmoradi *et al.* developed a magnetically controlled MEMS device for on-demand release of an antiproliferative drug, docetaxel (DTX) [67]. The LOC device consisted of a drug-loaded micro-reservoir (6 mm × 550 μm) which was sealed by an elastic magnetic PDMS membrane (6 mm × 40 μm), and a laser-drilled aperture (~100 × 100 μm). By applying a magnetic field, the drug solution was released due to the deformation of the magnetic PDMS membrane. Controlled DTX release at a rate of 171 ± 16.7 ng per actuation interval was achieved for 35 days under the 255- mT magnetic fields, in which the background leakage of drug solutions through the aperture could be negligible. Moreover, the biological activity of the released drug was investigated by studying cell apoptosis of two cell lines, Human umbilical vein endothelial cells and PC3 (prostate cancer) cells. Reproducible release rates were achieved and the full pharmacological efficacy of drugs were maintained within the device for more than two months. Although this device was at the proof-of-concept stage, it provided a promising platform for drug delivery in nanomolar concentrations, especially for hydrophobic drugs. More recently, another pressure-driven drug release study was performed on an implantable microfluidic LOC device based on induction heating by Jo *et al.* [85]. The delivery device consisted of a drug reservoir, a microchannel, and an actuator chamber, all of which were integrated on a semicircular copper disc (5 mm × 6 mm × 100 μm) with a thermally conductive tape in between. Nitrogen gas was generated by induction heating of azobisisobutyronitrile to act as the driving force, and thus the entire drug solution (28 μL) was driven out of reservoirs and released through micro-channels at the rate of 6 μL/s under the magnetic intensity of 160 μT. After implantation in the subcutaneous skin layer of a mouse, a highly concentrated calcein solution as a model drug was completely released from the device under the wireless actuation in 5 s, implying that more biological and medical applications could be achieved with this wireless actuating device.

In addition to these aforementioned microfluidic LOC devices for active drug delivery, there are also some other LOC devices focusing on the integration of microelectrodes to facilitate controlled drug delivery to research animals, humans, and brain-machine interfaces [86]. Those integrated microelectrodes serve different functions such as microheaters [54], catalysts [37], or microprobes [87]. For example, Spieth and his colleagues developed a *NeuroMedicator* device for behavioral studies in rodents and they further improved this device by integrating the wireless control to create a miniaturized electrodes-based drug delivery system using PMMA [54]. This compact device (20 × 17.5 ×5 mm^3) integrated with a microheater was composed of a microelectrodes-based PCB, individual liquid reservoirs with a thermally expandable layer for actuation, two silicon microprobes, and fluidic microchannels. All components were implemented into a cyclic olefin polymer plate and sealed by an elastic thermoplastic elastomer membrane. After drug loading, the expandable material under the reservoirs was locally heated and became inflated by the microheater, which was controlled and pre-programmed via the wireless microcontroller, allowing the delivery of drug solutions with the volume of 0.3 μL per reservoir. The *Neuromedicator* as a single wireless headstage was loaded with the NMDA receptor antagonist 3-((R)-2-Carboxypiperazin-4-yl)- propyl-1-phosphonic acid, and finally implanted into the medial

prefrontal cortex of a rat to perform a behavioral test of visual attention and impulsivity (the 5-choice serial reaction time task, 5-CSRTT). As a result, both electrophysiological recording and controlled drug delivery were successfully accomplished on this highly integrated device [48]. Similarly, a refillable and implantable micropump system integrated with a microelectrode-based actuator was developed by Gensler *et al.*, and for the first time applied for controlled drug delivery in small animals (e.g. mice) [37]. This device fabricated on the biocompatible silicone rubber included a drug reservoir, a refill port, a catheter, a highly integrated electrolysis actuator, and a check valve to ensure safe dosing. The bellows electrolysis actuator was constructed with a pair of interdigitated platinum electrodes and a bellows filled with electrolytes, possessing both ON and OFF states. When the electrolysis actuator was set to ON, hydrogen and oxygen gasses were generated by the electrolysis reaction, serving as the driving force to allow the fluid surrounding the bellows to flow out of the reservoir to the desired site. Inversely, the platinum microelectrodes acted as a catalyst to recombine water when at the OFF state. Therefore, the release rate of the drug could be adjusted to achieve the desired delivery regimen. The device was further implanted in mice for anti-cancer drug delivery, showing potential for not only drug delivery, but also highly flexible pharmaceutical studies in research animals.

Alternatively, Altuna *et al.* designed another microelectrode-based microfluidic device with multiple fluidic channels for simultaneous depth recording and drug delivery using the polymer SU-8 as the structural material [87]. The electrodes were employed to obtain the simultaneous recordings of neuronal activities at the microscale resolution via cyclic voltammetry. In addition, the tetrode-and linear-like electrode pattern was combined with both single and double fluidic microchannels, which enabled the independent drug delivery. The device acting as an encapsulated microprobe was capable of recording detailed spatiotemporal features of local field potentials and single-cell activities at the high resolution. Moreover, drug delivery in the brain was achieved with high spatial and temporal precision through *in vivo* studies of an anesthetized rat using a fluorescent vital dextran, Texas Red, as a model drug. The designed device was demonstrated to allow simultaneous monitoring of brain activities and drug delivery precisely in a range from tens of nanoliters to a few microliters.

3. Integration of Drug Carriers in Microfluidic Platforms

Drug carriers are defined as the substances which are incorporated to improve the delivery and the effectiveness of drugs [88-90]. A wide variety of drug carriers have been studied and employed in controlled drug delivery with some significant features such as the precise targeting ability, the accurate release of drugs, and the improved pharmacokinetic and biodistribution characteristics of drugs, and so on. Microfluidic platforms offer great opportunities especially for production and screening of drug carriers for controlled drug delivery [91]. The properties of the synthesized drug carriers using microfluidic platforms can be effectively and reproducibly modified at high throughput and low cost since the geometries and flow rates of the microfluidic devices can be easily adjusted. In this section, most widely used drug carries integrated into microfluidic platforms are categorized into three major types: microcapsules, nanoemulsions, and nanoparticles, and the synthetic process and applications of each type in controlled drug delivery are elaborated, as follows.

The main materials, the size, synthetic methods, drugs, and drug targets/applications of different drug carriers integrated into microfluidic platforms are summarized in Table 1.

3.1. Microcapsules

With a pore size of a few micrometers, excellent properties of biocompatibility and biodegradability, and capability of targeted or programmed drug release, microcapsules are very attractive drug carriers for controlled drug delivery [92]. The conventional approaches (e.g. the bulk layer-by-layer technique) for manufacturing microcapsules have the problem of low encapsulation efficiency because of the post-fabrication loading [93]. In addition, the functions and applications of the microcapsules are often restricted by lack of monodispersity, material stability, and diversity. The droplet-based microfluidic double emulsions, or in other words “emulsions of emulsions” or “droplets-in-droplets” (oil-water-oil or water-oil-water), are complex systems that the dispersed droplets contain one or more types of smaller dispersed droplets themselves. It provides a powerful tool with flexibility and reliability for manufacturing complex and uniform microcapsules with desired properties by precise control over the size distribution and scale-up possibility [94] and demonstrates enormous potential for drug carrier synthesis and controlled release of encapsulated actives [95, 96].

Glucose and temperature-responsive microcapsules have demonstrated promising applications for various biomedical applications including controlled drug (e.g. insulin) release and biomolecular sensing [97, 98]. However, the monodispersity of microcapsules as a critical factor for the precise loading control and the release kinetics of encapsulated substances is still a challenge [99], which affects the potential applications of glucose and temperature-responsive microcapsules. A microfluidic double-emulsion approach was developed to synthesize monodisperse microcapsules for glucose response at the physiological temperature, demonstrating a promising self-regulated drug delivery model for diabetes and cancer therapy [99]. In the polymer hydrogel shell of the synthesized microcapsules, the temperature-responsive poly(N-isopropylacrylamide) network, the glucose-responsive 3-aminophenylboronic acid moiety, and the acrylic acid moiety were used for actuation, glucose response, and adjusting the volume phase transition temperature of the shell, respectively. The prepared microcapsules demonstrated reversible and repeated swelling and shrinking response to glucose concertation changes within the physiological blood glucose level (0.4-4.5 g/L) at the physiological temperature of 37 °C. The potential application of the glucose-responsive microcapsules for controlled drug release was successfully demonstrated by using model drugs, rhodamine B and fluorescein-isothiocyanate-labeled insulin.

Controlled drug release of pH-responsive microcapsules has been achieved by using microfluidic double emulsions. The biocompatible pH-responsive polymer shells of the produced microcapsules could dissolve and degrade at a desired trigger pH, and release the active drug molecules or chemicals encapsulated in microcapsules at a prescribed rate. This goal was achieved by fabricating hybrid solid shells composed of a precisely controlled mixture of a pH-responsive polymer and another pH-unresponsive polymer with varying proportions on a glass capillary microfluidic device, and by carefully controlling the

thickness of the shells [100]. The poly(*N, N*-dimethylaminoethyl methacrylate) (PDM) with both biocompatibility and cationic pH-responsive properties was innovatively used for the preparation of pH-responsive microcapsules [101]. Because of the protonation of -$N(CH_3)_2$ groups in the cross-linked PDM networks, the prepared microcapsule swelled at low pH. High pH-sensitivity of the microcapsules was achieved at high pH and low cross-linking density during the synthesis process. The pH-responsive microcapsules can be used as carriers for controlled drug delivery for tumor therapy. Recently, dual pH-responsive microcapsules were presented as a remarkable candidate for dual-drug carriers [102]. Generated by combining both electrostatic droplets and microfluidic droplets, the microcapsules were composed of a monodisperse core (alginate) and shell (chitosan) structure with dual pH-responsive drug release functions in both acidic and alkaline environments. Two model drugs, ampicillin and diclofenac, respectively loaded in the chitosan shell and the monodisperse were used for the drug delivery study. Compare to the respective core or shell particles, the core-shell structure microcapsules exhibited better drug release efficiency than individual core or shell particles and demonstrated positive cell viability of about 80% in a biocompatibility test.

Calcium-alginate microcapsules with large cavities have been efficiently synthesized using microfluidic approaches to encapsulate drugs or nutrients such as therapeutic proteins for drug delivery and pharmaceutical applications. For example, by using gradient-droplet-based microfluidics, different sizes of monodisperse calcium-alginate microcapsules (diameters: 60-105 μm) with different concentrations of a model protein (bovine serum albumin, BSA) were simultaneously generated for drug release [103]. The preparation of calcium-alginate microcapsules was also reported via internal gelation in microfluidic double emulsions. The internal gelation was induced by crosslinking alginate polymers with Ca^{2+} ions initiated by UV exposure of the photoacid generator on $CaCO_3$ particles for double emulsions. Proteins such as BSA can be encapsulated after the preparation of microcapsules, providing an alternative route for loading active drugs or nutrients into microcapsule carriers without inactivation during the microcapsule preparation [104]. This microfluidic double emulsion approach was demonstrated as a powerful technique to develop microcapsule formulations of therapeutic proteins. With an 84% high encapsulation efficiency of proteins (i.e. BSA), the microcapsules were stable up to 4 weeks and released 30% of their content within 168 h [105].

Recently, a novel droplet-based microfluidic device with functions of both droplet merging and droplet storage for controlled drug release from microcapsules was reported for studying drug effects on specific cells [106]. The microcapsules were produced by using a simple layer-by-layer nanoassembly process with a drug model $MnCO_3$ encapsulated inside. The merging function unit and the storage function chambers were used for dynamically adding the control solution into the droplets and for collecting droplets that contained drugs within the microcapsules, respectively. The controlled release of drugs from specific microcapsules in the storage chambers could be monitored for an extended period of time. As a controlled drug release microfluidic platform, this system is especially useful for single cell analysis by studying the drug effects on specific cells in a controlled manner.

3.2. Nanoemulsions

Nanoemulsions refer to multiphase colloidal dispersion, which contains small particles or droplets with the average diameters ranging from 20 to 200 nm (transparent), or up to 500 nm (milky appearance) [107-110]. Since the preparation of first nanoemulsions in the 1940s, they have been widely used for drug delivery. Based on their compositions, there are three types of nanoemulsions: oil-in-water, water-in-oil, and bicontinuous. In all three types of nanoemulsions, the interface is stabilized by various surfactants and/or co-surfactants [111]. There are abundant merits for nanoemulsion-based delivery systems over other dosage forms, such as high surface area, unique transparent appearance, tunable rheology, good stability and bioavailability, and rapid and efficient penetration of the drug moiety [111-118]. Nanoemulsion is currently employed as an important drug carrier in the development of drug formulations for providing pharmaceutically accepted ingredients [112, 119-121].

There are currently several kinds of techniques for the preparation of nanoemulsions, namely, ultrasonication, the high-pressure valve homogenization, and the microfluidization technology [111, 122-124]. The microfluidization technology relies on microfluidic platforms, and the general principle of microfluidization involves the high-pressure streams (aqueous phase and oil phase) moving towards to the interaction chamber or an impingement area, thus causing a high shearing action and fine emulsions within the submicron range [124]. Microfluidization technology was reported to achieve the smallest particle sizes with less heat produced, thus resulting in a more efficient nanoemulsification process under the same homogenization conditions, compared to other nanoemulsion methods [125, 126]. In this section, we focus on recent advances of nanoemulsions as drug carriers for controlled drug delivery using microfluidic devices (Table 1) [118, 127].

Nanoemulsions have been applied to enhance numerous properties of drug molecules, including the stability, solubility, bioaccessibility, and bioavailability [109, 112, 119, 127-131]. The stable triglyceride nanoemulsions with the size ranging from 20 to 50 nm were developed for the first time by Zhigaltsev *et al.* for loading doxorubicin stably and efficiently [132]. The nanoemulsions were produced on a microfluidic mixing device, as illustrated in Fig. 3 (A), which was composed of a 200 μm wide and 79 μm high mixing channels fabricated by soft lithography. Lipids in ethanol and an aqueous buffer were pumped into two inlets respectively using a syringe pump, leading to the rapid mixing of the injected streams using a staggered herringbone micromixer (SHM). Doxorubicin hydrochloride was dissolved in saline and added to the ammonium sulfate-containing lipid nanoparticles (LNP), and the fluorescence intensities were measured to determine the loading efficiencies by varying the drug-to-lipid molar ratios. Approximately 100% of loading efficiencies were observed under the optimized drug-to-lipid ratios up to 0.2 (mol/mol). This method allowed the robust “bottom-up” synthesis of nanoemulsions with well-defined size.

Similarly, another nanoemulsions-based system was proposed by Zhong *et al.*, to study the effect of oils on β-Carotene (BC) bioaccessibility [133]. In this approach, six dietary lipids (corn oil, canola oil, olive oil, palm oil, coconut oil, and MCTs) were selected to produce BC carriers, and all six BC nanoemulsions were prepared by microfluidization. The positive

and linear correlation was observed between BC release and bile salts concentrations. In addition, the usage of pancreatin facilitated BC's release in simulated digestion. The relative bioaccessibility of BC in the nanoemulsion delivery systems was significantly improved to 70.9% as compared to 4.6% in the control (bulk oil). This nanoemulsions-based delivery system turned out to be beneficial to encapsulate and deliver BC as well as other bioactive lipophilic carotenoids in a wide range of commercial products. Chhabra *et al.* demonstrated another nanoemulsion-based system for amlodipine besylate (AB), in which both solubility and oral bioavailability of AB were enhanced [134]. The partition coefficient and the percent dissolution efficiency were correlated to predict the drug release from nanoemulsions to achieve localized delivery of drugs at the target site. It was demonstrated that the *in vitro* release of AB from nanoemulsions was significantly higher ($p < 0.01$) than the marketed tablet formulation. Furthermore, in almost all the tested organs, the uptake of AB from nanoemulsions was significantly higher ($p < 0.05$) than AB suspension, especially in the heart with a drug-targeting index of 44.1%, which also confirmed the high efficacy of nano-sized formulation at therapeutic sites. A relative bioavailability of 475% against AB suspensions was obtained in the pharmacokinetics and biodistribution studies with the optimized radiolabeled formulation in mice; a three-fold increase in the overall residence time further displayed the advantage of nanoemulsions as drug carriers for enhancing both solubility and bioavailability of AB.

Recently, many new nanoemulsion-based drug delivery systems have been explored for imaging guided therapy [135-137] [138] [139]. For example, Gianella *et al.* reported a 50 nm nanoemulsion-based platform for loading hydrophobic materials, which could be applied as a theranostic tool for simultaneous imaging-guided drug delivery in cancer [138]. The oil-in-water nanoemulsions were produced from soybean oil, PEGylated lipids, and oleic acid-coated iron oxide (FeO) nanocrystals for magnetic resonance imaging (MRI). The fluorescent dye Cy7 was introduced for near-infrared fluorescence (NIRF) imaging, while the hydrophobic glucocorticoid prednisolone acetate valerate (PAV) was applied for therapeutic purposes. When subcutaneous tumors were palpable, the nanoemulsions were controlled at a dose of 30 mg of FeO/kg and 10 mg of PAV/kg. MRI and NIRF imaging showed significant nanoparticle accumulation in the tumors, and tumor growth profiles revealed a potent inhibitory effect in all of the PAV nanoemulsion-treated animals, in comparison with the control samples treated with nanoemulsions, the free drug, and saline, respectively. This complex nanoemulsion-based system loaded with PAV, iron oxide nanocrystals, and Cy7 represented a flexible, versatile, and unique multifunctional theranostic platform for imaging guided therapy of cancer. Similarly, Hanlon *et al.* reported another theranostic platform for imaging-guided drug delivery and therapy.[139] The nanoemulsions with the average size of 180 nm and low polydispersity index (PDI) less than 0.2 were synthesized from perfluoropolyether (PFPE) by microfluidization, with PFPE-tyramide as a ^{19}F MRI tracer. Hydrocarbon oil, surfactants, and a near-infrared (NIR) dye, and a water-insoluble model nonsteroidal anti-inflammatory drug, celecoxib (0.2 mg/mL), were contained in this system. Therefore, with the aid of nanoemulsions, the whole formulation enabled the non-invasive monitoring of drug biodistributions using two imaging modalities, ^{19}F MRI and NIR optical imaging, as shown in Fig. 3 (B). The nanoemulsions

loaded into fetal skin dendritic cells (FSDCs) could remain stable for 30 days at 4 °C, resulting in a promising theranostic system for cancer imagings as well as treatments.

Alternatively, some nanoemulsions can be utilized as new templates for the synthesis of other particles for drug delivery using microfluidics. By using nanoemulsions as templates, Khan *et al.* developed a two-step semi-continuous process for the synthesis of poly(acrylamide) (PAM) Trojan microparticles for the delivery of ketoprofen via two different microfluidic devices [140]. An elongational-flow micromixer was first used to synthesize polymerizable nanoemulsions with the size varying from 98 to 132 nm, which were then emulsified into microdroplets in a co-axial capillary-based microfluidic droplet generator. The nanoemulsion droplets and microdroplets were both polymerized under UV irradiation. The polymerization using poly(ethyl acrylate) shrank the size of nanoemulsions down to 20 to 32 nm. While those microdroplets were lastly hardened into Trojan particles consisting of a crosslinked network of PAM chains. About 35 % of encapsulated ketoprofen was released over 24 h from the Trojan microparticles. These microparticles prepared using nanoemulsions as templates in microfluidic devices can potentially improve delivery of drug-loaded nanoparticles at the desired locations, such as in the gastrointestinal tract.

3.3. Nanoparticles (NPs)

With fine sizes usually between 1 and 100 nm, nanoparticles can be taken up by cells. Moreover, nanoparticles can be simply immobilized with small molecules, nucleic acids, peptides, and proteins to target particular tissues without being excluded by the immune system [141-143]. Therefore, nanoparticles have tremendous potential as drug carriers by loading drug molecules for controlled drug delivery. The recent advances of nanoparticles as drug carriers integrated on microfluidic platforms have been listed in Table 1. Lipid and/or polymer nanoparticles are common nanoparticle-based drug carriers due to their advantages such as biocompatible and biodegradable properties, low toxicity, and high efficacy [144, 145].

3.3.1. On-chip synthesis of nano-sized drug carriers—The unique properties (e.g. optical, thermal, magnetic and electrical properties) of nanoparticles are highly related to their sizes and morphology. However, conventional batch processes by bulk mixing and nanoprecipitation are technically challenging in fabricating monodisperse nanoparticles with a desired size and morphology, which compromises the properties of the produced nanoparticles [146]. Microfluidic systems have opened a new horizon for the development of novel nanoparticles as drug carriers [147, 148]. The rapid and tunable mixing in microfluidics makes it capable for precious control over the synthesis processes of nanoparticles by systematically varying parameters such as flow rates, reagent concentrations and compositions, temperature, and mixture time. Thus, nanoparticles with desirable sizes and morphology can be homogeneously and reproducibly synthesized in a high-throughput and reproducible manner [147]. In this section, we focus on the synthesis of four types of nanoparticle drug carriers using microfluidic platforms, including lipid nanoparticles, polymer nanoparticles, nano-sized polymeric conjugates, and lipid-polymer hybrid nanoparticles.

A) On-chip synthesis of lipid nanoparticles: Nanoparticles in the size range of 10-50 nm can progressively access and accumulate in target tissues in the body such as lymphatics and poorly vascularized tumors. Thus, the synthesis of such nanoparticles is attractive and important for drug delivery [149, 150]. However, producing lipid nanoparticles smaller than 80 nm is challenging due to the lack of effective methods with good scalability and reproducibility [132]. To solve this problem, Zhigaltsev *et al.* [132] reported a millisecond microfluidic mixing approach for the synthesis of two types of limit size (20-50 nm) lipid nanoparticle drug carriers with either polar (aqueous) or nonpolar (triglyceride) cores. In this approach, limit size lipid nanoparticles were synthesized by millisecond mixing of ethanol streams containing dissolved lipids and aqueous streams at high flow rates (> 2 mL/min) to drive a bottom-up synthesis process by the spontaneous assembly. The synthesized limit size lipid nanoparticles could be loaded with doxorubicin and other weak base drugs, indicating potential as ultrasmall lipid nanoparticle drug carriers.

Lipid nanoparticles are regarded as promising carriers of delivering siRNA for therapeutic applications [151]. To figure out the structure of lipid nanoparticles containing siRNA, Leung *et al.* [152] successfully synthesized lipid-siRNA nanoparticles (~15 nm) by employing a similar rapid microfluidic mixing approach to mix cationic lipids in an ethanol solution with siRNA in an aqueous medium, and applied various techniques (i.e. cryo-transmission electron microscopy and molecular modeling, *etc.*) to characterize the structure. It was discovered that a nanostructured electron-dense core was observed in the lipid-siRNA nanoparticles, which helped better understand and construct more sophisticated lipid-siRNA nanoparticles.

B) On-chip synthesis of polymer nanoparticles: Among different polymers, chitosan with three types of reactive functional groups and hydrophilic property is regarded as one of the most promising biopolymers for preparing nanoparticles for pharmaceutical applications thanks to its outstanding biologic properties such as bioactivity, biocompatibility, biodegradability, and the capacity to open tight junctions [153, 154]. However, chitosan is not appropriate for carrying hydrophobic drugs, and it is challenging to achieve monodisperse nanoparticles by using the conventional bulk mixing methods. To address these issues, Majedi *et al.* [155] presented a microfluidic hydrodynamic focusing and self-assembly approach to synthesize monodisperse chitosan-based nanoparticles as hydrophobic drug delivery agents. In this work, the self-assembly synthesis of monodisperse hydrophobically-modified chitosan-based nanoparticles occurred as a consequence of the changes in the physiological pH in a PDMS microfluidic device to provide hydrophobic drug packing. As a result, the synthesized monodisperse chitosan-based nanoparticles were capable of encapsulating hydrophobic anticancer drugs, which provided a sustainable release profile for controlled drug delivery [156]. The synthesized polymer nanoparticles were employed to encapsulate a common anticancer drug, paclitaxel, and compared them with the corresponding bulk synthesized nanoparticles for the *in vitro* investigation of the effectiveness of the microfluidic method-synthesized nanoparticles. It was found that compared to the bulk mixing method-generated nanoparticles, the microfluidic generated nanoparticles exhibited considerably smaller sizes, lower values of the diffusion coefficient, and extended t_{50} (the time of 50% drug release). The results are consistent with the results

reported by using microfluidic generated chitosan-based nanoparticles for a transdermal multidrug (clindamycin phosphate and tretinoin) delivery application, which exhibited a higher thermal stability, minimum inhibitory, and bactericidal concentrations, compared to the bulk mixing method generated nanoparticles as well [157].

Some other polymer nanoparticles have also been synthesized by rapid nanoprecipitation in microfluidic devices [145]. For instance, Liu *et al.* [158] reported a superfast sequential microfluidic nanoprecipitation approach for the synthesis of core/shell structured polymer nanoparticle drugs. The enteric coating polymer, hypromellose acetate succinate, was used to encapsulate two water-soluble anticancer drugs, sorafenib and paclitaxel. Through the superfast (i.e. milliseconds) sequential nanoprecipitation processes, the polymer nanoparticle drugs were stably synthesized in a homogeneous size distribution without using any stabilizers. A high-throughput production rate of ~700 g/day on a single microfluidic device was achieved. Othman *et al.* [159] reported another rapid nanoprecipitation approach for the synthesis of poly(d,l-lactide) polymer nanoparticles that encapsulated paracetamol drugs in a co-flow microfluidic device. The synthesized polymer nanoparticles exhibited a drug encapsulation efficiency of 38.5% and extended the drug release rate in simulated intestinal fluids at pH 7.4.

C) On-chip synthesis of nano-sized polymeric conjugates: Except for polymer nanoparticles, there is another category of polymer-based drug carriers, nano-sized polymeric conjugates, which have been integrated into microfluidic platforms for controlled drug delivery. Nano-sized polymeric conjugate, as a general name for a group of multifunctional systems, usually in the size range of 1 to 200 nm, has been applied to deliver bioactive agents to the desired sites. Unlike polymer nanoparticles, nano-sized polymeric conjugates are generally designed and synthesized by conjugating polymeric carriers and bioactive molecules directly, such as drugs, proteins, and oligonucleotides [160-163]. Nano-sized polymeric conjugates are advantageous over traditional polymeric drug carriers in controlled drug delivery systems, due to low nanotoxicity, adequate drug loading capacity, good aqueous solubility, excellent circulation and bioavailability, and enhanced permeation and retention effects [16, 27, 164-166].

In conventional synthetic methods, the polymeric conjugates, or polymer-drug conjugates are obtained via coupling reactions by the conjugation of drug molecules with hydrophilic polymers. However, multi-step conjugation reactions are often required, which take long reaction time and large consumption of drugs in order to get high drug coupling ratios. To solve these issues, microfluidics has emerged recently as a novel technology to generate polymeric conjugates, especially in nano-size, because of the rapid and accurate operations to deal with conjugation reactions within small volumes [167, 168].

Microfluidic devices have provided an excellent platform to synthesize polymeric drug conjugates for controlled drug delivery, generally via rapid mixing of polymers and drug molecules. An efficient synthetic method to obtain the nano-sized Heparin-folic acid-retinoic acid (HFR) bioconjugates was developed on a microfluidic device by Tran *et al.* [169]. This device was fabricated using perfluoropolyether, consisting of two inlets, one outlet, and a solvent resistant fluoropolymer microfluidic channel (500 μm × 50 μm × 40 cm). The

mixing and a single-step conjugation of unfractionated heparin, folic acid (FA), and aminated retinoic acid (RA) occurred in the microchannel to obtain HFR and the reaction time and rate were precisely controlled by a dual rack syringe pump. The approach demonstrated that well-defined HFR nanoparticles were produced with uniform size distribution in aqueous media, and HFR bioconjugates with high drug coupling ratios could be achieved within several minutes, providing a powerful tool to synthesize advanced polymeric conjugates. Microfluidic mixing techniques have also been explored by Shi *et al.* and Endres *et al.* to develop nano-sized particulate carriers for drug and gene delivery [170, 171]. Nano-suspensions were first prepared from acetone and amphiphilic cationic block copolymers, poly(ethylene glycol) (PEG), poly(ε-caprolactone) (PCL), and poly(ethylene imine) (PEI), via magnetically stirring. The Fluence Microfluidic Tool Kit (Epigem Ltd., Redcar, UK) consisting of a three-way mixing chip was then applied, where cationic NS and nucleic acid (siRNA) were driven and mixed with the aid of syringe-pump drives. The size of siRNA-loaded PEG-PCL-PEI nano-carriers through microfluidic mixing was characterized to be 179 ± 11 nm (PDI = 0.205 ± 0.028), which was smaller than that via classical pipetting (230 ± 97 nm, PDI = 0.353 ± 0.161). Additionally, the size distribution of the complexes on the microfluidic devices was unimodal, whereas two different size distributions were observed in classical pipetting. With uniform surface coating on the nano-sized carrier, less aggregation of RNA was observed through the microfluidic mixing process, thus enhancing RNA protection and transfection performance. The microfluidic complexation strategy provides an easy-to-use, uniform and stable formulation for drug and gene delivery [171].

D) On-chip synthesis of lipid-polymer hybrid nanoparticles: Lipid-polymer hybrid nanoparticles are emerging drug carriers for various medical therapy for cancer, cardiovascular diseases, and tuberculosis in a controlled manner [172]. Recently, three-dimensional monodisperse lipid-polymer hybrid nanoparticles were synthesized by using three-channel pathway and mixing microchannels in a microfluidic device, which accelerated the research and development process of lipid- polymer hybrid nanoparticles as drug carriers for controlled delivery [173]. The structure of the functionalized lipid shells was significant in the biocompatibility and *in vivo* stability of the lipid-polymer hybrid nanoparticles. To examine the structure and the effect on the cell-particle interaction of the lipid shells in nanoparticles, the structurally well-defined lipid-polymer hybrid nanoparticles covered with either a lipid-monolayer-shell as monolayer nanoparticles or lipid-bilayer-shell as bilayer nanoparticles were synthesized on a PDMS microfluidic device [174]. Compared to the bilayer nanoparticles, the monolayer nanoparticles exhibited lower flexibility, resulting in more efficient cellular uptake and thus enhanced anticancer effects. This flexibility-regulated cell-nanoparticle interaction study provides important implications for the design of lipid-polymer hybrid nanoparticle drug carriers.

3.3.2. Integrated nanoparticle drug carrier synthesis and drug delivery testing on a chip—

Microfluidic platforms can integrate both synthesis and optimization of nanoparticle drugs, which could potentially accelerate both the discovery and clinical translation of nanoparticle drugs. For instance, Valencia *et al.* [175] developed such a PDMS microfluidic system for integrated synthesis and screening of targeted nanoparticle drugs for

cancer therapy (see Fig. 4). In this system, numbers of polymeric nanoparticle precursors with varying sizes and surface compositions could be rapidly and reproducibly synthesized, followed by the rapid *in vitro* screening. By using this *in vitro* microfluidic screen approach, the nanoparticle drugs against prostate cancer cells with the low macrophage uptake level were selected. The *in vivo* pharmacokinetic studies demonstrated a 3.5-fold increase in the selected nanoparticle drugs in tumor accumulation in mice than non-targeted nanoparticle drugs.

Current technologies are limited to monitor the nanoparticles entering the treated cells, which is an important factor in developing nanoparticle drugs for anticancer treatment [176]. Microfluidic platforms have exhibited the potential in monitoring and assessing uptake of nanoparticles into target cells. For instance, Zhai *et al.* [177] have recently demonstrated a microfluidic approach of monitoring uptake of nanoparticles into living cells via surface-enhanced Raman spectroscopy. The fabricated beta-cyclodextrin-coated silver nanoparticles (Ag@CD NPs) were surface modified with para-aminothiophenol (p-ATP) and folic acid (FA). The p-ATP acted as the Raman reporter and the FA had a high affinity for folate receptors (FR) that are over-expressed on cancer cells surface. The FR-targeted dihydroartemisinin (DHA) was used as a model drug. The Ag@CD@p-ATP@FA NPs were successfully employed in a well-controlled way to quantitatively assess the number of nanoparticles entering FR-positive living cells and examine the FR-targeted DHA drug effect on cancer cells as well as the interaction between the nanoparticles and cells. Carvalho *et al.* [178] proposed a microfluidic platform for real-time monitoring of the cellular uptake of nanoparticles and tracking the fate of cancer cells. In this study, carboxymethylchitosan/poly(amidoamine) dendrimer nanoparticles were synthesized and labeled with fluorescein-5(6)-isothiocyanate. HeLa, HCT-116 and U87MG cancer cells were 3D dynamically cultured in a microfluidic device in the presence of those nanoparticles, and the subsequent investigation of cell viability and internalization efficiency was performed and compared with the standard 2D static culture. It was found that the dynamically cultured cancer cells with nanoparticles were viable and exhibited higher internalization levels as compared with statically cultured cells. Those studies demonstrated the potential application of the microfluidic-based platform for real-time monitoring and assessment of effects of nanoparticle drug release on cancer cells.

Although the development of specific nanoparticles as nanomedicine is attractive, considering the potential physical damage ability to cancer cells without the drug resistance obstacle in anticancer treatment, it is technically challenging to selectively target the specific nanoparticle drugs to cancer cells [179, 180]. Recently, a proof-of-concept of polymer nanoparticles synthesized via the microfluidic encapsulation for efficiently targeted cancer treatment has been reported [181]. In this work, the Prickly zinc-doped copper oxide (Zn-CuO) nanoparticle (Prickly NP) drug encapsulated in a spermine-modified activated dextran (SpAcDX) pH-responsive polymer with the surface modified with 3-(cyclooctylamine)-2,5,6-trifluoro-4-[(2-hydroxyethyl)sulfonyl] benzenesulfonamide (VD1142) through a polyethylene glycol (PEG) linker, named as Prickly@SpAcDX–PEG–VD1142, were produced in a microfluidic coflow focusing device. The encapsulation of the Prickly NPs was successfully achieved by using the microfluidic nanoprecipitation approach, which prevented the unspecific damaging from Prickly NPs to non-tumor receptor

negative cells. The VD1142 endows the Prickly NPs to specifically target to a transmembrane protein overexpressed in various tumors, carbonic anhydrase IX. The Prickly NPs disintegrate into small pieces intracellularly that could cause severe physical damage to the endoplasmic reticulum and mitochondria of cancer cells, demonstrating effective cancer cell antiproliferative capability.

4. Microneedle-based drug delivery

Transdermal administration is one of the most preferred routes of drug delivery because of the ease of use and convenience. It is minimally invasive and causes less discomfort to patients. It also avoids first pass metabolism and gastrointestinal degradation. It has significant advantages over hypodermic injections that are generally painful, produce medical waste, and pose a risk of disease transmission in underdeveloped countries by the reuse of the needles [182]. In addition, the transdermal system can be self-administered, provide long release periods, and are generally inexpensive.

Although transdermal drug delivery (TDD) had been one of the most innovative drug delivery systems, there are a limited number of transdermal drugs as they are limited to reach the systemic circulation due to the presence of skin which acts as an excellent biological barrier. After the first FDA-approved transdermal system, a three-day patch to deliver scopolamine to treat motion sickness for systemic delivery in 1979, FDA has approved 222 drug formulations (Supplementary Table S1). Skin, which has been considered as an impermeable barrier to exogenous chemicals have been treated with drug formulations upon its disruption by diseases or infections in the modern era. Skin is composed of three layers: 1) stratum corneum (SC) of dead tissues and 10-15 μm in thickness, 2) viable epidermis with living cells and nerves but without blood vessels and 50-100 μm in thickness, and 3) dermis with living cells, nerves, and blood vessels [183]. Macromolecules (molecular weight > 500 Da) may not be successfully administered transdermally. Similarly, hydrophilic drugs (Log P value below 1) are too hydrophilic to penetrate by passive diffusion and hydrophobic drugs (Log P value greater than 3) are so hydrophobic that they get entrapped within intracellular lipids of SC [184]. Because of the presence of SC, transdermal delivery of macromolecular agents such as peptides, DNA, and siRNA along with hydrophilic drugs have been problematic. As SC hinders TDD, different approaches including peptide enhancers, liposomes, ultrasound, thermal ablation, electroporation, laser micro-drilling, and MNs have been used to enhance skin permeability [185, 186].

MNs are minimally invasive devices that penetrate the SC barrier to access the microcirculation of the skin for the delivery of therapeutic drugs through transdermal routes. MNs consist of several micro-projections and a base support and are produced using microfabrication techniques. They are 25 to 2,000 μm in height with different shapes and made of different materials including silicon, metals, and polymers. While puncturing the skin with MNs, needles are long enough to penetrate the dermis but are of a small size to avoid contact with dermal nerves or blood vessels. They only create microscopic transient aqueous pores to enhance the dermal circulation for the drug diffusion [187]. Reversible disruption or by-pass of the SC molecular architecture is required for TDD; MNs can painlessly penetrate the SC barrier without drawing blood and have the potential to

overcome the aforementioned problems. MNs can be categorized into solid (SMNs), porous (PMNs), hollow (HMNs), coated (CMNs), and dissolvable microneedles (DMNs) based upon their structures, properties, and mechanisms of delivery of therapeutic drugs. Their specific fabrication methods, delivered drugs, delivery routes, applications, and study types are summarized in Table 2.

Varieties of factors influence the successful transdermal delivery of therapeutic drugs through MNs. Different factors including materials, the diameter of MNs, and the force applied affect the penetration of the skin. The choice of the material affects the mechanical strength while the tip sharpness can affect the force needed to insert the MN. Before using MNs in clinical practice a finer understanding of skin penetration by MNs is needed. The force at insertion linearly increased with the tip diameter, which shows that sharp MNs are required for well-controlled insertion [188]. Computerized tomography scans and finite element analysis showed a linear dependence of the mechanical strength on a number of vertices in polygon base of MNs. Penetration into ex vivo porcine skin revealed greater penetration depth for triangular and square-based MNs [189]. It was found that faster application speed could largely enhance the permeability but also increase the skin damage, while the shorter needle with large tip had insufficient penetration [190].

4.1. Solid Microneedles (SMNs)

SMNs usually used in a ‘poke, detach and diffuse' format can be applied to the skin's surface to physically disrupt SC. The removal of SMNs from the skin creates transient microchannels in SC, after which drug formulations in the form of solutions, gel, cream or transdermal patches can be applied. Drugs permeate through those microchannels to target sites through passive diffusion. Therapeutic drugs are then transported either for the systemic delivery or for a localized effect after skin capillaries take them up. SMNs enhance the transdermal delivery of different molecules that cannot be passed through the skin by passive diffusion alone. SMNs can increase the transdermal permeability of small molecules (up to 100 nm in diameter) by up to 4 folds [191].

SMNs can be fabricated from different materials such as silicon and metals like titanium, nickel, and tantalum [192]. In addition, polymers like photolithographic epoxy, co-polymer of methylvinyl ether and maleic anhydride, polyglycolic acid, and polylactic acid have also been used (Table 2) [193, 194]. Narayanan *et al.* developed SMNs made from silicon for drug delivery [192]. Etching factors and conditions for tetramethylammonium hydroxide were optimized to get SMNs 158 μm in height, 110.5 μm in base width, and 0.40 μm in tip diameter. They also obtained micro-hardness of 44.4 (HRC), which was 52.2 times higher than skin ultimate tensile strength, making insertion through the skin safer and easier.

Drug delivery efficiency can be significantly increased by the use of MN rollers. MN rollers are cylindrical stainless steel MNs that can roll over the surface of the skin to create micropores. Kaur *et al.* investigated stainless steel MN roller-based transdermal delivery of anti-hypersensitive drugs (verapamil hydrochloride and amlodipine besylate) across pigskin [195]. DermaRoller consisted of 540 MNs mounted on a cylindrical surface that could be rolled over the skin (Fig. 5(A-1)). Fig. 5(A-2) shows the side view of the MN roller. Percutaneous penetration of verapamil showed higher cumulative amounts of the drug in

MN-mediated diffusion as compared to passive diffusion (Fig. 5(A-3)). A statistically significant increase in the transdermal flux of verapamil was observed from 8.75 μg/cm^2/h to 49.96 μg/cm^2/h with the MN-roller treated porcine skin.

Similarly, the percutaneous flux of amlodipine besylate increased from 1.5 μg/cm^2/h to 22.39 μg/cm^2/h [195]. In addition, Nguyen *et al.* studied the influence of SMNs on the transdermal delivery of antiepileptic drugs tiagabine hydrochloride and carbamazepine in the porcine skin *in vitro* [196]. 12 h after the application of MN roller, a 6.74-fold increase in the percutaneous penetration of tiagabine hydrochloride from 12.83 ± 6.30 μg/cm^2/h to 86.42 ± 25.66 μg/cm^2/h was observed and was statistically significant. But in the case of carbamazepine, only a 1.38- to 1.39-fold increase in transdermal flux was seen when 20% and 30% ethanol solutions were applied, respectively, which was not statistically significant.

Pre-treatment of the skin surfaces increases the efficiency of drug delivery. For instance, pre-treatment of the mouse skin with SMNs helps the permeation of solid lipid NPs. It was found that transcutaneous immunization with ovalbumin NPs (230 nm) in the mouse skin pre-treated with SMNs induced stronger immune response than subcutaneous injection of the same ovalbumin NPs. Bacterial infection risks associated with MN treatment were similar to the hypodermic injection [197]. Guo *et al.* performed transcutaneous immunization against hepatitis B virus [198]. The pig skin was first poked by a functional microarray (FMA) to increase the permeation. Hepatitis B surface antigen (HBsAg) with cholera toxin B (CTB) as an adjuvant was then delivered by using a hydrogel patch. The use of hydrogel increased the thermostability. *In vitro* studies in the porcine skin and the rat abdominal skin showed better permeation by FMA compared to transcutaneous immunization. *In vivo* immunization in mice showed that FMA induced a more potent immune response (serum IgG titer, IgG2a/IgG1 ratio). They found that CTB adjuvant vaccine induced higher IgG titers compared to the group without CTB. Furthermore, cross-protection is very crucial for influenza vaccine, since regular mismatches occur between the viral vaccine and circulating viruses. Wang *et al.* treated skin with a nonablative fractional laser (as an adjuvant) before applying SMNs and PR8, a model influenza vaccine [199]. Rapid antigen uptake was observed and animals (mice and swine) were fully or partially protected from strains of influenza virus (H1N1, H3N2), while those treated only with SMNs (without the adjuvant) showed severe illness with similar viral challenges. However, animals with SMN treatments did not show skin irritation and lesion like intradermal injections.

SMNs have also been used to deliver peptides and siRNA. MN pretreatment enhances peptide permeation [200]. The permeation rates of peptides were also found to be dependent on the peptide's molecular weight, when studied using four model peptides, Gly–Gln–Pro–Arg (tetrapeptide), Val–Gly–Val–Ala–Pro–Gly (hexapeptide), AC–Glu– Glu–Met–Gln–Arg–Arg–NH_2 (acetyl hexapeptide), and Cys–Tyr–Ile–Gln–Asn–Cys– Pro–Leu–Gly–NH_2 (oxytocin). 20 % of known monogenic disorders are found to affect the skin and for most of them, no effective treatment is available [201]. Small interfering RNA (siRNA) therapies have been used for the treatment of diseases such as allergic skin diseases, pachyonychia congenital, alopecia, skin cancer, hyperpigmentation, and psoriasis caused by aberrant expression of the gene. Solid silicon microneedle arrays (MNAs) have been used to deliver

cholesterol-modified housekeeping gene (*Gapdh*) siRNA in the ear skin of mouse to reduce the expression of the gene by 66 % without accumulation in the major skin [202].

There are a few limitations of SMN-based drug delivery systems. One of the major limitations is the requirement of a two-step process where SMNs need to be inserted and removed followed by the application of therapeutic drugs. They also generate sharp bio-hazardous waste. Another problem of SMN-based drug delivery is the self-regeneration ability of the skin, which heals itself and prevents the delivery of molecules through micropores. The normal healing processes of the skin limit the duration of drug delivery windows. One of the strategies is to use a drug such as a cyclooxygenase inhibitor, which increases the pore lifetime by decreasing the local subclinical inflammatory response. Ghosh *et al.* studied a co-drug approach for sustained delivery of a therapeutic drug, naltrexone (NTX), across the SMN treated skin [203]. Diclofenac (DFC), a cyclooxygenase inhibitor, was used as a co-drug to NTX and the *in vitro* result showed a single patch could be used for a week for the transdermal drug delivery. In addition, an *in vivo* pore visualization study in a hairless guinea pig model showed that the skin concentration of DIC was high enough to keep the pores open for seven days. Enhancers such as fluvastatin also enhance the pore lifetime and deliver drugs for up to 7 days by inhibiting synthesis of cholesterol, a major component of SC lipids [204, 205].

4.2. Porous Microneedles (PMNs)

PMNs are similar to SMNs, but with porous tips through which drugs diffuse. For liquid drug formulations, once PMNs are pierced into the skin, the drugs pre-loaded in the pores of PMNs, start to diffuse from the MN matrix into the skin. In this diffusion-based process, when the drugs deplete, drugs diffuse from the MN back-plate through the MN into the skin. In contrast, for dry drug formulations, pre-loaded drugs that are dried by vacuum, heat or freeze-drying are first hydrated upon piercing into the skin by interstitial fluid. After hydration, drugs are diffused from the pores of PMNs into the skin [207].

PMNs can be fabricated from non-biodegradable materials. Silicon is the most widely used material for the fabrication of non-biodegradable PMNs. PMNs have been fabricated from porous silicon as well as non-porous silicon, simply by making the tips of MNs porous by methods such as electrochemical etching in acetonitrile/HF [208]. Ji *et al.* fabricated a silicon pyramidal MNA with porous tips by a dry etching technology using SF_6O_2 gas [208]. A thin silicon nitride layer was deposited over a thick photoresist layer. Reactive ion etching, followed by electrochemical etching was carried out to generate porous silicon on the tip of the MN. A 20 × 20 array of 100-150 μm high non-biodegradable pyramidal silicon MNs had porous tips of 30 μm high. Yan *et al.* fabricated porous metal MNs by using a process of cutting and wet etching [209]. Titanium MNs 400 μm in height, 800 μm in pitch distance, and 20 μm in micro-hole diameter could resist large shear forces and pierce the skin easily. They performed an *in vivo* experiment by injecting insulin into rats by a PMN patch. They studied the blood glucose level with and without insulin and found that the PMN delivery showed a similar effect as insulin delivered through the conventional hypodermic injection. Nevertheless, these kinds of non-biodegradable materials may have some health concerns.

The fragile tips of non-biodegradable PMNs may break inside the skin and remain there even after removing the patches.

PMNs fabricated from biodegradable materials including calcium phosphate, gelatin, and ceramics are preferred to non-biodegradable materials. Micro-porous calcium phosphate with varying degrees of porosity has been used to provide a biocompatible interface to immobilize trehalose on tips of stainless steel acupuncture PMNs [210]. Yu *et al.* fabricated biodegradable MN patches with abundant pores and channels using calcium sulfate and gelatin for drug release (Fig. 5(B)). They studied hypoglycemic effects of insulin in Sprague-Dawley rats *in vivo*, which was found to be more effective as compared to that of the subcutaneous injection route [206]. Yu *et al.* fabricated bioceramic composite MNs from gelatin and hydroxyapatite for transdermal delivery of insulin in diabetic rats [211]. The MNs with a number of pores and channels had low toxicity and excellent mechanical properties. Insulin released from the bioceramic composite MNs showed effective hypoglycemic effects along with a higher level of insulin in the blood plasma for a longer time as compared to delivery of insulin through subcutaneous injections.

Nanoporous materials have also been used to fabricate PMNs, primarily for the delivery of peptides, vaccines, and analgesics. Boks *et al.* fabricated a ceramic nanoporous MNA with an average pore size of 80 nm and back plate thickness of 0.8 ± 0.1 mm, where the material serves as a storage reservoir for vaccines [212]. OVA257-264 peptides with agonistic anti-CD40 antibodies as an adjuvant were delivered to a human ex vivo skin explant. The induced OVA-specific $CD8^+$ T cells were comparable to the intradermal injection using a syringe. But two nanoporous MNAs were required to induce IFN-γ- specific effector $CD8^+$ T cells, which were equivalent to those induced by the intradermal injection. Vernhoevan *et al.* developed an Al_2O_3 nanoporous MNA through micromolding process from PDMS molds [213]. Experiments in egg plants showed that these MNAs could be used to deliver therapeutic compounds in addition to extraction of compounds. Ex vivo human skin was used to deliver an FITC-labeled monoclonal antibody against a specific marker, DC-SIGN, which is a representative for dendritic cell (DC). Intradermally targeted DCs were found to be fully active in the post staining analysis. In addition, Kochhar *et al.* fabricated a microneedle integrated transdermal patch (MITP) using the photolithography technique [214]. Reservoir patches could hold a higher amount of a drug, lidocaine (up to 70 mg), so that the drug could be released for a prolonged period. PMN created micrometer-sized channels in the skin, where the drug could diffuse through the porous channels left by dissolving drug particles. MITP delivered a higher amount of the drug at a higher permeation rate *in vitro* through the rat skin as compared to commercial patches.

4.3. Hollow Microneedles (HMNs)

HMNs are the MNs which consist of fine perforates and can be used for body fluid sampling or continuous drug delivery from drug formulations stored at top reservoirs. Drugs can be delivered continuously as desired without the need to replace the drug patches as in the case of SMNs. Drugs can be delivered to the desired tissues at a certain flow rate from the defined duct using certain applicators or from a non-pressurized drug reservoir through passive diffusion. Drugs can also be released through pressure-driving force by combining

an MN injection applicator with a syringe pump or electromagnetic applicators [215, 216]. One advantage of HMNs over SMNs is the possibility of faster rates of drug delivery by force-driven flow [216]. Dosage can be controlled in a better way as desired by patients. Furthermore, HMNs may incorporate a microfluidic chip, micropump, or a heater for the release of drugs into the skin in a controlled way [217]. Norman *et al*. compared the reliability and accuracy of standard hypodermic syringes (Mantoux technique), hypodermic needle adapters, and HMNs for intradermal injection into the pig skin [218]. Reliability in terms of the percentage of administered drugs was similar among all three techniques, 95.4 ± 4.9 %, 97.6 ± 1.5 %, and 94.9 ± 0.3 %, respectively. Accuracy determined as the percentage of the dose localized in the dermis was also found to be similar, 97 ± 16 %, 92 ± 21 %, and 99 ± 12 %, respectively.

HMNs have been fabricated using different approaches including micromolding, laser micromachining, deep reactive-ion etching, and bottom-up assembly using carbon nanotubes. Norman *et al*. developed a sacrificial micromolding and selective electrodeposition method for the fabrication of HMNs used in intradermal injection [219]. Replicas were created from a laser ablated master structure, which was followed by sputtering gold seeds and electrodeposition of nickel, and finally dissolving sacrificial replicates to obtain HMNs. HMNs with 12 μm thickness of nickel electrodeposition were found to penetrate the skin with force 9 times less than their axial failure force. The *in vitro* injection in pig's skin and the *in vivo* injection in hairless guinea pig's skin showed 90 % of the material was targeted within the skin with minimal leakage. Deep reactive-ion etching technology has also been used for fabrication of HMNs for transdermal blood sampling and drug delivery [220]. Vinayakumar *et al*. fabricated a hollow stainless steel MNA in a single-step process using femtosecond laser micromachining and avoiding masks [221]. The *in-vivo* insulin study on diabetic rats was performed and the blood glucose level was dramatically reduced in the first hour. Normal blood glucose values (80–120 mg/dl) were observed after administering 5 times of the drug (5 h) and the rate was similar to subcutaneous delivery with a 32-G insulin needle. Lyon *et al*. developed a method using a composite of vertically aligned carbon nanotubes and polyimide for fabricating HMNs [222]. Patterned carbon nanotubes work as a porous scaffold where polyimide resin was wicked to reinforce the structure and provide strength to penetrate the skin (Fig. 6 (A)). Each MNA consisted of nine HMNs that were attached to a common 50-μm thick polyimide base. To demonstrate the utility of this bottom-up assembly, the methylene blue dye was successfully delivered to hydrogel and swine skin *in vitro*. Electron microscopy showed there was no structural damage to HMNs after delivery.

One of the most widely used applications of HMNs is immunization. HMNs have been used with different kinds of applicators to study the effect of immunization and the role of adjuvants has also been studied. Schipper *et al*. studied the repeated fractional intradermal dosing of inactivated polio vaccine (IPV) by utilizing an applicator and a single HMN [223]. They immunized rats intradermally with 5 D-antigen units (5 DU) of IPV1 at 150-μm skin depth as a bolus or repeated fractional dosing. 4 doses of 1.25 DU on 4 consecutive days, 8 doses of 0.625 DU on 8 consecutive days, or 4 exponentially increasing doses (0.04, 0.16, 0.8, and 4 DU) with or without CpG oligodeoxynucleotide 1826 (CpG) doses were given as fractional doses. The fractional doses resulted in up to 10-fold higher IPV1-specific IgG

response than intradermal and intramuscular bolus dosing. In addition, the combination with adjuvants did not show a significant increase in the response, indicating that repeated fractional dosing leads to superior response without the use of adjuvants. Schipper *et al.* studied the depth-dependent (50 to 550 μm) intradermal immunogenicity of IPV with CpG or cholera toxin (CT) as adjuvants using HMNs [224]. An applicator was used so that the rat skin could be microinjected accurately with required depths (50–900 μm), volumes (1–100 μL), and rates (up to 60 μL/min). IgG and virus neutralizing antibody titers were found to be similar to conventional intramuscular immunization, while IgG titers were found to be independent of injection depth. A 7-fold increase in IgG titer was found in the CpG and CT adjuvanted groups, signifying the importance of adjuvanted groups. HMNs have also been fabricated by hydrofluoric acid etching of fused silica capillaries for immunization studies [215]. HMNs with an inner diameter of 20 μm were evaluated in ex vivo human skin with the use of an electromagnetic applicator for IPV vaccination. In addition, rats were immunized with 9 μL of IPV by intradermal microinjection at 1m/s to a depth of 300 μm. Microinjection with HMNs created IPV-specific IgG and virus neutralizing antibodies that were comparable to conventional intramuscular immunization.

Ex-vivo delivery of drugs to the eye of human and other animals have also attracted a lot of attention. Drug delivery to the highly sensitive eye should be minimally invasive, simple, safe, well targeted (limiting exposure to other areas of the eye), and capable of sustained delivery minimizing frequent administration. Patel *et al.* inserted a single HMN with NPs and microparticles into the suprachoroidal space (between sclera and choroid tissues) of rabbit, pig, and human eyes ex vivo [225]. The needle length of 800–1,000 μm and the applied pressure of 250–300 kPa were found to be the most reliable for controlled drug delivery to the back of the eye. The distribution and clearance of HMN injected NPs and microparticles from the suprachoroidal space (3mm posterior to the limbus) using HMNsof New Zealand white rabbit eyes have also been studied [226]. Drug delivery to the suprachoroidal space can be used to treat posterior-segment diseases including age-related macular degeneration. 50 μL of non-biodegradable and fluorescently labeled polystyrene particles were injected into the suprachoroidal space. It was found that the particles spread over the suprachoroidal area up to 200 mm^2 and decreased by 9-35 % between 14 and 112 days. 28-69 % of particles appeared to be cleared during the time period. But further studies are required to see if the clearance is due to the removal by macrophages or due to the reduction in fluorescence intensity of particles.

HMNs have also been used for *in vivo* delivery of therapeutic drugs in animal models as well as humans. Jun *et al.* used HMNs for the delivery of phenylephrine into the anal sphincter muscle through the perianal skin for the treatment of fecal incontinence [227]. As compared to intravenous injection (IV), subcutaneous (SC) injection, and intramuscular (IM) injection, HMNs produced greater anal pressure over 12 h after injection, with maximum anal pressure between 5 and 6 h. HMNs have also been tested in humans. 16 children and adolescent with type 1 diabetes were given Lispro insulin by single HMNs and subcutaneous administration [228]. HMNs resulted in less insertion pain and faster insulin onset and offset time as compared to a subcutaneous insulin pump catheter. Maaden *et al.* developed HMNs by hydrofluoric acid etching of fused silica capillaries for dermal vaccination using an electromagnetic applicator [215]. HMNs were first evaluated in ex vivo human skin before

immunizing rats with IPV to generate IPV-specific IgG. The immune response elicited was comparable to that of the conventional intramuscular immunization.

4.4. Coated Microneedles (CMNs)

CMNs are the SMNs coated and dried with therapeutic drug formulations so that they can directly be applied to the desired area for the instant and rapid delivery of drugs. Drugs can be rapidly dissolved once in contact with interstitial fluids so that the drugs can be delivered into the desired tissues in a rapid manner. MNs can be coated and dried with desired drugs to enhance the long-term stability of drug formulations. Different varieties of water-soluble macromolecular drugs including proteins, peptides, DNA, and oligonucleotides, small molecules including lidocaine hydrochloride and vitamin B, and vaccines including influenza virus have been delivered using CMNs [230, 258].

CMNs can be fabricated by different ways including dip coating, spray-coating, and inkjet printing. CMN surfaces can be coated with aqueous solutions containing the therapeutic drugs and excipients, but water insoluble drugs possess several obstacles including slow dissolution in interstitial fluids of tissues and reduced bioavailability [259]. Dip coating of MNs works by submerging the MNs into drug solutions but may have uncontrollable material deposition, weight variation, and limited drug loading. Thus, coating solutions may need to be optimized. Ma *et al.* demonstrated the coating of solid dispersions on CMNs to deliver a water-insoluble drug lidocaine in the hydrophilic polyethylene glycol matrix [230]. *In vitro* studies in porcine skin showed faster delivery of lidocaine in just 3 min as compared to 1 h topical applications of 0.15 g EMLA®, a commercially available lidocaine-prilocaine cream. This molten dip-coating method of coating solid dispersion revealed that water insoluble lidocaine diffused up to 4.8 mm deep in the porcine skin. Titanium deep reactive ion etching was used to fabricate the MNs followed by coating using the aqueous formulation of 15 % PVP and 1 % Rhodamine B for ocular drug delivery [231]. The spray-coating method has also been used to coat live recombinant adenovirus and modified vaccinia virus Ankara (MVA) on MNAs [232]. The result showed the delivery of the virus in the mice resulted in transcutaneous infection and induction of antibody comparable to that obtained by a syringe intradermal immunization. Recently, inkjet printing has also been used to coat CMNs with different drugs, including anticancer agents 5-fluorouracil, curcumin, and cisplatin for transdermal delivery [233], and antifungal agents such as voriconazole and polyglycolic acid [260]. But the nozzle size, the applied voltage, and the duration of the pulse during inkjet printing may need optimization to achieve the desired coating. A piezoelectric microdispenser can be used to coat a wide range of tiny droplets to form a uniform layer on the needle surface [233]. Additionally, nano-and micrometer-scaled coating of pharmaceuticals have been demonstrated utilizing electrohydrodynamic atomization in stainless steel CMNs [261]. But some studies showed that drugs deposited in oral cavity mucosal tissues using CMNs could be lost due to salivary washout [262].

CMNs have been used for the delivery of biologics including nucleic acids and proteins. CMN-based delivery of nucleic acids to the skin could be used for the treatment of genetic diseases, cutaneous cancers, and intracutaneous genetic immunization [234]. The plasmid DNA coated onto CMN dips was found to lead reporter gene expression in the viable human

skin after the delivery. Similarly, siRNA targeting the reporter (luciferase/GFP) gene was coated onto steel CMNs and delivered to mouse footpad. The results showed functional *in vivo* gene silencing in a mouse model [235]. Therapeutic proteins have various applications including enzymes for metabolic complementation, neutralizing antibodies, engineered transcription factors, and programmable enzymes for gene editing [263]. Witting *et al.* conducted a feasibility study of the intraepidermal delivery of a model protein, asparaginase B (AsnB) [237]. Insertion experiments in pig's skin were performed where CMN coating dissolved in few minutes and the protein diffused homogenously, indicating coating was stable enough to withstand the insertion process. CMNs 300 μm in length yielded effective delivery of 68.0 ± 11.7 % of the coated AsnB in the reconstructed human skin. The AsnB bioactivity (90 %) was maintained for 3 months by polysorbate solutions with hyaluronic acid as a viscosity enhancer.

CMNs as a tool for vaccine delivery are finding increasing interest, as this is a low-cost, simple and reliable method of self-administration, which can be easily removed after use. Researches have shown that CMNs induce a stronger immune response, as compared to conventional intramuscular syringe injection for vaccine delivery. Kim *et al.* developed a CMN patch with virus-like particles (influenza virus heterologous M2 extracellular domain) without any adjuvants which were stable for 8 weeks at RT [238]. Strong humoral and mucosal immunity was elicited against different influenza viruses (H1N1, H3N2, and H5N1) compared to conventional intramuscular injection. IgG2a isotypes and IFN-γ producing cells were also induced at higher levels. Other CMN patches were developed for vaccination in 6-week-old female BALB/c mice [239]. Lips and tongue have also shown to be appropriate immunogenic sites for vaccination. HIV antigens, a virus-like particle, and a DNA vaccine were used for oral vaccination to compare with intramuscular vaccination; and a similar level of IgG was elicited in the serum [240]. In contrast, the CMN-based oral cavity vaccination group elicited both the systemic and mucosal immunity, while the intramuscular injection only elicited the systemic immunity. Uses of appropriate adjuvants have been found to increase the immunogenicity of vaccines. MF59, an adjuvant approved in Europe, have demonstrated enhanced immunogenicity of trivalent influenza vaccine in young children, and avian influenza vaccine in elderly. Similarly, in the US, aluminum hydroxide, aluminum phosphate, alum, and AS04 have been approved as adjuvants [239]. Weldon *et al.* found that imiquimod-adjuvanted monovalent H1N1 vaccine induced higher levels of serum IgG2a antibodies and robust IFN-γ cellular response, revealing improved protection as compared to influenza subunit vaccine alone.

CMNs have also been used for the delivery of anti-cancer drugs and insulin as an implantable device [229, 236]. Ma *et al.* fabricated CMNs with the coatings of poly(lactic-co-glycolic) acid (PLGA) nanoparticles encapsulating doxorubicin (DOX) for injection into porcine cadaver buccal tissues to study cellular cytotoxicity [236]. In contrast, hypodermic injection showed 25% leakage of the injected volume in addition to causing pain and poor distribution of the drug in the tumor, showing the potential benefit of CMNs for the treatment of cancer. Traverso *et al.* developed a device (2×1 cm) with a metallic core and 25G needles protruding 5mm from the surface. The device with both HMNs and CMNs could be endoscopically placed in the stomach of Yorkshire pigs, passed and excreted safely from the GI tract [229]. In the HMN-based device, the reservoir was compressed with

peristalsis to release insulin, while in the CMN-based device, the CMNs penetrated tissues and broke off from the device, leaving the needle to release the insulin. As compared to the subcutaneous route, MN-based delivery showed improved blood glucose response kinetics

CMNs have also been used for other applications including the treatment of injury, delivery of analgesics, and for neovascularization. For instance, Kim *et al.* showed that intracorneal delivery of bevacizumab using CMNs could be used to treat injury-induced neovascularization in the eye of New Zealand white rabbits with much lower dosages as compared to eye drops or subconjunctival injection [241]. Zhang *et al.* fabricated lidocaine-coated CMNs and inserted into domestic swine and found that co-formulation with 0.03% vasoconstrictor, epinephrine maintained the lidocaine in the tissues above 100 ng/mg for approximately 90 min [243]. Lidocaine dissolved into the skin within 1 min to achieve the tissue level needed to cause analgesia. Furthermore, Song *et al.* designed a CMN pen, a single 140 μm MN with a spring-loaded applicator to provide impact insertion [242]. The MN pen successfully delivered the rhodamine dye deep into the stromal layer with a small entry about 1000 μm^2. Sunitinib malate, an inhibitor of *in vitro* angiogenesis, was coated on the surface of the MN using the dip-coating method and delivered to a suture-induced angiogenesis model. As compared to a 30 G needle tip, only the MN pen could effectively inhibit corneal neovascularization *in vivo* in 8-week-old C57BL/6J mice.

CMNs have several advantages as discussed earlier, however, they have some limitations as well. One of the drawbacks of CMNs is the limited amounts of drugs that can be coated onto CMNs. There have been efforts to overcome the limitation, one of which is to coat alternate layers of drugs and fabrication materials. Maaden *et al.* coated pH-sensitive 200 μm long MNAs, alternately with 10 layers of IPV and N-trimethyl chitosan chloride (TMC) through electrostatic interactions (Fig. 6 (B)) [244].They fluorescently evaluated the release of IPV and TMC from the CMNs in ex vivo human skin. IPV-specific antibody response was elicited after the administration of IPV–TMC-coated CMNs in rats. Other issues involving the vaccine delivery through CMNs include the long-term stability of the coated vaccine. Transmission electron microscopy (TEM) has shown damaged morphology of inactivated virus upon crystallization and phase-separated coating. Similarly, reduced vaccine immunogenicity was observed during *in vivo* immunization with inactivated PR8 influenza vaccine in 6-8 weeks female mice [245].

4.5. Dissolvable Microneedles (DMNs)

DMNs are micron-sized needles where therapeutic drugs are encapsulated within the matrix made up of biodegradable polymers. Once the DMNs are inserted into the skin, the drugs are released for systematic or local delivery as the polymer dissolves or get biodegraded after getting into contact with the interstitial fluid of the skin. DMNs remain in the skin and slowly dissolve over the time at the rate that is predetermined by the rate of dissolution of the polymer to release the drug in tissues. As compared to other MNs, DMNs evade the risk of metal and silicon needles breaking *in vivo* as they act by releasing the drugs through the dissolution of the substrate used for the fabrication of the MNs [249]. Polymer DMNs are preferred drug delivery systems due to cost-effective materials and fabrication, their minimum pain on delivery, patient convenience, and biocompatibility [264, 265]. In

addition, they can completely dissolve within the skin so that there are no sharp biohazards left behind after the treatment, unlike solid and coated MNs.

DMNs can be fabricated from different materials including polylactic acid, hyaluronic acid, poloxamer, silk fibroin, and polyvinyl alcohol (PVA) (Table 2) [246-249, 266-268]. DMN tips need sufficient mechanical strength to perforate the SC while the bases need to be flexibly adherent to skin and to transmit the force to the tip. Cha *et al.* fabricated a polylactic acid MNA by a PDMS mold made from a master template of acupuncture MNs [266]. Compression tests and accelerated degradation tests were used to characterize the mechanical force and degradation behaviors. Penetration and staining tests on pig's skin showed that mechanical strength was enough to penetrate the skin and could be used to deliver a vaccine or drug by the transdermal route. Mönkäre *et al.* developed hyaluronan-based DMNs in a PDMS mold with a tip length of 280 μm for intradermal delivery of monoclonal IgG (Fig. 7) [246]. 80 % of IgG was recovered after dissolving MNs in PBS. MNs dissolved in 10 min when penetrated into the epidermis of the ex-vivo human skin, while co-depositing IgG and hyaluronan up to a depth of 150- 200 μm. Liu *et al.* developed hyaluronic acid-based DMNs to deliver fluorescein isothiocyanate-labeled dextran (4 kDa) as a model drug [267]. The DMN could puncture the skin to form a drug permeation pathway, indicated by an increase in transepidermal water loss and reduction in transcutaneous electrical resistance. Both of them returned to normal level rapidly, indicating that they were safe to use. Lu *et al.* developed poly(propylene fumarate) (PPF)-based MNAs loaded with Dacarbazine using microstereolithography for the treatment of skin cancer [247]. Each DMN had a cylindrical base of 700 μm and a conical tip with the height of 300 μm. Dacarbazine could be released at a controlled rate for 5 weeks. The amount of drug released could be altered by the loading amount of drug as well as changing the molecular weight of PPF.

In addition, Sivaraman *et al.* developed in situ forming hydrogel DMNs from the amphiphilic thermo-sensitive copolymer, poloxamer, for transdermal delivery of methotrexate to treat solid tumors [248]. The average cumulative drug amounts of methotrexate formulations that were administered using hydrogel MNs were found to be 32.2 ± 15.76 and 114.54 ± 40.89 μg/cm^2 for porcine ear skin and 3.89 ± 0.60 and 10.27 ± 6.98 μg/cm^2 for dermatomed human skin from 0.2 % and 0.4 % *w*/*w* methotrexate in hydrogels, respectively. Lau *et al.* developed multilayered pyramidal DMN patches to increase the efficiency of drug delivery and stability [249]. The DMN was composed of silk fibroin tips for good mechanical strength and rapid dissolution, and PVA for the structure support. The DMN patch could be inserted to a depth of 150 μm into the abdominal skin of mice for the release of encapsulated insulin to cause a hypoglycemic effect. More than 99% of insulin remained in silk fibroin of MNs for 20 days at room temperature.

Several strategies such as electric current, ultrasound, and near-infra red light have been tried either to improve the permeation of drugs or to trigger the release of drugs through DMNs. Garland *et al.* studied the electrically facilitated iontophoretic transdermal delivery of bovine insulin [250]. The amount of insulin permeated through porcine skin at 6h using soluble poly (methyl vinyl ether-co-maleic acid) (PMVE/MA) was found to be 150 μg (3.25%), 227 μg (4.85%), and 462 μg (9.87%) for iontophoresis (ITP), DMNs, and DMNs/ITP delivery

strategies, respectively, showing the efficiency increase due to the application of electric current. Nayak *et al.* explored the combination of DMNs and sonophoresis to study their effects on the percutaneous delivery of lidocaine from a polymeric hydrogel [251]. Different ratios of gelatin and carboxymethylcellulose were loaded with lidocaine. Ex vivo studies were performed in the porcine skin where an increase in permeability was observed from combined MNs and ultrasound pre-treatment. A 4.8-fold increase in the combined application was observed as compared to separate pre-treatment. Applications of MNs increased permeability by up to ~17 folds at 0.5 h and the time required to reach therapeutic levels of lidocaine was decreased to less than 7 min. Drug delivery systems which can be triggered by an external stimulus enable on- demand drug delivery adaptable to the patient as well as delivery of multiple dosages through a single administration. Chen *et al.* developed near-infrared light responsive DMNs for on-demand delivery of drugs [252]. Silica-coated lanthanum hexaboride nanostructures were introduced into polycaprolactone DMNs, to absorb NIR light and melt the DMNs at 50 °C to release the drugs. The release of the drugs was evaluated for four cycles, where samples were irradiated for 3 min so that the temperature reaches 50°C to release the drug.

Vaccine delivery to the skin tissues heavily occupied with antigen presenting cells can increase the immune response[253]. In addition, control over the kinetics of vaccine delivery can boost immunity as it can mimic the natural acute infection kinetics in a better way. DMNs have been widely used for vaccine delivery. DeMuth *et al.* developed DMNs composed of implantable silk composites for transcutaneous immunization by the programmable release of the vaccine [253]. Silk MN Tips were fabricated on PAA bases which were rapidly dissolved and delivered a bolus of protein subunit vaccine. In contrast, a low-level of the cutaneous vaccine was delivered at a sustained rate for 1-2 weeks from persistent silk hydrogel depots into the skin. C57Bl/6 mice were immunized with 9 μg of ovalbumin and 150 ng of polyI:C using a MNA. The process resulted in more than a 10-fold increase in antigen-specific T-cell and humoral immunity as compared to traditional parenteral needle-based immunization. Zhu *et al.* developed sodium hyaluronate-based DMNs loaded with EV71 virus-like particles for vaccination against the hand-foot-and-mouth disease with a spring-operated applicator [272]. *In vivo* experiments in mice induced a high level of the antibody but only with $1/10^{th}$ the dosage of conventional IM injection. Guo *et al.* fabricated polyvinylpyrrolidone MNAs where the tips were loaded with OVA antigen and CpG oligonucleotide (CpG OND) as an adjuvant encapsulated in a liposome (Lip) [254]. Mice were transcutaneously immunized with different combinations of the antigen and adjuvants, with or without liposome. Among them, the highest amount of anti-OVA IgG was elicited in DMNs containing OVA-CpG OND encapsulated in Lip.

Reducing the dependency on the cold chain to transfer or store a vaccine to a certain place would be very beneficial to many biomedical applications, particularly in low-resource settings. Mistilis *et al.* developed DMN patches from arginine and calcium heptagluconate for three strains of seasonal influenza vaccines, which could be stored at room temperature for 6 months in the presence of buffer salts, surfactants, and stabilizers [269]. Vassilieva *et al.* evaluated the immunogenicity of H1N1, H3N2, and B seasonal influenza virus vaccines administered by a DMN patch [255]. The DMN patch retained the antigenic activity for at least 3 months at room temperature conformed by an *in vitro* single radial diffusion assay

and mouse immunization studies *in vivo*. After a single immunization, superior neutralizing antibody titers to intramuscular immunization was observed. In addition, mice immunized with DMN patches with influenza vaccine were fully protected against lethal influenza. Recently, Ebola DNA vaccines have been coated on polylactic-*co*-glycolic acid—poly-l-lysine/poly-γ-glutamic acid NPs to be administered by a CMN patch [256]. The nanoparticle formulation increased the stability, enhanced transfection efficiency and storage at elevated temperatures, and showed a strong immune response *in vivo* in mice. Enabling transport without a cold chain can be beneficial for delivery of other drugs as well, such as insulin [249].

Some limitations of DMNs include difficulties in fully inserting them into the skin and requirements of a long time to be dissolved into the skin, which may lead to low drug efficiency. Delivery of full amounts of encapsulated drugs is complicated, as DMNs on a flat patch does not completely penetrate the viscoelastic skin even with strong insertion force [270]. Zhu *et al*. developed rapidly separating MNs, where drug loaded DMNs (PVA/Sucrose gel) were mounted on the top of SMNs, made of biodegradable polylactic acid, and achieved over 90 % drug delivery efficiency in 30 s compared to 2 min in traditional MNs [257]. *In vivo* tests in mice showed that the micro-pores healed in 1 h. Similarly, Kim *et al*. developed rapidly separating DMNs formed by cyclic contact and drying on pillars. Such DMNs were applied to pig cadaver skin, which took only 15 s for over 90 % of encapsulated rhodamine B to be delivered and had high penetration efficiency as well [271]. The separation of DMNs was found to be more rapid and complete as compared to other DMNs because of the minimal junction between DMNs and pillars and easy permeation of interstitial fluid between DMNs and pillars.

5. Conclusion & Future Prospects

An ideal goal of a controlled drug delivery system is to provide clinically relevant drug formulations at desired kinetics to help treat patients effectively from different pathological conditions, reduce side effects, and increase patient convenience and compliance. With the rapid development of microtechnology, numerous microfluidic platforms have been developed for controlled drug delivery, including carrier-free micro-reservoir-based drug delivery systems, highly integrated carrier-free microfluidic LOC systems, drug carrier-integrated microfluidic systems, and five different types of microneedles (i.e. SMNs, PMNs, HMNs, CMNs, and DMNs). These different micro-systems have significantly advanced the field of controlled drug delivery in many different applications, through precise control of drug delivery rates, time, and locations, and increased efficacy while with fewer side effects. It is worthy to mention that a number of such microdevices are implantable and have gone through *in vivo* testing. Micro-reservoir systems provide precise control over delivery rates in an interactive format with increased drug stability and prolonged delivery time. In addition to micro-reservoirs, various components and functions can be further integrated into microfluidic platforms such as microchannels and drug carrier synthesis and testing. Furthermore, microneedle systems are minimally invasive and several *in vivo* studies have shown that MNs are more efficient for transdermal drug delivery as compared to conventional injections. Researches have also discovered that MNs induce stronger immune response than convention methods of immunization.

However, multiple challenges still exist in front of microfluidic platforms for controlled drug delivery. One of the major challenges of controlled drug delivery using microdevices is that it is difficult to achieve the targeted drug delivery to specific cells or tissues. Most drugs are simply randomly distributed with a minor portion of the administered drugs ending up in target sites. The combination of drug carriers which are tagged with specific antibodies, nucleic acids, or peptides to certain targets with microfluidic platforms will help address this challenge. This might require close collaborations of people working in the field of microfluidics, nanomaterials, biology, and clinical medicine. Secondly, most current controlled drug delivery systems deliver drugs at preset rates, and are incapable of changing delivery parameters upon the changes of patient conditions, especially once implanted in human bodies. An optimum drug delivery system should be capable of monitoring patient conditions (e.g. biomarker levels) through a feedback system, and monitoring and changing the drug delivery parameters in response to the information from the feedback system. On-demand self-tuning dynamic drug delivery systems have tremendous potential for personalized drug delivery and disease treatment. However, this will require more advanced integration of microfluidics, biosensors, bioelectronics, automation, and so on. In addition, most of the current microneedles act simply as miniaturized “conventional needles”. The integration of more microfluidic and electronic components will enable more powerful “super microneedles”. Another major challenge is the lack of mature commercial products of microfluidic drug delivery systems for clinical applications, limiting the wide applications of those microfluidic drug delivery systems developed in research laboratories. Sealing the gap between laboratory research and industrial/clinical applications could be one of the major focuses in the future. To achieve the successful translation of microfluidic drug delivery systems into clinical applications, more thorough and stringent *in vivo* testing and clinical trials is essential. Despite these challenges, thanks to unique advantages of microfluidic platforms for controlled drug delivery, we envision that more and more efficient, advanced, and robust microfluidic drug delivery systems will be developed in the near future for effective personalized drug delivery and therapy.

Supplementary Material

Refer to Web version on PubMed Central for supplementary material.

Acknowledgments

The authors would like to acknowledge the financial support of the NIH/NIAID under award number R21AI107415, the NIH/NIGMS under award number SC2GM105584, and the NIH/NIMHD/RCMI under award number 5G12MD007593-22. Financial support from the Emily Koenig Meningitis Fund from the Philadelphia Foundation, Emily's Dash Foundation, the Medical Center of the Americas (MCA) Foundation, the U.S. NSF-PREM program (DMR 1205302), the NIH BUILD program, the NIH BUILDing Scholar Summer Sabbatical Award (RL5GM118969, TL4GM118971, and UL1GM118970), University of Texas System for the STARS Award, and the IDR Program at the University of Texas at El Paso, is also gratefully acknowledged.

References

1. Li H, Yu Y, Faraji Dana S, Li B, Lee CY, Kang L. Novel engineered systems for oral, mucosal and transdermal drug delivery. Journal of drug targeting. 2013; 21:611–629. [PubMed: 23869879]
2. Blanco E, Shen H, Ferrari M. Principles of nanoparticle design for overcoming biological barriers to drug delivery. Nature biotechnology. 2015; 33:941–951.

3. Muheem A, Shakeel F, Jahangir MA, Anwar M, Mallick N, Jain GK, Warsi MH, Ahmad FJ. A review on the strategies for oral delivery of proteins and peptides and their clinical perspectives. Saudi Pharmaceutical Journal. 2016; 24:413–428. [PubMed: 27330372]
4. Cheung K, Das DB. Microneedles for drug delivery: trends and progress. Drug delivery. 2014:1–17.
5. Rajput M, Sharma R, Kumar S, Jamil F, Sissodia N, Sharma S. Pulsatile drug delivery system: a review. International Journal of Research in Pharmaceutical and Biomedical Sciences. 2012; 3:118–124.
6. Chiang WL, Ke CJ, Liao ZX, Chen SY, Chen FR, Tsai CY, Xia Y, Sung HW. Pulsatile drug release from PLGA hollow microspheres by controlling the permeability of their walls with a magnetic field. Small. 2012; 8:3584–3588. [PubMed: 22893436]
7. Park K. Controlled drug delivery systems: past forward and future back. Journal of Controlled Release. 2014; 190:3–8. [PubMed: 24794901]
8. Yang K, Feng L, Liu Z. Stimuli responsive drug delivery systems based on nano-graphene for cancer therapy. Advanced drug delivery reviews. 2016; 105:228–241. [PubMed: 27233212]
9. Sanjay ST, Dou M, Fu G, Xu F, Li X. Controlled drug delivery using microdevices. Current pharmaceutical biotechnology. 2016; 17:772–787. [PubMed: 26813304]
10. Li, XJ., Zhou, Y. Microfluidic devices for biomedical applications. Elsevier; 2013.
11. Sanjay ST, Fu G, Dou M, Xu F, Liu R, Qi H, Li X. Biomarker detection for disease diagnosis using cost-effective microfluidic platforms. Analyst. 2015; 140:7062–7081. [PubMed: 26171467]
12. Shen F, Li X, Li PC. Study of flow behaviors on single-cell manipulation and shear stress reduction in microfluidic chips using computational fluid dynamics simulations. Biomicrofluidics. 2014; 8:014109. [PubMed: 24753729]
13. Li XJ, Valadez AV, Zuo P, Nie Z. Microfluidic 3D cell culture: potential application for tissue-based bioassays. 2012
14. Dou M, Sanjay ST, Dominguez DC, Zhan S, Li X. A paper/polymer hybrid CD-like microfluidic SpinChip integrated with DNA-functionalized graphene oxide nanosensors for multiplex qLAMP detection. Chemical communications. 2017
15. Belliveau NM, Huft J, Lin PJ, Chen S, Leung AK, Leaver TJ, Wild AW, Lee JB, Taylor RJ, Tam YK. Microfluidic synthesis of highly potent limit-size lipid nanoparticles for in vivo delivery of siRNA. Molecular Therapy—Nucleic Acids. 2012; 1:e37. [PubMed: 23344179]
16. Khan IU, Serra CA, Anton N, Vandamme T. Microfluidics: A focus on improved cancer targeted drug delivery systems. Journal Of Controlled Release. 2013; 172:1065–1074. [PubMed: 23933524]
17. Dou MW, Lopez J, Rios M, Garcia O, Xiao C, Eastman M, Li XJ. A fully batterypowered inexpensive spectrophotometric system for high-sensitivity point-of-care analysis on a microfluidic chip. Analyst. 2016; 141:3898–3903. [PubMed: 27143408]
18. Dou MW, Garcia JM, Zhan SH, Li XJ. Interfacial nano-biosensing in microfluidic droplets for high-sensitivity detection of low-solubility molecules. Chem Commun. 2016; 52:3470–3473.
19. Wang J, Kaplan JA, Colson YL, Grinstaff MW. Mechanoresponsive materials for drug delivery: Harnessing forces for controlled release. Advanced drug delivery reviews. 2017; 108:68–82. [PubMed: 27856307]
20. Lu DR, Øie S. Cellular drug delivery: principles and practice. Springer Science & Business Media. 2004
21. Riahi R, Tamayol A, Shaegh SAM, Ghaemmaghami AM, Dokmeci MR, Khademhosseini A. Microfluidics for advanced drug delivery systems. Current Opinion in Chemical Engineering. 2015; 7:101–112.
22. Bhise NS, Ribas J, Manoharan V, Zhang YS, Polini A, Massa S, Dokmeci MR, Khademhosseini A. Organ-on-a-chip platforms for studying drug delivery systems. Journal Of Controlled Release. 2014; 190:82–93. [PubMed: 24818770]
23. Nguyen NT, Shaegh SAM, Kashaninejad N, Phan DT. Design, fabrication and characterization of drug delivery systems based on lab-on-a-chip technology. Adv Drug Deliver Rev. 2013; 65:1403–1419.
24. Sant S, Tao SL, Fisher OZ, Xu QB, Peppas NA, Khademhosseini A. Microfabrication technologies for oral drug delivery. Adv Drug Deliver Rev. 2012; 64:496–507.

25. Vladisavljevic GT, Khalid N, Neves MA, Kuroiwa T, Nakajima M, Uemura K, Ichikawa S, Kobayashi I. Industrial lab-on-a-chip: Design, applications and scale-up for drug discovery and delivery. Adv Drug Deliver Rev. 2013; 65:1626–1663.
26. Sanjay ST, Dou MW, Sun JJ, Li XJ. A paper/polymer hybrid microfluidic microplate for rapid quantitative detection of multiple disease biomarkers. Sci Rep-Uk. 2016; 6:30474.
27. Zhang Y, Chan HF, Leong KW. Advanced materials and processing for drug delivery: The past and the future. Adv Drug Deliver Rev. 2013; 65:104–120.
28. Dou MW, Sanjay ST, Dominguez DC, Liu P, Xu F, Li XJ. Multiplexed instrument-free meningitis diagnosis on a polymer/paper hybrid microfluidic biochip. Biosens Bioelectron. 2017; 87:865–873. [PubMed: 27657849]
29. Dou M, Sanjay ST, Benhabib M, Xu F, Li X. Low-cost bioanalysis on paper-based and its hybrid microfluidic platforms. Talanta. 2015; 145:43–54. [PubMed: 26459442]
30. Herrlich S, Spieth S, Messner S, Zengerle R. Osmotic micropumps for drug delivery. Adv Drug Deliver Rev. 2012; 64:1617–1627.
31. Sharei A, Zoldan J, Adamo A, Sim WY, Cho N, Jackson E, Mao S, Schneider S, Han MJ, Lytton-Jean A, Basto PA, Jhunjhunwala S, Lee J, Heller DA, Kang JW, Hartoularos GC, Kim KS, Anderson DG, Langer R, Jensen KF. A vector-free microfluidic platform for intracellular delivery. P Natl Acad Sci USA. 2013; 110:2082–2087.
32. Kusunose J, Zhang H, Gagnon MKJ, Pan TR, Simon SI, Ferrara KW. Microfluidic System for Facilitated Quantification of Nanoparticle Accumulation to Cells Under Laminar Flow. Ann Biomed Eng. 2013; 41:89–99. [PubMed: 22855121]
33. Pararas EEL, Borkholder DA, Borenstein JT. Microsystems technologies for drug delivery to the inner ear. Adv Drug Deliver Rev. 2012; 64:1650–1660.
34. Khalid N, Kobayashi I, Nakajima M. Recent lab-on-chip developments for novel drug discovery, Wiley interdisciplinary reviews. Systems biology and medicine. 2017; doi: 10.1002/wsbm.1381
35. Scholten K, Meng E. Materials for microfabricated implantable devices: a review. Lab on a chip. 2015; 15:4256–4272. [PubMed: 26400550]
36. Khan I, Khan M, Umar MN, Oh DH. Nanobiotechnology and its applications in drug delivery system: a review. Iet Nanobiotechnol. 2015; 9:396–400. [PubMed: 26647817]
37. Gensler H, Sheybani R, Li PY, Lo Mann R, Meng E. An implantable MEMS micropump system for drug delivery in small animals. Biomed Microdevices. 2012; 14:483–496. [PubMed: 22273985]
38. Stevenson CL, Santini JT, Langer R. Reservoir-based drug delivery systems utilizing microtechnology. Advanced drug delivery reviews. 2012; 64:1590–1602. [PubMed: 22465783]
39. Lee HP, Ryu W. Wet microcontact printing (microCP) for micro-reservoir drug delivery systems. Biofabrication. 2013; 5:025011. [PubMed: 23624468]
40. Meng E, Sheybani R. Micro-and nano-fabricated implantable drug-delivery systems: current state and future perspectives. Therapeutic delivery. 2014; 5:1167–1170. [PubMed: 25491666]
41. Meng E, Hoang T. Micro-and nano-fabricated implantable drug-delivery systems. Therapeutic delivery. 2012; 3:1457–1467. [PubMed: 23323562]
42. Hwang TH, Kim JB, Yang DS, Park YI, Ryu W. Targeted electrohydrodynamic printing for micro-reservoir drug delivery systems. J Micromech Microeng. 2013; 23:035012.
43. Eltorai AEM, Fox H, McGurrin E, Guang S. Microchips in Medicine: Current and Future Applications. Biomed Res Int. 2016
44. Zhou JW, Kim A, Ochoa M, Jiang HJ, Ziaie B. An Ultrasonically Powered Micropump for on Demand In-Situ Drug Delivery. Proc Ieee Micr Elect. 2016:349–352.
45. Cobo A, Sheybani R, Meng E. MEMS: Enabled Drug Delivery Systems. Adv Healthc Mater. 2015; 4:969–982. [PubMed: 25703045]
46. Song PY, Hu R, Tng DJH, Yong KT. Moving towards individualized medicine with microfluidics technology. Rsc Adv. 2014; 4:11499–11511.
47. Wang B, Ni JH, Litvin Y, Pfaff DW, Lin Q. A Microfluidic Approach to Pulsatile Delivery of Drugs for Neurobiological Studies. J Microelectromech S. 2012; 21:53–61.

48. Spieth S, Schumacher A, Holtzman T, Rich PD, Theobald DE, Dalley JW, Nouna R, Messner S, Zengerle R. An intra-cerebral drug delivery system for freely moving animals. Biomed Microdevices. 2012; 14:799–809. [PubMed: 22622711]
49. Honda W, Harada S, Arie T, Akita S, Takei K. Wearable, Human-Interactive, Health-Monitoring, Wireless Devices Fabricated by Macroscale Printing Techniques. Adv Funct Mater. 2014; 24:3299–3304.
50. Garg T. Current nanotechnological approaches for an effective delivery of bio-active drug molecules in the treatment of acne. Artif Cell Nanomed B. 2016; 44:98–105.
51. Lue SJ, Chen CH, Shih CM, Tsai MC, Kuo CY, Lai JY. Grafting of poly(N-isopropylacrylamide-co-acrylic acid) on micro-porous polycarbonate films: Regulating lower critical solution temperatures for drug controlled release. J Membrane Sci. 2011; 379:330–340.
52. Adrus N, Ulbricht M. Novel hydrogel pore-filled composite membranes with tunable and temperature-responsive size-selectivity. J Mater Chem. 2012; 22:3088–3098.
53. Epstein-Barash H, Stefanescu CF, Kohane DS. An in situ cross-linking hybrid hydrogel for controlled release of proteins. Acta Biomater. 2012; 8:1703–1709. [PubMed: 22342597]
54. Spieth S, Schumacher A, Kallenbach C, Messner S, Zengerle R. The NeuroMedicator-a micropump integrated with silicon microprobes for drug delivery in neural research. J Micromech Microeng. 2012; 22:065020.
55. Timko BP, Kohane DS. Materials to Clinical Devices: Technologies for Remotely Triggered Drug Delivery. Clin Ther. 2012; 34:S25–S35. [PubMed: 23149010]
56. Nicu L, Alava T, Leichle T, Saya D, Pourciel LB, Mathieu F, Soyer C, Remiens D, Ayela C, Haupt K. Integrative technology-based approach of microelectromechanical systems (MEMS) for biosensing applications. Ieee Eng Med Bio. 2012:4475–4478.
57. Meng E, Sheybani R. Micro-and nano-fabricated implantable drug-delivery systems: current state and future perspectives. Therapeutic delivery. 2014; 5:1167–1170. [PubMed: 25491666]
58. Nuxoll E. BioMEMS in drug delivery. Adv Drug Deliver Rev. 2013; 65:1611–1625.
59. Song PY, Jian D, Tng H, Hu R, Lin GM, Meng E, Yong KT. An Electrochemically Actuated MEMS Device for Individualized Drug Delivery: an In Vitro Study. Adv Healthc Mater. 2013; 2:1170–1178. [PubMed: 23495127]
60. Zhuang Y, Hou W, Zheng X, Wang Z, Zheng J, Pi X, Cui J, Jiang Y, Qian S, Peng C. A MEMS-based electronic capsule for time controlled drug delivery in the alimentary canal. Sensors and Actuators A: Physical. 2011; 169:211–216.
61. Pirmoradi FN, Jackson JK, Burt HM, Chiao M. A magnetically controlled MEMS device for drug delivery: design, fabrication, and testing. Lab on a Chip. 2011; 11:3072–3080. [PubMed: 21860883]
62. Jeong JW, McCall JG, Shin G, Zhang YH, Al-Hasani R, Kim M, Li S, Sim JY, Jang KI, Shi Y, Hong DY, Liu YH, Schmitz GP, Xia L, He ZB, Gamble P, Ray WZ, Huang YG, Bruchas MR, Rogers JA. Wireless Optofluidic Systems for Programmable In Vivo Pharmacology and Optogenetics. Cell. 2015; 162:662–674. [PubMed: 26189679]
63. Fong J, Xiao ZM, Takahata K. Wireless implantable chip with integrated nitinol-based pump for radio-controlled local drug delivery. Lab Chip. 2015; 15:1050–1058. [PubMed: 25473933]
64. Farra R, Sheppard NF, McCabe L, Neer RM, Anderson JM, Santini JT, Cima MJ, Langer R. First-in-human testing of a wirelessly controlled drug delivery microchip. Science translational medicine. 2012; 4:122ra121–122ra121.
65. Rahimi, S., Takahata, K. A Wireless Implantable Drug Delivery Device with Hydrogel Microvalves Controlled by Field-Frequency Tuning. 2011 Ieee 24th International Conference on Micro Electro Mechanical Systems (Mems); 2011; p. 1019-1022.
66. Huang PL, Kuo PH, Huang YJ, Liao HH, Yang YJJ, Wang T, Wang YH, Lu SS. A Controlled-Release Drug Delivery System on a Chip Using Electrolysis. Ieee T Ind Electron. 2012; 59:1578–1587.
67. Pirmoradi FN, Jackson JK, Burt HM, Chiao M. On-demand controlled release of docetaxel from a battery-less MEMS drug delivery device. Lab Chip. 2011; 11:2744–2752. [PubMed: 21698338]
68. Chirra HD, Desai TA. Multi-Reservoir Bioadhesive Microdevices for Independent Rate-Controlled Delivery of Multiple Drugs. Small. 2012; 8:3839–3846. [PubMed: 22962019]

69. Fox CB, Chirra HD, Desai TA. Planar Bioadhesive Microdevices: A New Technology for Oral Drug Delivery. Curr Pharm Biotechno. 2014; 15:673–683.
70. Liu YQ, Song PY, Liu JW, Tng DJH, Hu R, Chen HY, Hu YZ, Tan CH, Wang JH, Liu J, Ye L, Yong KT. An in-vivo evaluation of a MEMS drug delivery device using Kunming mice model. Biomed Microdevices. 2015; 17:6. [PubMed: 25653064]
71. Tng DJH, Hu R, Song PY, Roy I, Yong KT. Approaches and Challenges of Engineering Implantable Microelectromechanical Systems (MEMS) Drug Delivery Systems for in Vitro and in Vivo Applications. Micromachinevs-Basel. 2012; 3:615–631.
72. Yasin MN, Svirskis D, Seyfoddin A, Rupenthal ID. Implants for drug delivery to the posterior segment of the eye: A focus on stimuli-responsive and tunable release systems. Journal Of Controlled Release. 2014; 196:208–221. [PubMed: 25307997]
73. Molokhia SA, Thomas SC, Garff KJ, Mandell KJ, Wirostko BM. Anterior Eye Segment Drug Delivery Systems: Current Treatments and Future Challenges. J Ocul Pharmacol Th. 2013; 29:92–105.
74. Pearce W, Hsu J, Yeh S. Advances in drug delivery to the posterior segment. Curr Opin Ophthalmol. 2015; 26:233–239. [PubMed: 25759965]
75. McRoberts W, Prager J, Hamza M. Severe Hypertension Following Accidental Clonidine Overdose During the Refilling of an Implanted Intrathecal Drug Delivery System COMMENTS. Neuromodulation. 2012; 15:34–34.
76. Prager J, Deer T, Levy R, Bruel B, Buchser E, Caraway D, Cousins M, Jacobs M, McGlothlen G, Rauck R, Staats P, Stearns L. Best Practices for Intrathecal Drug Delivery for Pain. Neuromodulation. 2014; 17:354–372. [PubMed: 24446870]
77. Bertrand N, Wu J, Xu XY, Kamaly N, Farokhzad OC. Cancer nanotechnology: The impact of passive and active targeting in the era of modern cancer biology. Adv Drug Deliver Rev. 2014; 66:2–25.
78. Vashist A, Vashist A, Gupta YK, Ahmad S. Recent advances in hydrogel based drug delivery systems for the human body. J Mater Chem B. 2014; 2:147–166.
79. Lee KJ, Yang SY, Ryu W. Controlled release of bupivacaine HCl through microchannels of biodegradable drug delivery device. Biomed Microdevices. 2012; 14:583–593. [PubMed: 22374474]
80. Lee SH, Park M, Park CG, Kim B-H, Lee J, Choi S, Nam Sr, Park SH, Choy YB. Implantable micro-chip for controlled delivery of diclofenac sodium. Journal of Controlled Release. 2014; 196:52–59. [PubMed: 25270113]
81. Marsh J, Pidaparti RM. Design Optimization of an Implantable Device Concept for Passive Ocular Drug Delivery. J Med Devices. 2014; 8:021005.
82. Ferrati S, Fine D, You JP, De Rosa E, Hudson L, Zabre E, Hosali S, Zhang L, Hickman C, Bansal SS, Cordero-Reyes AM, Geninatti T, Sih J, Goodall R, Palapattu G, Kloc M, Ghobrial RM, Ferrari M, Grattoni A. Leveraging nanochannels for universal, zero-order drug delivery in vivo. Journal Of Controlled Release. 2013; 172:1011–1019. [PubMed: 24095805]
83. Lee K, Kim C, Kim Y, Ahn B, Bang J, Kim J, Panchapakesan R, Yoon YK, Kang JY, Oh KW. Microfluidic concentration-on-demand combinatorial dilutions. Microfluidics and nanofluidics. 2011; 11:75–86.
84. Nagai N, Kaji H, Onami H, Katsukura Y, Ishikawa Y, Nezhad ZK, Sampei K, Iwata S, Ito S, Nishizawa M. A Platform for Controlled Dual-Drug Delivery to the Retina: Protective Effects against Light-Induced Retinal Damage in Rats. Advanced healthcare materials. 2014; 3:1555–1560. [PubMed: 24753450]
85. Jo WJ, Baek SK, Park JH. A wireless actuating drug delivery system. J Micromech Microeng. 2015; 25:045014.
86. Park H, Yang S, Kang JY, Park MH. On-Demand Drug Delivery System Using Micro-organogels with Gold Nanorods. Acs Med Chem Lett. 2016; 7:1087–1091. [PubMed: 27994743]
87. Altuna A, Bellistri E, Cid E, Aivar P, Gal B, Berganzo J, Gabriel G, Guimerà A, Villa R, Fernández LJ. SU-8 based microprobes for simultaneous neural depth recording and drug delivery in the brain. Lab on a Chip. 2013; 13:1422–1430. [PubMed: 23407672]

88. Hassan, S., Yoon, J. Nano carriers based targeted drug delivery path planning using hybrid particle swarm optimizer and artificial magnetic fields. 2012 12th International Conference on Control, Automation and Systems (Iccas); 2012; p. 1700-1705.

89. Vyas A, Sonker AK, Gidwani B. Carrier-Based Drug Delivery System for Treatment of Acne. Sci World J. 2014

90. Ustundag-Okur N, Gokce EH, Bozbiyik DI, Egrilmez S, Ertan G, Ozer O. Novel nanostructured lipid carrier-based inserts for controlled ocular drug delivery: evaluation of corneal bioavailability and treatment efficacy in bacterial keratitis. Expert Opin Drug Del. 2015; 12:1791–1807.

91. Tsui JH, Lee W, Pun SH, Kim J, Kim DH. Microfluidics-assisted in vitro drug screening and carrier production. Advanced drug delivery reviews. 2013; 65:1575–1588. [PubMed: 23856409]

92. Wei J, Ju XJ, Zou XY, Xie R, Wang W, Liu YM, Chu LY. Drug delivery: multi- stimuli-responsive microcapsules for adjustable controlled-release. Advanced Functional Materials. 2014; 24:3290–3290.

93. Zhao CX. Multiphase flow microfluidics for the production of single or multiple emulsions for drug delivery. Advanced Drug Delivery Reviews. 2013; 65:1420–1446. [PubMed: 23770061]

94. Bawazer LA, McNally CS, Empson CJ, Marchant WJ, Comyn TP, Niu X, Cho S, McPherson MJ, Binks BP, Meldrum FC. Combinatorial microfluidic droplet engineering for biomimetic material synthesis. Science Advances. 2016; 2:e1600567. [PubMed: 27730209]

95. Iqbal M, Zafar N, Fessi H, Elaissari A. Double emulsion solvent evaporation techniques used for drug encapsulation. International Journal of Pharmaceutics. 2015; 496:173–190. [PubMed: 26522982]

96. Ramazani F, Chen W, van Nostrum CF, Storm G, Kiessling F, Lammers T, Hennink WE, Kok RJ. Strategies for encapsulation of small hydrophilic and amphiphilic drugs in PLGA microspheres: state-of-the-art and challenges. International Journal of Pharmaceutics. 2016; 499:358–367. [PubMed: 26795193]

97. Xie X, Zhang W, Abbaspourrad A, Ahn J, Bader A, Bose S, Vegas A, Lin J, Tao J, Hang T. Microfluidic Fabrication of Colloidal Nanomaterials-Encapsulated Microcapsules for Biomolecular Sensing. Nano Letters. 2017; 17:2015–2020. [PubMed: 28152589]

98. Li J, Yang L, Fan X, Zhang J, Wang F, Wang Z. Temperature and glucose dual-responsive carriers bearing poly (N-isopropylacrylamide) and phenylboronic acid for insulin controlled release: a review. International Journal of Polymeric Materials and Polymeric Biomaterials. 2017

99. Zhang MJ, Wang W, Xie R, Ju XJ, Liu L, Gu YY, Chu LY. Microfluidic fabrication of monodisperse microcapsules for glucose-response at physiological temperature. Soft Matter. 2013; 9:4150–4159.

100. Abbaspourrad A, Datta SS, Weitz DA. Controlling release from pH-responsive microcapsules. Langmuir. 2013; 29:12697–12702. [PubMed: 24041287]

101. Wei J, Ju XJ, Xie R, Mou CL, Lin X, Chu LY. Novel cationic pH-responsive poly (N, N-dimethylaminoethyl methacrylate) microcapsules prepared by a microfluidic technique. Journal of Colloid and Interface Science. 2011; 357:101–108. [PubMed: 21345438]

102. Yang CH, Wang CY, Grumezescu AM, Wang AHJ, Hsiao CJ, Chen ZY, Huang KS. Core-shell structure microcapsules with dual pH-responsive drug release function. Electrophoresis. 2014; 35:2673–2680. [PubMed: 24917513]

103. Yeh CH, Chen YC, Lin YC. Generation of droplets with different concentrations using gradient-microfluidic droplet generator. Microfluidics and Nanofluidics. 2011; 11:245–253.

104. Liu L, Wu F, Ju XJ, Xie R, Wang W, Niu CH, Chu LY. Preparation of monodisperse calcium alginate microcapsules via internal gelation in microfluidic-generated double emulsions. Journal of Colloid and Interface Science. 2013; 404:85–90. [PubMed: 23711658]

105. Pessi J, Santos HA, Miroshnyk I, Weitz DA, Mirza S. Microfluidics-assisted engineering of polymeric microcapsules with high encapsulation efficiency for protein drug delivery. International Journal of Pharmaceutics. 2014; 472:82–87. [PubMed: 24928131]

106. Cheng WC, He Y, Chang AY, Que L. A microfluidic chip for controlled release of drugs from microcapsules. Biomicrofluidics. 2013; 7:064102.

107. Yukuyama MN, Ghisleni DD, Pinto TJ, Bou-Chacra NA. Nanoemulsion: process selection and application in cosmetics--a review. International journal of cosmetic science. 2016; 38:13–24. [PubMed: 26171789]
108. Gao YA, Qi XJ, Zheng YP, Ji HY, Wu LH, Zheng NN, Tang JL. Nanoemulsion enhances alpha-tocopherol succinate bioavailability in rats. Int J Pharmaceut. 2016; 515:506–514.
109. de Paula LB, Primo FL, Pinto MR, Morais PC, Tedesco AC. Evaluation of a chloroaluminium phthalocyanine-loaded magnetic nanoemulsion as a drug delivery device to treat glioblastoma using hyperthermia and photodynamic therapy. Rsc Adv. 2017; 7:9115–9122.
110. Soltani S, Zakeri-Milani P, Barzegar-Jalali M, Jelvehgari M. Design of eudragit RL nanoparticles by nanoemulsion method as carriers for ophthalmic drug delivery of ketotifen fumarate. Iran J Basic Med Sci. 2016; 19:850–860.
111. Patel RP, Joshi JR. An overview on nanoemulsion: A novel approach. International Journal of Pharmaceutical Sciences and Research. 2012; 3:4640.
112. Tan SL, Stanslas J, Basri M, Karjiban RAA, Kirby BP, Sani D, Bin Basri H. Nanoemulsion-based Parenteral Drug Delivery System of Carbamazepine: Preparation, Characterization, Stability Evaluation and Blood-Brain Pharmacokinetics. Curr Drug Deliv. 2016; 12:795–804.
113. Yildiz E, Demirkesen I, Mert B. High Pressure Microfluidization of Agro by-product to Functionalized Dietary Fiber and Evaluation as a Novel Bakery Ingredient. J Food Quality. 2016; 39:599–610.
114. Durukan O, Kahraman I, Parlevliet P, Geistbeck M, Seyhan AT. Microfluidization, time-effective and solvent free processing of nanoparticle containing thermosetting matrix resin suspensions for producing composites with enhanced thermal properties. Eur Polym J. 2016; 85:575–587.
115. Seok SH, Kang SY, Seo JW, Kim SH, Hwang KM, Park ES. Formulation of Nanoparticle Containing Everolimus Using Microfluidization and Freeze-Drying. Chem Pharm Bull. 2016; 64:1445–1449. [PubMed: 27725499]
116. Sun CX, Dai L, Liu FG, Gao YX. Dynamic high pressure microfluidization treatment of zein in aqueous ethanol solution. Food Chem. 2016; 210:388–395. [PubMed: 27211662]
117. Uluata S, Decker EA, McClements DJ. Optimization of Nanoemulsion Fabrication Using Microfluidization: Role of Surfactant Concentration on Formation and Stability. Food Biophys. 2016; 11:52–59.
118. Choi CH, Kim J, Nam JO, Kang SM, Jeong SG, Lee CS. Microfluidic design of complex emulsions. ChemPhysChem. 2014; 15:21–29. [PubMed: 24399799]
119. Hussain A, Samad A, Singh SK, Ahsan MN, Haque MW, Faruk A, Ahmed FJ. Nanoemulsion gel-based topical delivery of an antifungal drug: in vitro activity and in vivo evaluation. Drug Deliv. 2016; 23:652–667.
120. Khani S, Keyhanfar F, Amani A. Design and evaluation of oral nanoemulsion drug delivery system of mebudipine. Drug Deliv. 2016; 23:2035–2043. [PubMed: 26406153]
121. Salim N, Ahmad N, Musa SH, Hashim R, Tadros TF, Basri M. Nanoemulsion as a topical delivery system of antipsoriatic drugs. Rsc Adv. 2016; 6:6234–6250.
122. Jo YJ, Kwon YJ. Characterization of beta-carotene nanoemulsions prepared by microfluidization technique. Food Sci Biotechnol. 2014; 23:107–113.
123. Sivakumar M, Tang SY, Tan KW. Cavitation technology - a greener processing technique for the generation of pharmaceutical nanoemulsions. Ultrasonics sonochemistry. 2014; 21:2069–2083. [PubMed: 24755340]
124. Lu Y, Park K. Polymeric micelles and alternative nanonized delivery vehicles for poorly soluble drugs. International journal of pharmaceutics. 2013; 453:198–214. [PubMed: 22944304]
125. Salvia-Trujillo L, Rojas-Grau A, Soliva-Fortuny R, Martin-Belloso O. Physicochemical characterization and antimicrobial activity of food-grade emulsions and nanoemulsions incorporating essential oils. Food Hydrocolloid. 2015; 43:547–556.
126. Ostertag F, Weiss J, McClements DJ. Low-energy formation of edible nanoemulsions: Factors influencing droplet size produced by emulsion phase inversion. J Colloid Interf Sci. 2012; 388:95–102.

127. Shakeel F, Shafiq S, Haq N, Alanazi FK, Alsarra IA. Nanoemulsions as potential vehicles for transdermal and dermal delivery of hydrophobic compounds: an overview. Expert Opin Drug Del. 2012; 9:953–974.
128. Ahmed K, Li Y, McClements DJ, Xiao H. Nanoemulsion-and emulsion-based delivery systems for curcumin: Encapsulation and release properties. Food Chem. 2012; 132:799–807.
129. Tang SY, Shridharan P, Sivakumar M. Impact of process parameters in the generation of novel aspirin nanoemulsions - Comparative studies between ultrasound cavitation and microfluidizer. Ultrasonics sonochemistry. 2013; 20:485–497. [PubMed: 22633626]
130. Choi CH, Weitz DA, Lee CS. One Step Formation of Controllable Complex Emulsions: From Functional Particles to Simultaneous Encapsulation of Hydrophilic and Hydrophobic Agents into Desired Position. Adv Mater. 2013; 25:2536–2541. [PubMed: 23526714]
131. Zheng Y, Ouyang WQ, Wei YP, Syed SF, Hao CS, Wang BZ, Shang YH. Effects of Carbopol (R) 934 proportion on nanoemulsion gel for topical and transdermal drug delivery: a skin permeation study. Int J Nanomed. 2016; 11:5971–5987.
132. Zhigaltsev IV, Belliveau N, Hafez I, Leung AK, Huft J, Hansen C, Cullis PR. Bottom-up design and synthesis of limit size lipid nanoparticle systems with aqueous and triglyceride cores using millisecond microfluidic mixing. Langmuir. 2012; 28:3633–3640. [PubMed: 22268499]
133. Yi J, Zhong F, Zhang Y, Yokoyama W, Zhao L. Effects of lipids on in vitro release and cellular uptake of β-carotene in nanoemulsion-based delivery systems. Journal of agricultural and food chemistry. 2015; 63:10831–10837. [PubMed: 26629789]
134. Chhabra G, Chuttani K, Mishra AK, Pathak K. Design and development of nanoemulsion drug delivery system of amlodipine besilate for improvement of oral bioavailability. Drug development and industrial pharmacy. 2011; 37:907–916. [PubMed: 21401341]
135. He W, Lu Y, Qi JP, Chen LY, Hu FQ, Wu W. Nanoemulsion-templated shell-crosslinked nanocapsules as drug delivery systems. Int J Pharmaceut. 2013; 445:69–78.
136. Tatham LM, Rannard SP, Owen A. Nanoformulation strategies for the enhanced oral bioavailability of antiretroviral therapeutics. Therapeutic delivery. 2015; 6:469–490. [PubMed: 25996045]
137. Singh Y, Meher JG, Raval K, Khan FA, Chaurasia M, Jain NK, Chourasia MK. Nanoemulsion: Concepts, development and applications in drug delivery. Journal of controlled release: official journal of the Controlled Release Society. 2017; 252:28–49. [PubMed: 28279798]
138. Gianella A, Jarzyna PA, Mani V, Ramachandran S, Calcagno C, Tang J, Kann B, Dijk WJ, Thijssen VL, Griffioen AW. Multifunctional nanoemulsion platform for imaging guided therapy evaluated in experimental cancer. ACS nano. 2011; 5:4422–4433. [PubMed: 21557611]
139. O'Hanlon CE, Amede KG, Meredith R, Janjic JM. NIR-labeled perfluoropolyether nanoemulsions for drug delivery and imaging. Journal of fluorine chemistry. 2012; 137:27–33. [PubMed: 22675234]
140. Khan IU, Serra CA, Anton N, Er-Rafik M, Blanck C, Schmutz M, Kraus I, Messaddeq N, Sutter C, Anton H. Microfluidic conceived Trojan microcarriers for oral delivery of nanoparticles. International journal of pharmaceutics. 2015; 493:7–15. [PubMed: 26116014]
141. Paranjpe M, Müller-Goymann CC. Nanoparticle-mediated pulmonary drug delivery: a review. International journal of molecular sciences. 2014; 15:5852–5873. [PubMed: 24717409]
142. Fu G, Sanjay ST, Dou M, Li X. Nanoparticle-mediated photothermal effect enables a new method for quantitative biochemical analysis using a thermometer. Nanoscale. 2016; 8:5422–5427. [PubMed: 26838516]
143. Fu G, Sanjay ST, Li X. Cost-effective and sensitive colorimetric immunosensing using an iron oxide-to-Prussian blue nanoparticle conversion strategy. Analyst. 2016; 141:3883–3889. [PubMed: 27140740]
144. Kraft JC, Freeling JP, Wang Z, Ho RJY. Emerging research and clinical development trends of liposome and lipid nanoparticle drug delivery systems. Journal of Pharmaceutical Sciences. 2014; 103:29–52. [PubMed: 24338748]
145. Ding S, Anton N, Vandamme TF, Serra CA. Microfluidic nanoprecipitation systems for preparing pure drug or polymeric drug loaded nanoparticles: an overview. Expert opinion on drug delivery. 2016; 13:1447–1460. [PubMed: 27253154]

146. Karnik R, Gu F, Basto P, Cannizzaro C, Dean L, Kyei-Manu W, Langer R, Farokhzad OC. Microfluidic platform for controlled synthesis of polymeric nanoparticles. Nano Letters. 2008; 8:2906–2912. [PubMed: 18656990]

147. Ma J, Lee SMY, Yi C, Li CW. Controllable synthesis of functional nanoparticles by microfluidic platforms for biomedical applications–a review. Lab on a Chip. 2017; 17:209–226. [PubMed: 27991629]

148. Liu Y, Du J, Choi Js, Chen KJ, Hou S, Yan M, Lin WY, Chen KS, Ro T, Lipshutz GS. A high-throughput platform for formulating and screening multifunctional nanoparticles capable of simultaneous delivery of genes and transcription factors. Angewandte Chemie International Edition. 2016; 55:169–173. [PubMed: 26768819]

149. Rao DA, Robinson JR. Effect of size and surface properties of biodegradable PLGA-PMA: PLA: PEG nanoparticles on lymphatic uptake and retention in rats. Journal of Controlled Release. 2008; 132:e45–e47.

150. Cabral H, Matsumoto Y, Mizuno K, Chen Q, Murakami M, Kimura M, Terada Y, Kano MR, Miyazono K, Uesaka M. Accumulation of sub-100 nm polymeric micelles in poorly permeable tumours depends on size. Nature Nanotechnology. 2011; 6:815–823.

151. Semple SC, Akinc A, Chen J, Sandhu AP, Mui BL, Cho CK, Sah DWY, Stebbing D, Crosley EJ, Yaworski E. Rational design of cationic lipids for siRNA delivery. Nature Biotechnology. 2010; 28:172–176.

152. Leung AKK, Hafez IM, Baoukina S, Belliveau NM, Zhigaltsev IV, Afshinmanesh E, Tieleman DP, Hansen CL, Hope MJ, Cullis PR. Lipid nanoparticles containing siRNA synthesized by microfluidic mixing exhibit an electron-dense nanostructured core. The Journal of Physical Chemistry C. 2012; 116:18440–18450.

153. Park JH, Saravanakumar G, Kim K, Kwon IC. Targeted delivery of low molecular drugs using chitosan and its derivatives. Advanced Drug Delivery Reviews. 2010; 62:28–41. [PubMed: 19874862]

154. Kumar MNVR, Muzzarelli RA, Muzzarelli C, Sashiwa H, Domb AJ. Chitosan chemistry and pharmaceutical perspectives. Chemical Reviews. 2004; 104:6017–6084. [PubMed: 15584695]

155. Majedi FS, Hasani-Sadrabadi MM, Emami SH, Shokrgozar MA, VanDersarl JJ, Dashtimoghadam E, Bertsch A, Renaud P. Microfluidic assisted self-assembly of chitosan based nanoparticles as drug delivery agents. Lab on a Chip. 2013; 13:204–207. [PubMed: 23196715]

156. Dashtimoghadam E, Mirzadeh H, Taromi FA, Nyström B. Microfluidic self-assembly of polymeric nanoparticles with tunable compactness for controlled drug delivery. Polymer. 2013; 54:4972–4979.

157. Shamsi M, Zahedi P, Ghourchian H, Minaeian S. Microfluidic-aided fabrication of nanoparticles blend based on chitosan for a transdermal multidrug delivery application. International Journal of Biological Macromolecules. 2017; 99:433–442. [PubMed: 28274863]

158. Liu D, Zhang H, Cito S, Fan J, Mäkilä EM, Salonen JJ, Hirvonen J, Sikanen TM, Weitz DA, Santos HA. Core/shell nanocomposites produced by superfast sequential microfluidic nanoprecipitation. Nano Letters. 2017; 17:606–614. [PubMed: 28060521]

159. Othman R, Vladisavljević GT, Thomas NL, Nagy ZK. Fabrication of composite poly (d, l-lactide)/montmorillonite nanoparticles for controlled delivery of acetaminophen by solvent-displacement method using glass capillary microfluidics. Colloids and Surfaces B: Biointerfaces. 2016; 141:187–195. [PubMed: 26852102]

160. Duan JH, Mansour HM, Zhang YD, Deng XM, Chen YX, Wang JW, Pan YF, Zhao JF. Reversion of multidrug resistance by co-encapsulation of doxorubicin and curcumin in chitosan/poly(butyl cyanoacrylate) nanoparticles. Int J Pharmaceut. 2012; 426:193–201.

161. Guimaraes PPG, Oliveira SR, Rodrigues GD, Gontijo SML, Lula IS, Cortes ME, Denadai AML, Sinisterra RD. Development of Sulfadiazine-Decorated PLGA Nanoparticles Loaded with 5-Fluorouracil and Cell Viability. Molecules. 2015; 20:879–899. [PubMed: 25580685]

162. Huang P, Zhao J, Wei CJ, Hou XH, Chen PZ, Tan Y, He CY, Wang ZY, Chen ZY. Erythrocyte membrane based cationic polymer-mcDNA complexes as an efficient gene delivery system. Biomater Sci-Uk. 2017; 5:120–127.

163. Jang M, Han HD, Ahn HJ. A RNA nanotechnology platform for a simultaneous two-in-one siRNA delivery and its application in synergistic RNAi therapy. Sci Rep-Uk. 2016; 6
164. Larson N, Ghandehari H. Polymeric Conjugates for Drug Delivery. Chem Mater. 2012; 24:840–853. [PubMed: 22707853]
165. Tosi G, Bortot B, Ruozi B, Dolcetta D, Vandelli MA, Forni F, Severini GM. Potential Use of Polymeric Nanoparticles for Drug Delivery Across the Blood-Brain Barrier. Curr Med Chem. 2013; 20:2212–2225. [PubMed: 23458620]
166. Chittasupho C, Thongnopkoon T, Kewsuwan P. Surface Modification of Poly(D,L-lactic-co-glycolic acid) Nanoparticles Using Sodium Carboxymethyl Cellulose as Colloidal Stabilizer. Curr Drug Deliv. 2016; 13:95–104. [PubMed: 26338259]
167. Wang B, Yuan HX, Zhu CL, Yang Q, Lv FT, Liu LB, Wang S. Polymer-drug conjugates for intracellar molecule-targeted photoinduced inactivation of protein and growth inhibition of cancer cells. Sci Rep-Uk. 2012; 2:766.
168. Costa MP, Feitosa ACS, Oliveira FCE, Cavalcanti BC, da Silva EN, Dias GG, Sales FAM, Sousa BL, Barroso-Neto IL, Pessoa C, Caetano EWS, Di Fiore S, Fischer R, Ladeira LO, Freire VN. Controlled Release of Nor--lapachone by PLGA Microparticles: A Strategy for Improving Cytotoxicity against Prostate Cancer Cells. Molecules. 2016; 21:873.
169. Tran TH, Nguyen CT, Kim DP, Lee YK, Huh KM. Microfluidic approach for highly efficient synthesis of heparin-based bioconjugates for drug delivery. Lab Chip. 2012; 12:589–594. [PubMed: 22134726]
170. Shi QS, Liu PF, Sun Y, Zhang HP, Du J, Li F, Du LF, Duan YR. siRNA Delivery Mediated by Copolymer Nanoparticles, Phospholipid Stabilized Sulphur Hexafluoride Microbubbles and Ultrasound. J Biomed Nanotechnol. 2014; 10:436–444. [PubMed: 24730239]
171. Endres T, Zheng MY, Beck-Broichsitter M, Samsonova O, Debus H, Kissel T. Optimising the self-assembly of siRNA loaded PEG-PCL-lPEI nano-carriers employing different preparation techniques. Journal Of Controlled Release. 2012; 160:583–591. [PubMed: 22525320]
172. Zhang L, Feng Q, Wang J, Sun J, Shi X, Jiang X. Microfluidic synthesis of rigid nanovesicles for hydrophilic reagents delivery. Angewandte Chemie International Edition. 2015; 54:3952–3956. [PubMed: 25704675]
173. Takami EA, Erogbogbo F. Microfluidic synthesis of lipid-polymer hybrid nanoparticles for targeted drug delivery. MRS Advances. 2016:1–6.
174. Zhang L, Feng Q, Wang J, Zhang S, Ding B, Wei Y, Dong M, Ryu JY, Yoon TY, Shi X. Microfluidic synthesis of hybrid nanoparticles with controlled lipid layers: understanding flexibility-regulated cell–nanoparticle interaction. ACS nano. 2015; 9:9912–9921. [PubMed: 26448362]
175. Valencia PM, Pridgen EM, Rhee M, Langer R, Farokhzad OC, Karnik R. Microfluidic platform for combinatorial synthesis and optimization of targeted nanoparticles for cancer therapy. ACS Nano. 2013; 7:10671–10680. [PubMed: 24215426]
176. Ozcelikkale A, Moon Hr, Linnes M, Han B. In vitro microfluidic models of tumor microenvironment to screen transport of drugs and nanoparticles. Wiley Interdisciplinary Reviews: Nanomedicine and Nanobiotechnology. 2017
177. Zhai Z, Zhang F, Chen X, Zhong J, Liu G, Tian Y, Huang Q. Uptake of silver nanoparticles by DHA-treated cancer cells examined by surface-enhanced Raman spectroscopy in a microfluidic chip. Lab on a Chip. 2017
178. Carvalho MR, Maia FR, Silva-Correia J, Costa BM, Reis RL, Oliveira JM. A semiautomated microfluidic platform for real-time investigation of nanoparticles' cellular uptake and cancer cells' tracking. Nanomedicine. 2017; 12:581–596. [PubMed: 28186438]
179. Lukianova-Hleb EY, Kim YS, Belatsarkouski I, Gillenwater AM, O'Neill BE, Lapotko DO. Intraoperative diagnostics and elimination of residual microtumours with plasmonic nanobubbles. Nature Nanotechnology. 2016; 11:525–532.
180. Ferrari M. Cancer nanotechnology: opportunities and challenges. Nature Reviews Cancer. 2005; 5:161–171. [PubMed: 15738981]
181. Zhang H, Liu D, Wang L, Liu Z, Wu R, Janoniene A, Ma M, Pan G, Baranauskiene L, Zhang L. Microfluidic encapsulation of Prickly zinc-doped copper oxide nanoparticles with VD1142

modified spermine acetalated dextran for efficient cancer therapy. Advanced Healthcare Materials. 2017

182. Prausnitz MR, Langer R. Transdermal drug delivery. Nature biotechnology. 2008; 26:1261–1268.
183. Kim BH, Seo YH. Transdermal Drug Delivery Devices Based on Microneedles: A Review. Journal of mucopolysaccharidosis and rare disease. 2015; 1:5–14.
184. Donnelly, RF., Singh, TRR., Morrow, DI., Woolfson, AD. Microneedle-mediated transdermal and intradermal drug delivery. John Wiley & Sons; 2012.
185. Mitragotri S, Nanotherapeutics TP, Hrkach J, Fan Z, Ho JC, Yerushalmi R, Javey A, Ozkan M, Ozkan CS, Lee JD. Recent developments in needle-free drug delivery. Frontiers of Engineering: Reports on Leading-Edge Engineering from the 2008 Symposium. 2009
186. Karande P, Jain A, Ergun K, Kispersky V, Mitragotri S. Design principles of chemical penetration enhancers for transdermal drug delivery. Proceedings of the national academy of sciences of the United States of America. 2005; 102:4688–4693. [PubMed: 15774584]
187. Prausnitz MR. Microneedles for transdermal drug delivery. Advanced drug delivery reviews. 2004; 56:581–587. [PubMed: 15019747]
188. Römgens A, Bader D, Bouwstra J, Baaijens F, Oomens C. Monitoring the penetration process of single microneedles with varying tip diameters. journal of the mechanical behavior of biomedical materials. 2014; 40:397–405. [PubMed: 25305633]
189. Loizidou EZ, Inoue NT, Ashton-Barnett J, Barrow DA, Allender CJ. Evaluation of geometrical effects of microneedles on skin penetration by CT scan and finite element analysis. European Journal of Pharmaceutics and Biopharmaceutics. 2016; 107:1–6. [PubMed: 27373753]
190. Watanabe T, Hagino K, Sato T. Evaluation of the effect of polymeric microneedle arrays of varying geometries in combination with a high-velocity applicator on skin permeability and irritation. Biomedical microdevices. 2014; 16:591–597. [PubMed: 24733417]
191. Li QY, Zhang JN, Chen BZ, Wang QL, Guo XD. A solid polymer microneedle patch pretreatment enhances the permeation of drug molecules into the skin. RSC Advances. 2017; 7:15408–15415.
192. Narayanan SP, Raghavan S. Solid silicon microneedles for drug delivery applications. The International Journal of Advanced Manufacturing Technology. 2016:1–16.
193. Kim YC, Park JH, Prausnitz MR. Microneedles for drug and vaccine delivery. Advanced drug delivery reviews. 2012; 64:1547–1568. [PubMed: 22575858]
194. Donnelly RF, Majithiya R, Singh TRR, Morrow DI, Garland MJ, Demir YK, Migalska K, Ryan E, Gillen D, Scott CJ. Design, optimization and characterisation of polymeric microneedle arrays prepared by a novel laser-based micromoulding technique. Pharmaceutical research. 2011; 28:41–57. [PubMed: 20490627]
195. Kaur M, Ita KB, Popova IE, Parikh SJ, Bair DA. Microneedle-assisted delivery of verapamil hydrochloride and amlodipine besylate. European Journal of Pharmaceutics and Biopharmaceutics. 2014; 86:284–291. [PubMed: 24176676]
196. Nguyen J, Ita KB, Morra MJ, Popova IE. The Influence of Solid Microneedles on the Transdermal Delivery of Selected Antiepileptic Drugs. Pharmaceutics. 2016; 8:33.
197. Kumar A, Li X, Sandoval MA, Rodriguez BL, Sloat BR, Cui Z. Permeation of antigen protein-conjugated nanoparticles and live bacteria through microneedle-treated mouse skin. Int J Nanomedicine. 2011; 6:1253–1264. [PubMed: 21753877]
198. Guo L, Qiu Y, Chen J, Zhang S, Xu B, Gao Y. Effective transcutaneous immunization against hepatitis B virus by a combined approach of hydrogel patch formulation and microneedle arrays. Biomedical microdevices. 2013; 15:1077–1085. [PubMed: 23893014]
199. Wang J, Li B, Wu MX. Effective and lesion-free cutaneous influenza vaccination. Proceedings of the National Academy of Sciences. 2015; 112:5005–5010.
200. Zhang S, Qiu Y, Gao Y. Enhanced delivery of hydrophilic peptides in vitro by transdermal microneedle pretreatment. Acta Pharmaceutica Sinica B. 2014; 4:100–104. [PubMed: 26579370]
201. Hickerson RP, Wey WC, Rimm DL, Speaker T, Suh S, Flores MA, Gonzalez-Gonzalez E, Leake D, Contag CH, Kaspar RL. Gene silencing in skin after deposition of self-delivery siRNA with a motorized microneedle array device. Molecular Therapy—Nucleic Acids. 2013; 2:e129. [PubMed: 24150576]

202. Deng Y, Chen J, Zhao Y, Yan X, Zhang L, Choy K, Hu J, Sant HJ, Gale BK, Tang T. Transdermal Delivery of siRNA through Microneedle Array. Scientific reports. 2016; 6

203. Ghosh P, Pinninti RR, Hammell DC, Paudel KS, Stinchcomb AL. Development of a codrug approach for sustained drug delivery across microneedle-treated skin. Journal of pharmaceutical sciences. 2013; 102:1458–1467. [PubMed: 23417751]

204. Ghosh P, Brogden NK, Stinchcomb AL. Fluvastatin as a Micropore Lifetime Enhancer for Sustained Delivery Across Microneedle-Treated Skin. Journal of pharmaceutical sciences. 2014; 103:652–660. [PubMed: 24395718]

205. Ghosh P. Formulation optimization for pore lifetime enhancement and sustained drug delivery across microneedle treated skin. 2013

206. Yu W, Jiang G, Liu D, Li L, Chen H, Liu Y, Huang Q, Tong Z, Yao J, Kong X. Fabrication of biodegradable composite microneedles based on calcium sulfate and gelatin for transdermal delivery of insulin. Materials Science and Engineering: C. 2017; 71:725–734. [PubMed: 27987766]

207. van der Maaden K, Luttge R, Vos PJ, Bouwstra J, Kersten G, Ploemen I. Microneedle-based drug and vaccine delivery via nanoporous microneedle arrays. Drug delivery and translational research. 2015; 5:397–406. [PubMed: 26044672]

208. Ji J, Tay FE, Miao J, Iliescu C. Microfabricated microneedle with porous tip for drug delivery. Journal of Micromechanics and Microengineering. 2006; 16:958.

209. Yan XX, Liu JQ, Jiang SD, Yang B, Yang CS. Fabrication and testing of porous Ti microneedles for drug delivery. Micro & Nano Letters. 2013; 8:906–908.

210. Shirkhanzadeh M. Microneedles coated with porous calcium phosphate ceramics: effective vehicles for transdermal delivery of solid trehalose. Journal of Materials Science: Materials in Medicine. 2005; 16:37–45. [PubMed: 15754142]

211. Yu W, Jiang G, Liu D, Li L, Tong Z, Yao J, Kong X. Transdermal delivery of insulin with bioceramic composite microneedles fabricated by gelatin and hydroxyapatite. Materials Science and Engineering: C. 2017; 73:425–428. [PubMed: 28183628]

212. Boks MA, Unger WW, Engels S, Ambrosini M, van Kooyk Y, Luttge R. Controlled release of a model vaccine by nanoporous ceramic microneedle arrays. International journal of pharmaceutics. 2015; 491:375–383. [PubMed: 26116016]

213. Verhoeven M, Bystrova S, Winnubst L, Qureshi H, De Gruijl TD, Scheper RJ, Luttge R. Applying ceramic nanoporous microneedle arrays as a transport interface in egg plants and an ex-vivo human skin model. Microelectronic engineering. 2012; 98:659–662.

214. Kochhar JS, Lim WXS, Zou S, Foo WY, Pan J, Kang L. Microneedle integrated transdermal patch for fast onset and sustained delivery of lidocaine. Molecular pharmaceutics. 2013; 10:4272–4280. [PubMed: 24044683]

215. van der Maaden K, Trietsch SJ, Kraan H, Varypataki EM, Romeijn S, Zwier R, van der Linden HJ, Kersten G, Hankemeier T, Jiskoot W. Novel hollow microneedle technology for depth-controlled microinjection-mediated dermal vaccination: a study with polio vaccine in rats. Pharmaceutical research. 2014; 31:1846–1854. [PubMed: 24469907]

216. Bal SM, Ding Z, van Riet E, Jiskoot W, Bouwstra JA. Advances in transcutaneous vaccine delivery: do all ways lead to Rome? Journal of controlled release. 2010; 148:266–282. [PubMed: 20869998]

217. van der Maaden K, Jiskoot W, Bouwstra J. Microneedle technologies for (trans) dermal drug and vaccine delivery. Journal of controlled release. 2012; 161:645–655. [PubMed: 22342643]

218. Norman JJ, Gupta J, Patel SR, Park S, Jarrahian C, Zehrung D, Prausnitz MR. Reliability and accuracy of intradermal injection by Mantoux technique, hypodermic needle adapter, and hollow microneedle in pigs. Drug delivery and translational research. 2014; 4:126–130. [PubMed: 25786726]

219. Norman JJ, Choi SO, Tong NT, Aiyar AR, Patel SR, Prausnitz MR, Allen MG. Hollow microneedles for intradermal injection fabricated by sacrificial micromolding and selective electrodeposition. Biomedical microdevices. 2013; 15:203–210. [PubMed: 23053452]

220. Liu Y, Eng PF, Guy OJ, Roberts K, Ashraf H, Knight N. Advanced deep reactive-ion etching technology for hollow microneedles for transdermal blood sampling and drug delivery. IET nanobiotechnology. 2013; 7:59–62. [PubMed: 24046906]

221. Vinayakumar K, Kulkarni PG, Nayak M, Dinesh N, Hegde GM, Ramachandra S, Rajanna K. A hollow stainless steel microneedle array to deliver insulin to a diabetic rat. Journal of Micromechanics and Microengineering. 2016; 26:065013.

222. Lyon BJ, Aria AI, Gharib M. Fabrication of carbon nanotube—polyimide composite hollow microneedles for transdermal drug delivery. Biomedical microdevices. 2014; 16:879–886. [PubMed: 25095899]

223. Schipper P, van der Maaden K, Romeijn S, Oomens C, Kersten G, Jiskoot W, Bouwstra J. Repeated fractional intradermal dosing of an inactivated polio vaccine by a single hollow microneedle leads to superior immune responses. Journal of Controlled Release. 2016; 242:141–147. [PubMed: 27496634]

224. Schipper P, van der Maaden K, Romeijn S, Oomens C, Kersten G, Jiskoot W, Bouwstra J. Determination of depth-dependent intradermal immunogenicity of adjuvanted inactivated polio vaccine delivered by microinjections via hollow microneedles. Pharmaceutical research. 2016; 33:2269–2279. [PubMed: 27317570]

225. Patel SR, Lin AS, Edelhauser HF, Prausnitz MR. Suprachoroidal drug delivery to the back of the eye using hollow microneedles. Pharmaceutical research. 2011; 28:166–176. [PubMed: 20857178]

226. Kim Y, Prausnitz M, Edelhauser H. Distribution And Clearance Of Microparticles And Nanoparticles In The Suprachoroidal Space After Injection Using Hollow Microneedles In Rabbits. Investigative Ophthalmology & Visual Science. 2013; 54:1098–1098.

227. Jun H, Han MR, Kang NG, Park JH, Park JH. Use of hollow microneedles for targeted delivery of phenylephrine to treat fecal incontinence. Journal of Controlled Release. 2015; 207:1–6. [PubMed: 25828366]

228. Norman JJ, Brown MR, Raviele NA, Prausnitz MR, Felner EI. Faster pharmacokinetics and increased patient acceptance of intradermal insulin delivery using a single hollow microneedle in children and adolescents with type 1 diabetes. Pediatric diabetes. 2013; 14:459–465. [PubMed: 23517449]

229. Traverso G, Schoellhammer CM, Schroeder A, Maa R, Lauwers GY, Polat BE, Anderson DG, Blankschtein D, Langer R. Microneedles for drug delivery via the gastrointestinal tract. Journal of pharmaceutical sciences. 2015; 104:362–367. [PubMed: 25250829]

230. Ma Y, Gill HS. Coating Solid Dispersions on Microneedles via a Molten Dip- Coating Method: Development and In Vitro Evaluation for Transdermal Delivery of a Water-Insoluble Drug. Journal of pharmaceutical sciences. 2014; 103:3621–3630. [PubMed: 25213295]

231. Khandan O, Kahook MY, Rao MP. Fenestrated microneedles for ocular drug delivery. Sensors and Actuators B: Chemical. 2016; 223:15–23.

232. Vrdoljak A, McGrath MG, Carey JB, Draper SJ, Hill AV, O'Mahony C, Crean AM, Moore AC. Coated microneedle arrays for transcutaneous delivery of live virus vaccines. Journal of controlled release. 2012; 159:34–42. [PubMed: 22245683]

233. Uddin MJ, Scoutaris N, Klepetsanis P, Chowdhry B, Prausnitz MR, Douroumis D. Inkjet printing of transdermal microneedles for the delivery of anticancer agents. International journal of pharmaceutics. 2015; 494:593–602. [PubMed: 25617676]

234. Pearton M, Saller V, Coulman SA, Gateley C, Anstey AV, Zarnitsyn V, Birchall JC. Microneedle delivery of plasmid DNA to living human skin: Formulation coating, skin insertion and gene expression. Journal of controlled release. 2012; 160:561–569. [PubMed: 22516089]

235. Chong RH, Gonzalez-Gonzalez E, Lara MF, Speaker TJ, Contag CH, Kaspar RL, Coulman SA, Hargest R, Birchall JC. Gene silencing following siRNA delivery to skin via coated steel microneedles: in vitro and in vivo proof-of-concept. Journal of Controlled Release. 2013; 166:211–219. [PubMed: 23313112]

236. Ma Y, Boese SE, Luo Z, Nitin N, Gill HS. Drug coated microneedles for minimally-invasive treatment of oral carcinomas: development and in vitro evaluation. Biomedical microdevices. 2015; 17:44. [PubMed: 25787934]

237. Witting M, Obst K, Pietzsch M, Friess W, Hedtrich S. Feasibility study for intraepidermal delivery of proteins using a solid microneedle array. International journal of pharmaceutics. 2015; 486:52–58. [PubMed: 25819344]

238. Kim MC, Lee JW, Choi HJ, Lee YN, Hwang HS, Lee J, Kim C, Lee JS, Montemagno C, Prausnitz MR. Microneedle patch delivery to the skin of virus-like particles containing heterologous M2e extracellular domains of influenza virus induces broad heterosubtypic cross-protection. Journal of Controlled Release. 2015; 210:208–216. [PubMed: 26003039]

239. Weldon WC, Zarnitsyn VG, Esser ES, Taherbhai MT, Koutsonanos DG, Vassilieva EV, Skountzou I, Prausnitz MR, Compans RW. Effect of adjuvants on responses to skin immunization by microneedles coated with influenza subunit vaccine. PloS one. 2012; 7:e41501. [PubMed: 22848514]

240. Ma Y, Tao W, Krebs SJ, Sutton WF, Haigwood NL, Gill HS. Vaccine delivery to the oral cavity using coated microneedles induces systemic and mucosal immunity. Pharmaceutical research. 2014; 31:2393–2403. [PubMed: 24623480]

241. Kim YC, Edelhauser HF, Prausnitz MR. Intracorneal delivery of bevacizumab using microneedles to treat injury-induced neovascularization. Investigative Ophthalmology & Visual Science. 2012; 53:507–507.

242. Song HB, Lee KJ, Seo IH, Lee JY, Lee SM, Kim JH, Kim JH, Ryu W. Impact insertion of transfer-molded microneedle for localized and minimally invasive ocular drug delivery. Journal of Controlled Release. 2015; 209:272–279. [PubMed: 25937320]

243. Zhang Y, Brown K, Siebenaler K, Determan A, Dohmeier D, Hansen K. Development of lidocaine-coated microneedle product for rapid, safe, and prolonged local analgesic action. Pharmaceutical research. 2012; 29:170–177. [PubMed: 21735335]

244. van der Maaden K, Sekerdag E, Schipper P, Kersten G, Jiskoot W, Bouwstra J. Layer-by-layer assembly of inactivated poliovirus and N-trimethyl chitosan on pH-sensitive microneedles for dermal vaccination. Langmuir. 2015; 31:8654–8660. [PubMed: 26145437]

245. Choi HJ, Yoo DG, Bondy BJ, Quan FS, Compans RW, Kang SM, Prausnitz MR. Stability of influenza vaccine coated onto microneedles. Biomaterials. 2012; 33:3756–3769. [PubMed: 22361098]

246. Mönkäre J, Nejadnik MR, Baccouche K, Romeijn S, Jiskoot W, Bouwstra JA. IgG-loaded hyaluronan-based dissolving microneedles for intradermal protein delivery. Journal of Controlled Release. 2015; 218:53–62. [PubMed: 26437262]

247. Lu Y, Mantha SN, Crowder DC, Chinchilla S, Shah KN, Yun YH, Wicker RB, Choi JW. Microstereolithography and characterization of poly (propylene fumarate)-based drug-loaded microneedle arrays. Biofabrication. 2015; 7:045001. [PubMed: 26418306]

248. Sivaraman A, Banga AK. Novel in situ forming hydrogel microneedles for transdermal drug delivery. Drug Delivery and Translational Research. 2016:1–11. [PubMed: 26712122]

249. Lau S, Fei J, Liu H, Chen W, Liu R. Multilayered pyramidal dissolving microneedle patches with flexible pedestals for improving effective drug delivery. Journal of Controlled Release. 2016

250. Garland MJ, Caffarel-Salvador E, Migalska K, Woolfson AD, Donnelly RF. Dissolving polymeric microneedle arrays for electrically assisted transdermal drug delivery. Journal of controlled release. 2012; 159:52–59. [PubMed: 22265694]

251. Nayak A, Babla H, Han T, Das DB. Lidocaine carboxymethylcellulose with gelatine co-polymer hydrogel delivery by combined microneedle and ultrasound. Drug delivery. 2016; 23:658–669. [PubMed: 25034877]

252. Chen MC, Ling MH, Wang KW, Lin ZW, Lai BH, Chen DH. Near-infrared light-responsive composite microneedles for on-demand transdermal drug delivery. Biomacromolecules. 2015; 16:1598–1607. [PubMed: 25839774]

253. DeMuth PC, Min Y, Irvine DJ, Hammond PT. Implantable silk composite microneedles for programmable vaccine release kinetics and enhanced immunogenicity in transcutaneous immunization. Advanced healthcare materials. 2014; 3:47–58. [PubMed: 23847143]

254. Guo L, Chen J, Qiu Y, Zhang S, Xu B, Gao Y. Enhanced transcutaneous immunization via dissolving microneedle array loaded with liposome encapsulated antigen and adjuvant. International journal of pharmaceutics. 2013; 447:22–30. [PubMed: 23410987]

255. Vassilieva EV, Kalluri H, McAllister D, Taherbhai MT, Esser ES, Pewin WP, Pulit-Penaloza JA, Prausnitz MR, Compans RW, Skountzou I. Improved immunogenicity of individual influenza vaccine components delivered with a novel dissolving microneedle patch stable at room temperature. Drug delivery and translational research. 2015; 5:360–371. [PubMed: 25895053]

256. Yang HW, Ye L, Guo XD, Yang C, Compans RW, Prausnitz MR. Ebola Vaccination Using a DNA Vaccine Coated on PLGA-PLL/γPGA Nanoparticles Administered Using a Microneedle Patch. Advanced Healthcare Materials. 2016

257. Zhu DD, Wang QL, Liu XB, Guo XD. Rapidly Separating Microneedles for Transdermal Drug Delivery. Acta biomaterialia. 2016

258. Gill HS, Prausnitz MR. Coated microneedles for transdermal delivery. Journal of controlled release. 2007; 117:227–237. [PubMed: 17169459]

259. Gill HS, Prausnitz MR. Coating fomulations for microneedles. Pharmaceutical research. 2007; 24:1369–1380. [PubMed: 17385011]

260. Boehm RD, Daniels J, Stafslien S, Nasir A, Lefebvre J, Narayan RJ. Polyglycolic acid microneedles modified with inkjet-deposited antifungal coatings. Biointerphases. 10(2015): 011004.

261. Khan H, Mehta P, Msallam H, Armitage D, Ahmad Z. Smart microneedle coatings for controlled delivery and biomedical analysis. Journal of drug targeting. 2014; 22:790–795. [PubMed: 24892742]

262. Serpe L, Jain A, de Macedo CG, Volpato MC, Groppo FC, Gill HS, Franz-Montan M. Influence of salivary washout on drug delivery to the oral cavity using coated microneedles: An in vitro evaluation. European Journal of Pharmaceutical Sciences. 2016; 93:215–223. [PubMed: 27523787]

263. Zuris JA, Thompson DB, Shu Y, Guilinger JP, Bessen JL, Hu JH, Maeder ML, Joung JK, Chen ZY, Liu DR. Efficient Delivery of Genome-Editing Proteins In Vitro and In Vivo. Nature biotechnology. 2015; 33:73.

264. Kim M, Yang H, Kim H, Jung H. Novel cosmetic patches for wrinkle improvement: retinyl retinoate-and ascorbic acid-loaded dissolving microneedles. International journal of cosmetic science. 2014; 36:207–212. [PubMed: 24910870]

265. Donnelly RF, Singh TRR, Woolfson AD. Microneedle-based drug delivery systems: microfabrication, drug delivery, and safety. Drug delivery. 2010; 17:187–207. [PubMed: 20297904]

266. Cha KJ, Kim T, Park SJ, Kim DS. Simple and cost-effective fabrication of solid biodegradable polymer microneedle arrays with adjustable aspect ratio for transdermal drug delivery using acupuncture microneedles. Journal of Micromechanics and Microengineering. 2014; 24:115015.

267. Liu S, Jin Mn, Quan Ys, Kamiyama F, Kusamori K, Katsumi H, Sakane T, Yamamoto A. Transdermal delivery of relatively high molecular weight drugs using novel self-dissolving microneedle arrays fabricated from hyaluronic acid and their characteristics and safety after application to the skin. European Journal of Pharmaceutics and Biopharmaceutics. 2014; 86:267–276. [PubMed: 24120887]

268. Wang Q, Yao G, Dong P, Gong Z, Li G, Zhang K, Wu C. Investigation on fabrication process of dissolving microneedle arrays to improve effective needle drug distribution. European Journal of Pharmaceutical Sciences. 2015; 66:148–156. [PubMed: 25446513]

269. Mistilis MJ, Bommarius AS, Prausnitz MR. Development of a thermostable microneedle patch for influenza vaccination. Journal of pharmaceutical sciences. 2015; 104:740–749. [PubMed: 25448542]

270. Crichton ML, Donose BC, Chen X, Raphael AP, Huang H, Kendall MA. The viscoelastic, hyperelastic and scale dependent behaviour of freshly excised individual skin layers. Biomaterials. 2011; 32:4670–4681. [PubMed: 21458062]

271. Kim M, Yang H, Kim S, Lee C, Jung H. The Troy Microneedle: A Rapidly Separating, Dissolving Microneedle Formed by Cyclic Contact and Drying on the Pillar (CCDP). PloS one. 2015; 10:e0136513. [PubMed: 26308945]

272. Zhu Z, Ye X, Ku Z, Liu Q, Shen C, Luo H, Luan H, Zhang C, Tian S, Lim C, Huang Z. Transcutaneous immunization via rapidly dissolvable microneedles protects against hand-foot-

and-mouth disease caused by enterovirus 71. Journal of Controlled Release. 2016; 243:291–302. [PubMed: 27793685]

Abbreviations

AB	Amlodipine besylate
AsnB	Asparaginase B
Ag@CD NPs	Beta-cyclodextrin-coated silver NPs
BSA	Bovine serum albumin
BHCl	Bupivacaine hydrochloride
CTB	Cholera toxin B
CMNs	Coated microneedles
CpG OND	CpG oligonucleotide
DC	Dendritic cell
DFC	Diclofenac
DS	Diclofenac sodium
DHA	Dihydroartemisinin
DMNs	Dissolvable microneedles
DTX	Docetaxel
DOX	Doxorubicin
EDV	Edaravone
FSDCs	Fetal skin dendritic cells
FA	Folic acid
FMA	Functional microarray
HFR	Heparin-folic acid-retinoic acid
HBsAg	Hepatitis B surface antigen
HMNs	Hollow microneedles
IPV	Inactivated polio vaccine
IM	Intramuscular
ITP	Iontophoresis
FeO	Iron oxide

LOC	Lab-on-a-chip
LNP	Lipid nanoparticles
MRI	Magnetic resonance imaging
MEMS	Microelectromechanical system
MNs	Microneedles
MNAs	Microneedle arrays
MITP	Microneedle integrated transdermal patch
NTX	Naltrexone
NPs	Nanoparticles
NIR	Near-infrared
NIRF	Near-infrared fluorescence
TMC	N-trimethyl chitosan chloride
p-ATP	Para-aminothiophenol
PFPE	Perfluoropolyether
PAM	Poly(acrylamide)
PEI	Poly(ethylene imine)
PEGDM	Poly(ethyleneglycol)dimethacrylate
PLGA	Poly(lactic-co-glycolic) acid
PMVE/MA	Poly (methyl vinyl ether-co-maleic acid)
PMMA	Poly(methyl methacrylate)
PDM	Poly(N, N-dimethylaminoethyl methacrylate)
PDMS	Polydimethylsiloxane
PDI	Polydispersity index
PEG	Polyethylene glycol
PPF	Poly(propylene fumarate
PCL	Poly(ε-caprolactone)
PVA	Polyvinyl alcohol
PMNs	Porous microneedles
PAV	Prednisolone acetate valerate

PCB	Printed circuit board
RA	Retinoic acid
SMNs	Solid microneedles
SpAcDX	Spermine-modified activated dextran
SHM	Staggered herringbone micromixer
SC	Stratum corneum
TDD	Transdermal drug delivery
TEM	Transmission electron microscope
UNO	Unoprostone
BC	β-Carotene
VD1142	3-(cyclooctylaminee)-2,5,6-trifluoro-4-[(2-hydroxyethyl)sulfonyl] Benzenesulfonamide

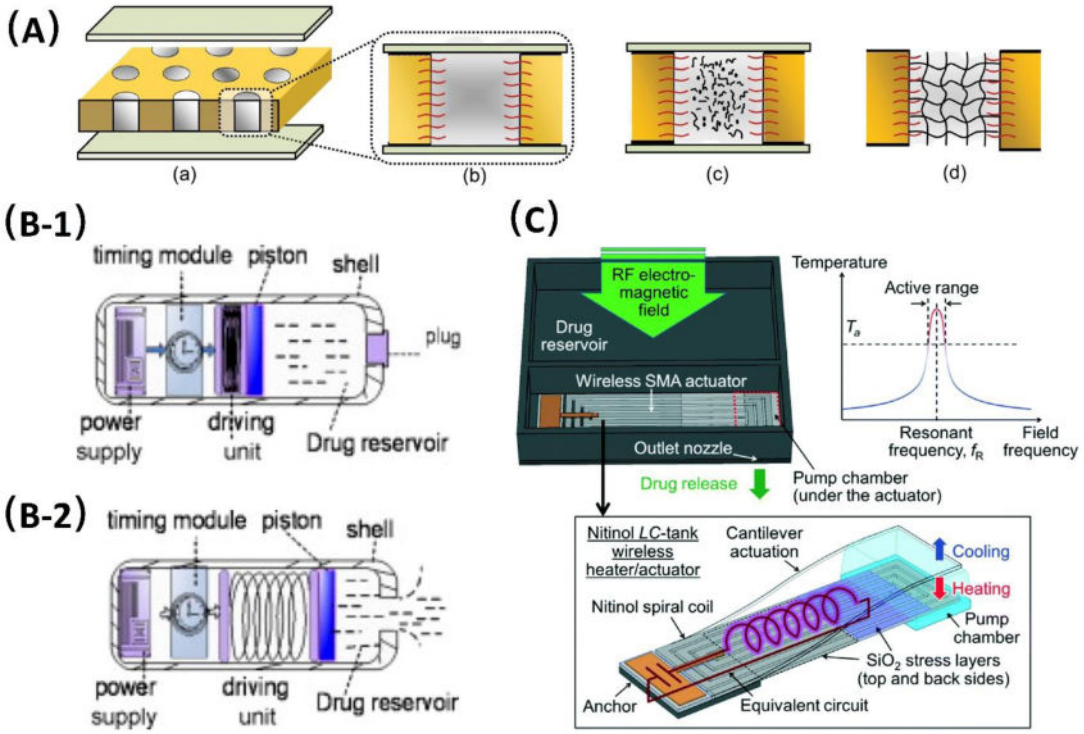

Fig 1.

Drug carrier-free micro-reservoir systems for controlled drug delivery in passive mode (A) and active mode (B and C). (A) Schematic illustration of pore-filling functionalization via in situ photopolymerization during different stages including (a) filling and equilibration of the membrane, (b) during equilibration with reaction mixtures, (c) during UV initiated in situ crosslinking polymerization, and (d) after complete reaction toward hydrogel pore-filled composite membrane. Adapt from Adrus et al. [52]. Copyright RSC 2012. (B) Schematic illustration of two stages of actively controlled drug delivery using a piston: drug inside the electronic capsule (B-1) and drug being released (B-2). Adapted from Zhuang et al. [60]. Copyright Elsevier 2011. (C) Conceptual diagram and frequency-sensitive working principle of the Radio-frequency (RF) powered and implantable chip for local drug delivery operated using tuned RF electromagnetic fields. Adapted from Fong et al. [63]. Copyright RSC 2014.

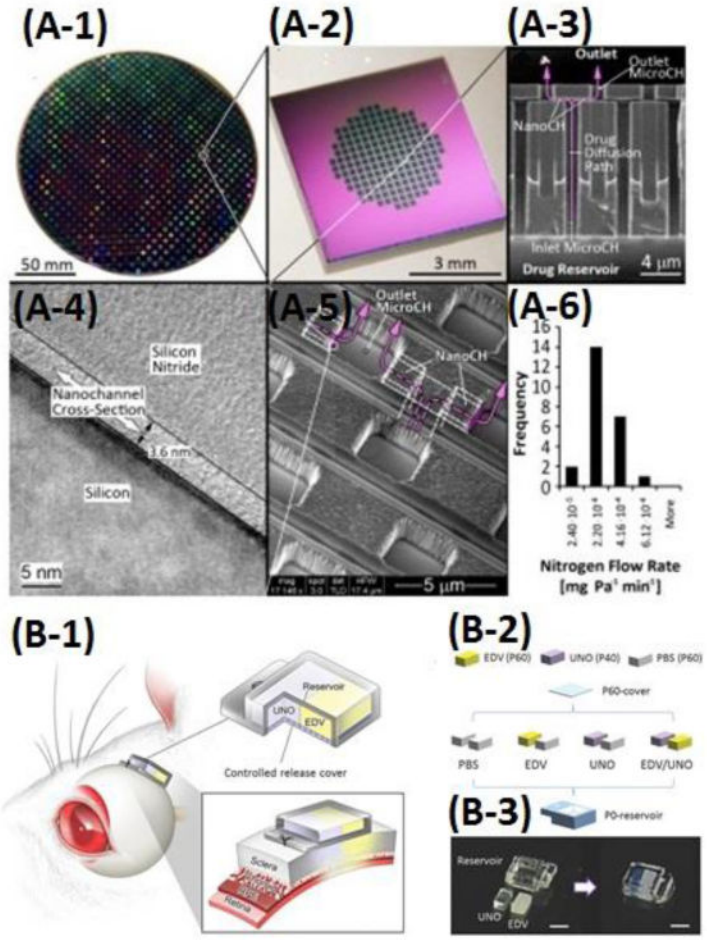

Fig 2.

Drug carrier-free microfluidic LOC systems for controlled drug delivery. (A1-A6) A nanochannel-controlled drug delivery system. (A-1) Image of a wafer containing ~700 nanochannel membranes; (A-2) A nanochannel membrane; (A-3) A cross section showing the vertically oriented inlet and outlet microchannels connected by the horizontally oriented nanochannels; (A-4) A transmission electron micrograph (TEM) of a nanochannel; (A-5) A scanning electron micrograph (SEM) of the outlet microchannels; (A-6) A histogram showing the results of quality-control gas testing performed on 24 membranes. The pink arrows depict the drug delivery path. Adapted from Ferrati et al. [82]. Copyright 2013 Elsevier. (B-1) Schematic of an implantable device on the rat sclera. (B-2) Device conditions for in vivo study of synergistic protective effects of EDV and UNO. (B-3) Photographs of the device before assembling and after assembling. Adapted from Nagai et al. [84]. Copyright 1999-2017 John Wiley & Sons, Inc.

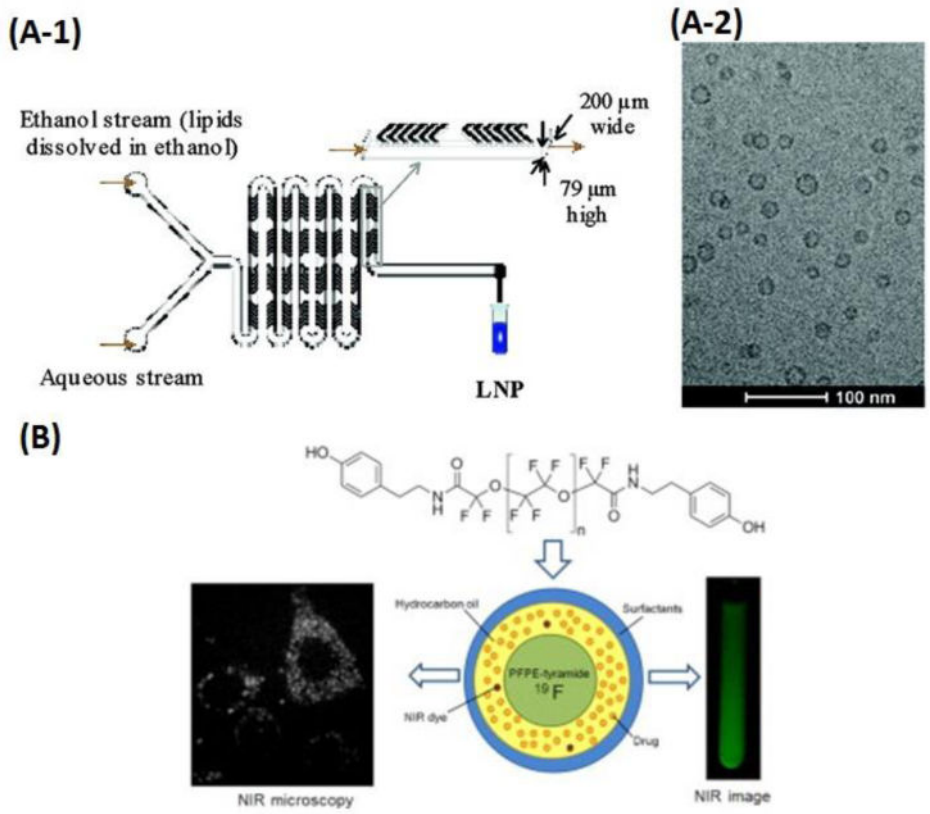

Fig 3.

Syntheses of nanoemulsions-based drug carriers in microfluidic platforms. (A-1) Schematic of LNP formulation process employing a staggered herringbone micromixer. (A-2) Cryo-TEM micrographs of limit size LNP with the total lipid concentration in the ethanol phase of 10 mg/mL. Adapted from Zhigaltsev *et al.* [132]. Copyright 2012 American Chemical Society. (B) Schematic of the PFPE-tyramide nanoemulsions for imaging-guided drug delivery. FSDCs cellular uptake of nanoemulsions visualized by NIR microscopy (left) and NIR fluorescence imaging (at 800 nm, right). Adapted from Hanlon et al. [139]. Copyright 2012 Elsevier.

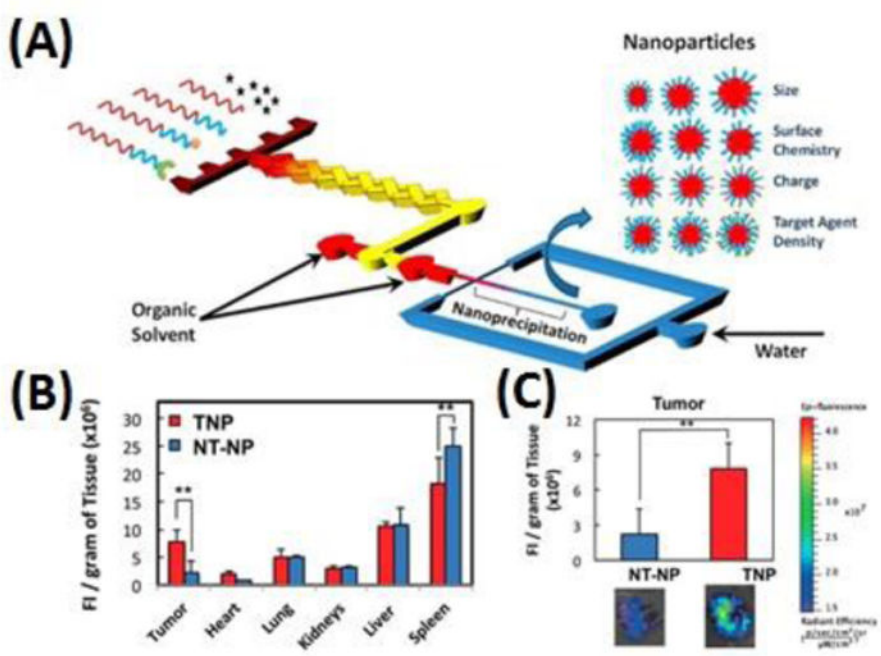

Fig 4.

A microfluidic system for integrated synthesis and screening of nanoparticle drug carriers for cancer therapy. (A) Schematic of rapid synthesis of nanoparticles on a PDMS microfluidic device upon self-assembly through nanoprecipitation. (B) Biodistribution and (C) tumor accumulation of the targeted nanoparticle drugs and non-targeted nanoparticle drugs. Adapted from Valencia et al.[175]. Copyright 2012 ACS.

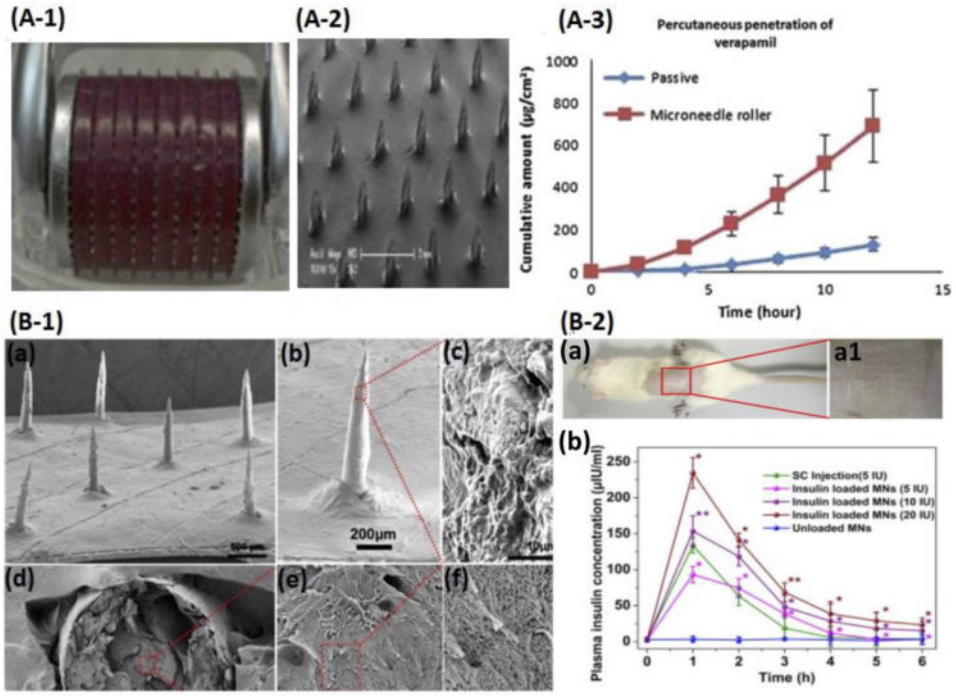

Fig 5.

Solid (A) and Porous (B) Microneedles. (A-1) DermaRoller with 540 MNs. (A-2) Side view of SMNs. (A-3) Passive diffusion and MN-mediated diffusion of verapamil with MN rollers across pig skin. Adapted from Kaur *et al.* [195]. Copyright 2014 Elsevier. (B-1) SEM images of PMNs with different magnifications (a, 500 μm; b, 200 μm), surface region (c,10 μm), and cross-sections (d-f) at different magnifications of 500, 10,000 and 30,000 folds. (B-2) Insulin delivery using PMNs during the treatment process in diabetic rats (a) and plasma insulin levels after administration of insulin-loaded PMN patches (b). Adapted from Yu et al. [206]. Copyright 2014 Elsevier.

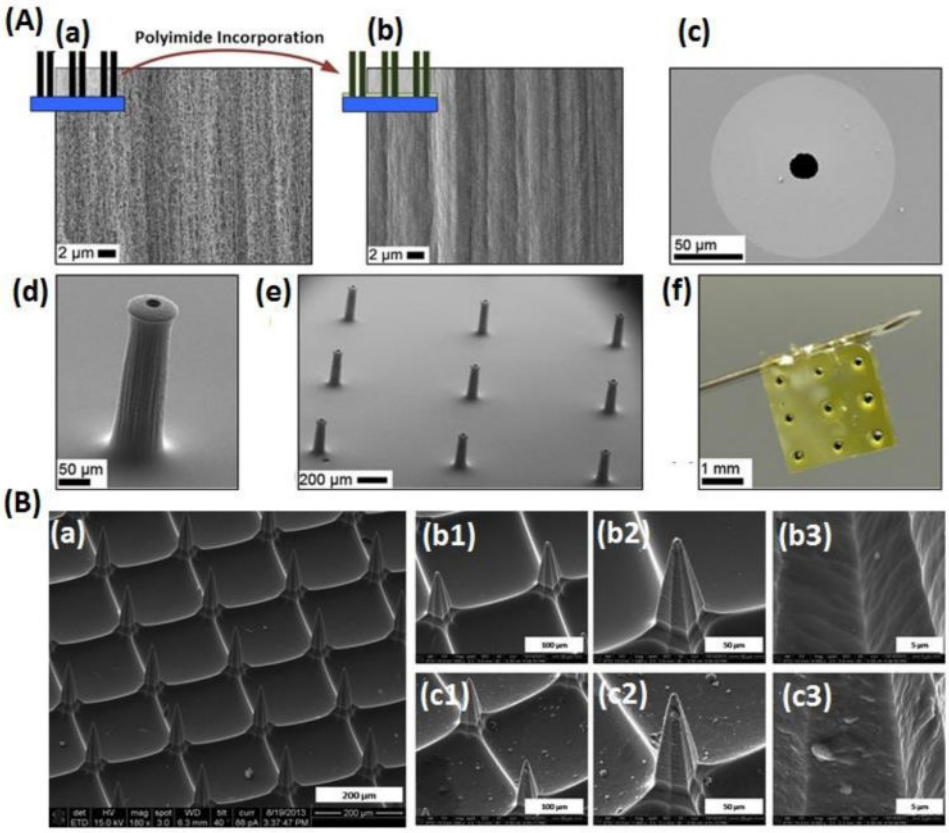

Fig 6.

Hollow (A) and coated (B) MNs. (A) Carbon nanotube-polyimide composite HMNs. (a) The porous structure of CNTs before incorporation of polyimide. (b) Non-porous nanotube-polyimide composite. (c) The underside of an MN showing a clear inner channel. (d) A single HMN. (e) 3 × 3 MNA. (f) Size comparison of HMNs with 30 G hypodermic needle. Adapted from Lyon *et al.* [222]. Copyright 2014 Springer. (B) Scanning electron microscope images of CMNs. Unmodified MNs (a and b) and a pH-sensitive MNA coated with 10 alternate layers of IPV and TMC (c) at different magnifications of 500 (1), 1000 (2), and 8000 (3). Adapted from Maaden et al. [244]. Copyright 2015 ACS.

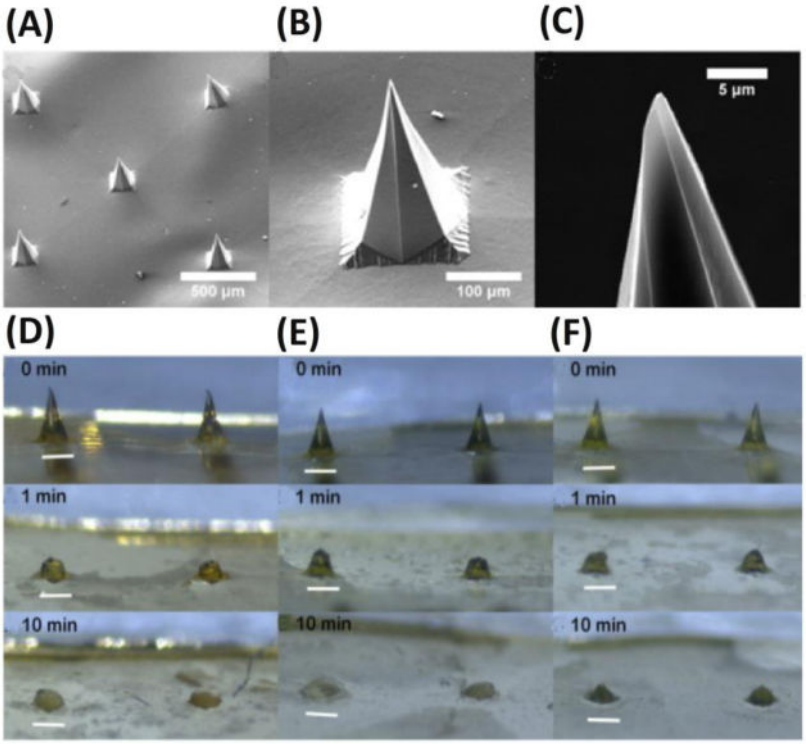

Fig 7.

SEM images of DMNs. (A) SEM image of a MNA. (B) A single DMN. (C) MN tip with 2% IgG. Microscopic images of microneedle tips without IgG (D) and with 2% (E) or 10% (w/w) IgG (F) into ex vivo human skin after different application time periods. Scale bar is 200 µm. Adapted from Mönkäre *et al.* [246] Copyright 2015 Elsevier.

Table 1

Summary of different drug carriers integrated into microfluidic platforms

Drug Carrier Type		Main Material	Size	Synthetic Method	Drug	Target/Application	Ref.
Microcapsules		P(NIPAM-*co*-AAPBA-*co*-AAc)	ID ~240 μm; OD ~360 μm	Microfluidic double emulsion	Rhodamine B; insulin	Glucose-responsive controlled release	[99]
		PAA-b-PMMA	OD ~120-150 μm	Microfluidic double emulsion	--	pH-responsive controlled release	[100]
		PDM	ID ~294 μm; OD ~402 μm	Microfluidic double emulsion	--	pH-responsive controlled release	[101]
		Alginate; chitosan	OD 472-740 μm	Electrostatic microfluidic droplets	Ampicillin; diclofenac	pH-responsive controlled release; Dual-drug carriers	[102]
		Ca-alginate	OD 60-105 μm	gradient-microfluidic droplets	BSA	Pharmaceutical area; Therapeutic proteins	[103]
		Ca-alginate	ID ~383 μm; OD ~467 μm	Microfluidic double emulsion	BSA	Pharmaceutical area; Therapeutic proteins	[104]
		PVA, PCL, PEG	OD 23-47 μm	Microfluidic double emulsion	BSA	Pharmaceutical area; Therapeutic proteins	[105]
		PAH, PSS, FITC	OD 50-80 μm	Microfluidic droplet merging and droplet storage functions	$MnCO_3$	Drug effects on specific cells	[106]
Nanoemulsions		Six dietary lipids (corn oil, canola oil, olive oil, palm oil, coconut oil, MCTs)	~160-180 nm	Micro-fluidization	BC	Caco-2 cells	[133]
		Labrafil M, Tween 80, ethanol	~30-50 nm	Spontaneous emulsification	AB	Heart	[134]
		Soybean oil, PEGylated lipids, oleic acid-coated FeO, Cy7	50 nm	Immediate evaporation	PAV	Kidney, liver	[138]
		PFPE	180 nm	Self-assembly and high energy emulsification	Celecoxib	FSDCs	[139]
		PAM	20-32 nm	Rapid microfluidic mixing	Ketoprofen	Gastro intestinal tract	[140]
NPs	Lipid NPs	POPC, cholesterol, triglyceride triolein	20-50 nm	Rapid microfluidic mixing	Doxorubicin	Pharmaceutical area	[132]
		DLinKC2-DMA, phospholipid, cholesterol, PEG	~80 nm	Rapid microfluidic mixing	siRNA	Therapeutic siRNA	[152]
	Polymer NPs	Chitosan	75-122 nm	Rapid microfluidic mixing	Paclitaxel	Anticancer drug	[155]
		Chitosan	~73-216 nm	Rapid microfluidic mixing	Paclitaxel	Anticancer drug	[156]
		Chitosan	200-300 nm	Rapid microfluidic mixing	Clindamycin phosphate; tretinoin	Transdermal multidrug delivery	[157]
		PLGA-PEG	25-200 nm	Rapid microfluidic mixing	Docetaxel	Drug discovery and clinical translation	[175]

Drug Carrier Type		Main Material	Size	Synthetic Method	Drug	Target/Application	Ref.
		Ag@CD NPs	20-60 nm	Conventional method	Dihydro-artemisinin	Monitoring of drug effect on cancer cells	[177]
		Carboxymethyl chitosan, PAMAM dendrimer	~50 nm	Conventional method	--	Monitoring of drug effect on cancer cells	[178]
	Nano-sized polymeric conjugates	FA, RA	130 nm	Rapid microfluidic mixing	Heparin	KB and A549 cells	[169]
		PEG, PCL, PEI	179 ± 11 nm	Rapid microfluidic mixing	siRNA	SKOV3 cells	[171]
	Hybrid NPs	PLGA, cholesterol	~103-106 nm	Rapid microfluidic mixing	Doxorubicin; combretastatin A4	Anticancer drug	[174]

Note, chemical structures and formulas of small molecular drugs are shown in supplementary Table S2.

Table 2

Summary of controlled drug delivery using different MNs

Devices	Device Features	Fabrication materials	Drugs	Delivery routes	Applications	Study types	Ref.
SMNs	- Simple and low-cost processing - A large variety of materials for the fabrication	Stainless steel	Verapamil & Amlodipine	Pig skin/Transcutaneous	Anti-hypersensitive	In-vitro	[195]
		MN roller	Tiagabine & Carbamazepine	Pig skin/Transdermal	Anti-epileptic	In-vitro	[196]
		Dermaroller	Ovalbumin Ag	Mouse skin/Transcutaneous	Immunization	In-vitro/In-vivo	[197]
		Silicon	HBsAg	Pig skin/Rat abdomen Transcutaneous	Immunization	In-vitro/In-vivo	[198]
		PVP	Influenza vaccine/PR8	Mice/Swine/Cutaneous	Vaccination	In-vivo	[199]
		Silicon	Peptides	Pig ear skin Transdermal	Delivery of Therapeutic peptides	In-vitro	[200]
		Silicon	(*Gapdh*) siRNA	Mouse ear skin	Gene expression	In-vivo	[202]
		--	Naltrexone with diclofenac	Pig skin	Opioid antagonist/ Enhance pore lifetime	In-vitro/In-vivo	[203]
PMNs	-Delivery of dry and liquid drug formation -Continuous drug delivery -Flexible and multi-functional TDD systems	Titanium	Insulin	Rat skin/Transdermal	Insulin therapy	In-vivo	[209]
		Calcium sulfate & gelatin	Insulin	Rat skin/Transdermal	Insulin therapy	In-vivo	[206]
		Gelatin & hydroxyapatite	Insulin	Rat skin/Transdermal	Insulin therapy	In-vivo	[211]
		Ceramics	OVApeptides	Rat & Human skin	Vaccination	In-vivo/Ex-vivo	[212]
		Al2O3 Ceramics	DC-SIGN	Human skin/Intradermal	Vaccination	Ex-vivo	[213]
		Poly(ethylene glycol)diacrylate	Lidocaine	Rat skin	Analgesic	In-vitro	[214]
HMNs	-Direct delivery of liquid drug formulation -Continuous delivery of drugs -Unlimited dose of drugs -Can be used for tissue	Silica capillaries	IPV	Human & Rat skin/ Intradermal	Vaccination	Ex-vivo/In-vivo	[215]
		-	-	Pig skin/Intradermal	Vaccination	In-vivo	[218]
		Stainless steel	Insulin	Rat skin	Insulin therapy	In-vivo	[221]
		Polyimide coated fused-silica	IPV	Rat skin/Intradermal	Vaccination	In-vivo	[223] [224]
		Borosilicate	Sulfo-rhodamine B	Rabbit, pig & human eye	Eye treatment (proof of concept)	Ex-vivo	[225]
		Metal MN	Polystyrene particle	Rabbit eye	Eye treatment (proof of concept)	In-vivo	[226]
		Modified NanoFil needle	Phenylephrine	Perianal skin/rat	Fecal incontinence	In-vivo	[227]
		-	Lispro insulin	Human/Subcutaneous	Treatment of diabetes	In-vivo	[228]
		Acrylic	Insulin	Pig skin	Insulin therapy	In-vivo	[229]
CMNs	- Higher immune response	Stainless steel	Lidocaine	Pig skin	Analgesic	In-vitro	[230]

Devices	Device Features	Fabrication materials	Drugs	Delivery routes	Applications	Study types	Ref.
	-Rapid release of the drugs	Titanium	Rhodamine B	Rabbit cornea	Eye treatment (proof of concept)	Ex-vivo	[231]
		Silicon	Adenovirus	Mouse skin/Transcutaneous	Vaccination	In-vivo	[232]
		Stainless steel	5-fluororacil, curcumin and cisplatin	Pig skin/Transdermal	Anti-cancer	In-vitro	[233]
		Stainless steel	Plasmid DNA	Human skin	Skin disease & immunization	Ex-vivo	[234]
		Steel	siRNA	Mouse footpad	Gene silencing	In-vivo	[235]
		Stainless steel	Doxorubicin	Pig buccal tissues	Anti-cancer	In-vitro	[236]
		Stainless steel	Asparginase	Pig & Human skin/ Intraepidermal	Vaccination	Ex-vivo/In-vitro	[237]
		Stainless steel	Influenza virus	Mice skin	Vaccination	In-vivo	[238]
		Stainless steel	H1N1	Mice skin	Vaccination	In-vivo	[239]
		Stainless steel	HIV antigen	Rabbit lip & tongue	Vaccination	In-vivo	[240]
		-	Bevacizumab	Rabbit/Intracorneal	Neo-vascularization	In-vivo	[241]
		Silicon	Sunitinib malate	Mice/Intracorneal	Angiogenesis	In-vivo	[242]
		Polymer	Lidocaine	Swine/Intramuscular	Analgesia	In-vivo	[243]
		Pyridine-modified Silicon MNs	IPV	Human skin/Dermal Rat	Vaccination	Ex-vivo/In-vivo	[244]
		Titanium	PR8 influenza	Mice skin	Vaccination	In-vitro/In-vivo	[245]
DMNs	-No bio-hazardous sharp wastes -Fabrication from bio-compatible and bio-degradable materials	Hyaluronan	IgG	Human skin	Immunization	Ex-vivo	[246]
		PPF	Dacarbazine	-	Skin cancer	In-vitro	[247]
		Poloxamer	Methotrexate	Pig & human skin/ Transdermal	Solid tumor	In-vitro	[248]
		Silk fibrion/PVA	Insulin	Mice skin	Insulin therapy	In-vivo	[249]
		PMVE/MA	Insulin	Pig skin	Insulin therapy	In-vivo	[250]
		Polymeric hydrogel	Lidocaine	Pig skin	Analgesia	Ex-vivo	[251]
		Poly-caprolactone	Doxorubicin	Porcine skin & Rat skin	Anti-cancer	In-vitro/In-vivo	[252]
		Silk/PAA	Ovalbumin	Mice/Transcutaneous	Immunization	In-vivo	[253]
		Sodium hyaluronate	EV71	Mice skin	Vaccination	In-vivo	[272]
		Poly-vinylpyrrolidone	OVA Ag	Mice skin	Vaccination	In-vivo	[254]
		-	Influenza vaccine	Mice skin	Vaccination	In-vivo	[255]

Devices	Device Features	Fabrication materials	Drugs	Delivery routes	Applications	Study types	Ref.
		PLGA/PLL	Ebola DNA vaccine	Mice skin	Vaccination	In-vivo	[256]
		Polylactic acid	Sulfo-rhodamine B	Mice skin	Proof-of-concept	In-vivo	[257]

Note, chemical structures and formulas of small molecular drugs are shown in supplementary Table S2.